Reconciling organizational and cellular discrepancies between the mammalian and the avian cerebellum

by

Iulia Craciun

A thesis submitted in partial fulfillment of the requirements for the degree of

Master of Science

Neuroscience
University of Alberta

Abstract

Birds and mammals have highly developed cerebella. There are many similarities at both the cellular level and the systems level between these classes, although there are some apparent differences. In this thesis, we explored two of these discrepancies. The first is a difference at the systems level. Mammalian literature has determined that climbing fibres, originating from the inferior olive, innervate the cerebellum such that a particular subnucleus will only innervate either zebrin II immunopositive (ZII+) or zebrin II immunonegative (ZII-) stripes. Seemingly contrary this this scheme, avian literature has found that ZII+ and ZII- stripes of a functional pair are innervated by a common region of the inferior olive. Through retrograde tracing techniques, we demonstrate that ZII+ and ZII- are in fact innervated by separate, but adjacent areas of the inferior olive, thus aligning with the mammalian schematic organization. The second apparent difference we explore is one at a cellular level. Lugaro cells, which are well-characterized inhibitory interneurons in the mammalian cerebellum, have never been definitively described in an avian species. Here, we propose the existence of the avian Lugaro cell based on a number of similarities between these and mammalian Lugaro cells. The shared characteristics include fusiform somata with dendrites emerging from either end, residence in the granule cell layer just below the Purkinje cell layer, collateral innervation by Purkinje cells, and long axonal projections into the molecular layer akin to the parallel fibres of granule cells. In conclusion, these data highlight the similarity between with cerebella in birds and mammals at both the cellular and systems levels.

Preface

This thesis is an original work by Iulia Craciun. The research projects, of which this this is a part, received research ethics approval from the University of Alberta Research Ethics Board, Project Name “Structure-Function of the Pigeon Accessory Optic-Olivocerebellar System - Anatomical Studies”, AUP00000623.

The data in chapter 2 was acquired and analyzed with the assistance of D.R. Wylie and J.R. Corfield. C. Gutiérrez-Ibáñez also contributed greatly to data analysis in chapter 2. Protocol optimization for data acquisition in chapter 3 was aided by C. Gutiérrez-Ibáñez.

The work in this thesis was supported by Canadian Institutes of Health Research (CIHR) (Chapter 2) and Natural Science and Engineering Council of Canada (NSERC) (Chapter 3) grants to Douglas Wylie, as well as an NSERC Alexander Graham Bell Canada Graduate Scholarship – Masters (CGS-M) awarded to myself.

This thesis is an original work by Iulia Craciun. Chapter 2 of this thesis has been previously published.

Acknowledgments

First and foremost, I would like to thank my supervisor, Dr. Doug Wylie, for encouraging me to pursue graduate school in the first place, for always being around when help was needed, and for pushing me and my fellow lab mates to give it our best. Though we all know he can be demanding at times, what people often don't hear through the door is the encouragement, motivation, and laughter that comes along with that. I will forever be grateful for the many opportunities for growth that he has given me, as well as the resilience that has come from being under his mentorship.

I would like to extend a special thank you to the lab members that have been a great help throughout the years, especially to Dr. Cristián Gutiérrez-Ibáñez for providing insight time and time again, lending a hand when it was often needed, and for sharing his delicious meals and beer. A special shout-out to Becky Long, as we were able to keep each other "sane" while being under pressure, as the song goes. I will cherish our friendship for years to come.

Besides my supervisor and collegues, thank you to my committee members Drs Peter Hurd and Ian Winship for their insights and suggestions, as well as a sincere thanks to Dr. Jeremy Corfield who was a principal mentor upon my arrival in the lab and the two years following.

Thank you also to the Neuroscience and Mental Health Institute team, especially to Amber Lapointe, who continues to coordinate and make graduate students' lives easier. I'm grateful to have had to chance to work with the many wonderful people whom I've met over the years.

Finally, thanks to family and friends for motivating me to stay focused and for their continuous encouragement.

Table of Contents

List of Tables:

List of Figures:

List of Abbreviations:

AOS	accessory optic system
BDA	biotinylated dextran amine
CB	Calbindin D28-k
CR	Calretinin
CTB	cholera toxin subunit B
CF	climbing fibre
dl	dorsal lamella of the inferior olive
gcl	granular layer of the cerebellum
IO	inferior olive
IXcd	folium IXcd of the cerebellum
mcIO	medial column of the inferior olive
mF	mossy fibre
mcl	molecular layer of the cerebellum
NADPH-d	nicotinamide adenine dinucleotide phosphate-diaphorase
PC	Purkinje cell
PC CSA	Purkinje cell complex spike activity
pcl	Purkinje cell layer of the cerebellum
HA	rotation about an horizontal axis
SCGN	secretagogin
VA	rotation about the vertical axis
VbC	vestibulocerebellum
vl	ventral lamella of the inferior olive
wm	white matter of cerebellum
ZII+/-	zebrin II immunopositive/immunonegative

Chapter 1: **Introduction**

Although we have a wealth of knowledge regarding the organization and function of cerebral cortex, comparatively little is known about that of the cerebellum, despite it containing up to 80% of all the neurons in the brain (Lange, 1975). A more comprehensive understanding of the general principles of cerebellar organization is required as more research demonstrates that the cerebellum is involved in many behaviours and compromised in several disease states including vertigo (Bronstein, 2004), oculomotor ataxia (Onodera, 2006), and Alzheimer's disease (Larner, 1997). Cerebellar organization appears deceivingly simple, as we have known about the few cells types in the cerebellar circuit since they were described by Ramón y Cajal (1911). The cerebellar cortex is comprised of three layers: the innermost granule cell layer (gcl), the Purkinje cell (PC) monolayer (pcl), and the outermost molecular cell layer (mcl), through which the dendritic arbour of PCs extends (Figure 1.1). Though this structure may appear simple, in recent years we have learned that there is a lot more complexity in cerebellar structure and function. The cerebellum has transverse anatomical separations called "lobules or "folia", but we are now aware that the functionality of the cerebellum lies in the sagittal plane, with parasagittal zones exhibiting different properties (Voogd and Bigaré, 1980; Arends and Voogd, 1989; Seil et al., 1995; Herrup and Kuemerle, 1997; Voogd and Ruigrok, 1997; Voogd and Glickstein, 1998; Rivkin and Herrup, 2003; Pijpers et al., 2005). These parasagittal "zones" comprise the functional units of the cerebellum. First, zones can be defined with respect to the distribution of afferent input from climbing fibres (CFs), which originate from the inferior olive (IO) and mossy fibres, which originate from various areas of the brain (Voogd and Bigaré, 1980; Wu et al., 1999; Ruigrok, 2003; Pakan and Wylie, 2008). Second, the projection patterns of efferent PC outputs are zonally organized (Voogd and Glickstein, 1998; Wylie et al., 2003a, 2003b).

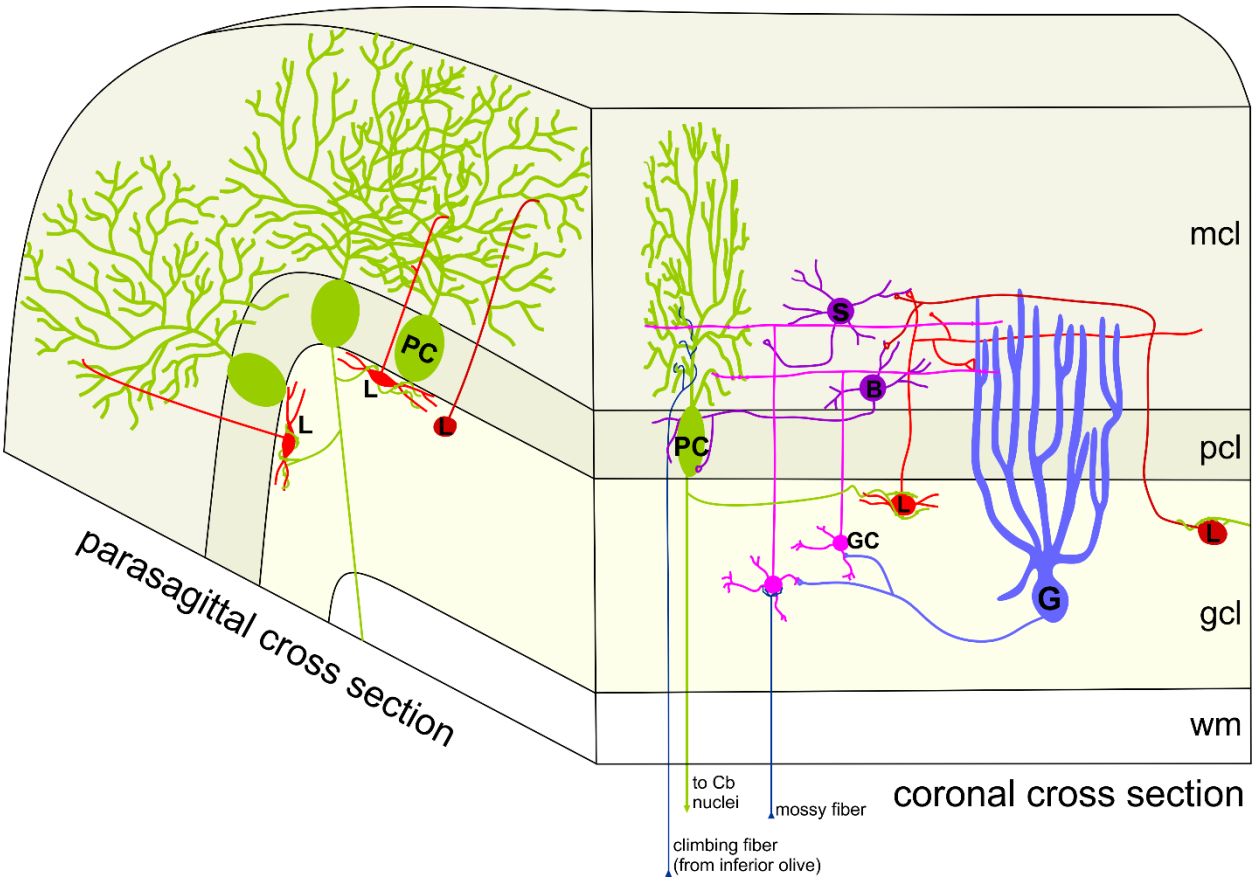

Figure 1.1 Simplified cerebellar circuitry. The schematic shows simple cerebellar connectivity, and a view of a cerebellar folium in the parasagittal and coronal planes. Climbing fibres (CFs; navy) and mossy fibres (mFs; navy) are the two main inputs into the cerebellum. CFs come from the inferior olive and synapse directly onto the Purkinje cells (PCs; green) while mFs terminate on granule cells (GC; magenta) and Golgi cells (G; blue) in the granular cell layer (gcl). Granule cells project their axons into the molecular cell layer (mcl) and bifurcate to send off parallel fibres that synapse extensively onto the PCs. Lugaro cells (L; red) also project their axons into the mcl, and their axons travel through the coronal plane alongside granule cell parallel fibres to synapse on basket (B) and stellate (S) cells (purple). Basket and stellate cells in turn synapse on PCs, and PC collaterals synapse on Lugaro cells. Lugaro cells also synapse onto

Golgi cells. Note both fusiform (bright red) and globular (dark red) types of Lugaro cells. The fusiform somata are only noticeable in parasagittal cross sections. pcl = Purkinje cell layer; wm = white matter.

Third, PCs within a sagittal band exhibit similar response properties (Apps and Garwicz, 2005; Graham and Wylie, 2012), and tend to fire synchronously (Llinás and Sasaki, 1989). Finally, several molecular markers exhibit parasagittal expression in the cerebellum (Herrup and Kuemerle, 1997).

The most extensively studied marker is zebrin II (ZII), whose antibody recognizes the 36-kDa metabolic isoenzyme aldolase C, and is expressed almost exclusively by PCs in their somata, dendrites, axons, and terminals (Brochu et al., 1990; Ahn et al., 1994; Hawkes and Herrup, 1995; Pakan et al., 2007). ZII is heterogeneously expressed such that regions of PCs that strongly express ZII (ZII+) alternate with regions that express little or no ZII (ZII-) (Figure 1.2). ZII stripes have been demonstrated in several mammalian (Leclerc et al., 1992; Ozol et al., 1999; Armstrong and Hawkes, 2000; Sanchez et al., 2002; Marzban et al., 2003, 2015; Sillitoe et al., 2003; Marzban and Hawkes, 2011) and avian species (Pakan et al., 2007; Iwaniuk et al., 2009; Marzban et al., 2010; Corfield et al., 2015, 2016; Vibulyaseck et al., 2015), as well as in one genus of lizard (Wylie et al., 2016). The prevalence of ZII stripes across various species suggests that the role for ZII is highly conserved and is likely crucial to cerebellar function. In the pigeon vestibulocerebellum (VbC), which consists of folia IXcd and X (Figure 1.2), it has been shown that the ZII stripes coincide with functional properties of PCs and afferent inputs, so this ZII+/- stripe pair is called a functional zone (Pakan and Wylie, 2008; Pakan et al., 2010, 2011, 2014; Graham and Wylie, 2012; Wylie, 2013).

The highly conserved and well-studied pattern of ZII expression in the avian cerebellum is one aspect of the pigeon vestibulocerebellum (VbC) that makes the VbC an ideal model for studying parasagittal cerebellar organization. Second, the cerebellum is also highly conserved in terms of functionality. For instance, the flocculus is strikingly similar in pigeon, rodents, rats,

and non-human primates (for review, see Voogd and Wylie, 2004). Third, both the inputs and outputs of the VbC have been well described. For instance, mossy fibre input from the retinorecipient nuclei of the accessory optic system, the nucleus lentiformis mesencephali and nucleus of the basal optic root, and their mammalian homologs, the nucleus of the optic tract and medial terminal nucleus, are strikingly similar in terms of connectivity and response properties to stimuli (McKenna and Wallman, 1985; Wylie and Crowder, 2000; Crowder and Wylie, 2001, 2002; Ibbotson and Price, 2001; Wylie, 2001; Giolli et al., 2006). These nuclei provide most of the input to the VbC. Last, the functionality of the pigeon VbC has been thoroughly researched. It is now known that PCs in the VbC selectively respond to different types of optic flow depending on their parasagittal location, and that each functional parasagittal zone happens to coincide with a ZII+/- stripe pair in the pigeon VbC (see section 1.1) (Wylie and Frost, 1999; Pakan and Wylie, 2008; Pakan et al., 2010, 2011, 2014; Graham and Wylie, 2012; Wylie et al., 2013, 2017)

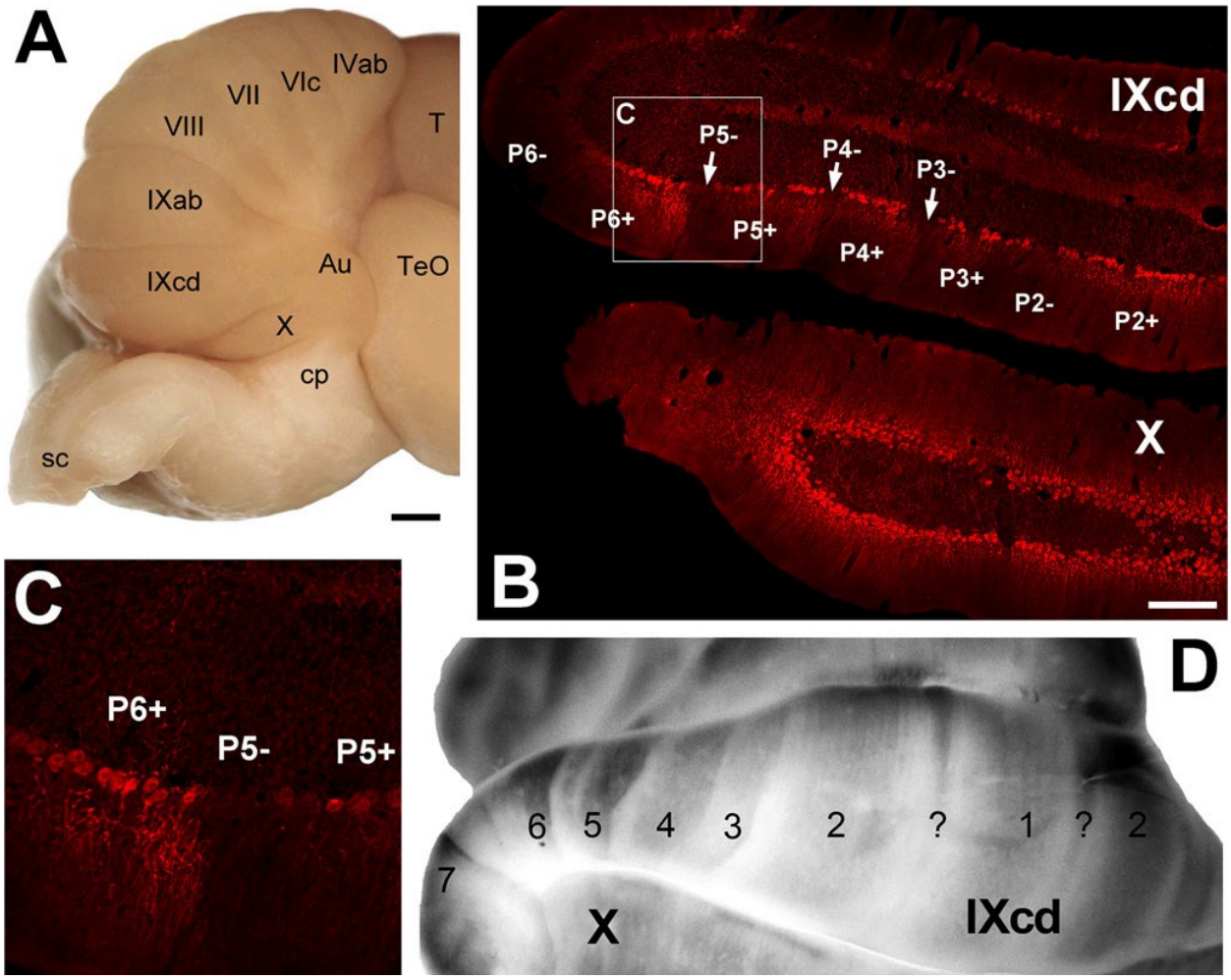

Figure 1.2 Pigeon cerebellum and zebrin II stripes. A Shows a lateral view of the pigeon cerebellum. **B-D** show the striped pattern of ZII immunolabelling in the pigeon cerebellum. **A** is a coronal section through the vestibulocerebellum (VbC; folia IXcd and X). ZII stripes are labelled from P1+/- most medially to P7+/- most laterally (not all shown here). **C** is a close-up image of the white box from B as an example of ZII+ and ZII- immunolabelling. **D** shows a dorsal view of the VbC with all 7 stripe pairs visible. Au = auricle, T = telencephalon, TeO = optic tectum, cp = cerebellar peduncle, sc = spinal cord. Scale bars = 1 mm in **A,D**; 250 μm in **B**. Adapted from Pakan et al. (2011).

Although the cerebellum is highly conserved, there are still some noted differences between mammalian and avian cerebellar organization. First there is an apparent discrepancy in ZII stripe innervation by CFs in mammals versus birds. According to the mammalian literature, separate olivary subnuclei either innervate a ZII+ or ZII- stripe but never both (Voogd et al., 2003; Sugihara and Shinoda, 2004; Voogd and Ruigrok, 2004; Pijpers et al., 2006; Sugihara and Quy, 2007). However, studies in pigeons have shown that a particular section of the medial column of the inferior olive (mcIO) goes to innervate both ZII+ and ZII- stripes within a functional pair (Pakan and Wylie, 2008; Pakan et al., 2014). Another difference between mammals and birds is in the apparent lack of certain cell types in the avian cerebellum. Lugaro cells are one such cell that is known to exist in mammals but has never been described in birds. This thesis provides a closer examination into these discrepancies at the organizational level and cellular level to reconcile these apparent differences between the avian and mammalian cerebellum.

1.1 Functional Cerebellar Organization

1.1.1 *Optic Flow Overview*

Optic flow refers to the pattern of motion across the retina as an animal moves through its environment with "self-motion" (Gibson, 1954). Self-motion refers to self-rotation, meaning the rotation of the head relative to the world, and self-translation, which entails moving from one location to another within the environment. Neurons that respond to translational optic flow respond to contraction, expansion, ascent, and descent. Contraction neurons respond to backwards translation, whereas expansion neurons respond to forward translation along the horizontal axis. Ascent neurons respond to upward translation along the vertical axis, while

descent neurons respond to downward translation along the vertical axis. Self-rotation can either be about the vertical axis (VA), or about an horizontal axis oriented 45° to the midline (HA)(Wylie and Frost, 1993).

1.1.2 *Optic Flow Zones and ZII Expression*

The pigeon VbC houses the cerebellar optic flow zones – areas in which PC complex spike activity (CSA) responds to particular patterns of optic flow. The ZII stripes in the pigeon VbC are named from P1+/- starting at the midline, to P7+/- (Figure 1.2). The "+/-" refers to adjacent immunopositive and immunonegative bands within a functional zone. Additionally, there is a satellite ZII+ band in folia IXcd named "?" within P1-, separating P1- into medial and lateral sections, and a satellite ZII- band we call the "notch" in P2+, separating it into medial and lateral sections (Figure 1.2). As previously mentioned, these optic flow zones coincide with ZII stripes, with the exception of folia X which is entirely ZII+, but contains the extension of the cerebellar optic flow zones based on the immunoreactivity of folia IXcd above (Figure 1.3). The functional organization of the optic flow zones is shown in Figure 1.3 (Pakan et al., 2011; Graham and Wylie, 2012; Wylie, 2013). In the lateral aspect of folia IXcd, also known as the flocculus, there are two interdigitated VA zones (P4+/- and P6+/-), and two HA zones (P5+/- and P7+/-). In these regions, PC CSA responds to responded to rotation about the vertical axis (VA neurons), and to rotation about the horizontal axis (HA neurons), respectively (Graham and Wylie, 2012). In the medial aspect of folia IXcd, the uvula, and folia X, known as the nodulus, PCs respond to self-translational patterns of optic flow (Wylie and Frost, 1999; Graham and Wylie, 2012). In these regions, neurons respond to contraction, expansion, ascent, and descent. My research focus is on the uvula, where the order of optic flow zones from medial to lateral is

as follows: contraction zone (P1+/P1-med), expansion/ascent zone (P1-lat/P2+med), and descent zone (P2+lat/P2-), as shown in Figure 1.3. The well characterized nature of these cerebellar optic flow zones is useful as it allows us to map the location of an electrode in the cerebellum through the use of electrophysiological recordings of PC responses to optokinetic stimuli.

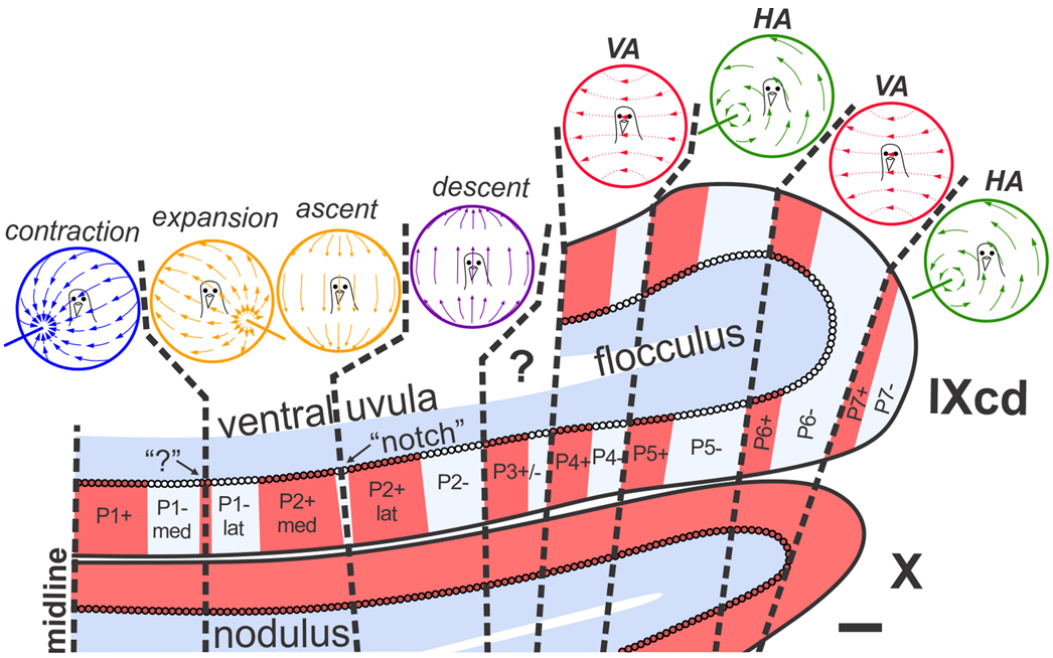

Figure 1.3 Vestibulocerebellar optic flow zones. Optic flow zones and zebrin II (ZII) pattern is depicted in a coronal section through the pigeon vestibulocerbellum (VbC; folia IXcd and X).The alternating ZII+ (red) and ZII- (pale blue) stripes are numbered from P1+/- most medially to P7+/- laterally, with ZII+ and ZII– stripes alternating. P1– is bisected by a satellite ZII+ band designated "?", dividing the stripe into medial and lateral halves (P1-med; P1-lat). P2+ is divided by a ZII– "notch", indicated by the inverted triangle (Wylie et al., 2007). In the uvula, the optic flow zones from medial to lateral are as follows: contraction zone (P1+/P1–med); expansion/ascent zone (P1–lat/P2+med); descent zone (P2+lat/P2–) (Graham and Wylie, 2012). Purkinje cells (PCs) in the floccular zones respond optic flow resulting from rotation about either the vertical axis (VA) or an horizontal axis (HA). There are two VA zones, spanning P4+/- and P6+/-, interdigitated with two HA zones, spanning P5+/- and P7+/- (Pakan et al., 2011). PCs in the P3+/- stripe do not respond to optic flow stimuli and their function is

unknown (Graham and Wylie, 2012). The sagittal organization of the optic flow zones extend into the nodulus (folia X), although all PCs are ZII+ (Graham and Wylie, 2012; Pakan et al., 2007, 2011, 2014; Pakan and Wylie, 2008). Scale bar = 200 μm.

1.1.3 *Zebrin II Stripes and Climbing Fibre Input*

According to anterograde tracing studies whereby biotinylated dextran amine (BDA) was injected in the inferior olive, it was suggested that an olivary subdivision innervated both ZII+ and ZII- stripes of a functional pain (Pakan and Wylie, 2008; Pakan et al., 2014). It was reported that the three translational optic flow zones of the uvula receive input from different regions in the dorsolateral portion of the medial column of the inferior olive (mcIO) (Pakan et al., 2014). The different regions of the dorsolateral mcIO project to the uvula as follows: the caudal-most portion innervates the *contraction* zone, the rostral-most portion innervates the *descent* zone, and a middle region in between the caudal and rostral dorsolateral mcIO innervates the *expansion/ascent* zone (Crowder et al., 2000; Pakan et al., 2011, 2014) (Figure 1.4A). Similarly, different regions of the dorsomedial mcIO project to the flocculus as follows: CFs from the caudal mcIO projected strictly to the P4+/- and P6+/- ZII bands (HA zones), and those from the rostral mcIO innervated only the P5+/- and P7+/- ZII bands (VA zones) (Pakan and Wylie, 2008).

These studies are seemingly at odds with what has been described in mammalian literature, being that CFs from a particular olivary subnucleus will innervate either a ZII+ or a ZII- stripe, but never both types (Voogd et al., 2003; Sugihara and Shinoda, 2004; Voogd and Ruigrok, 2004; Pijpers et al., 2006; Sugihara and Quy, 2007). Voogd et al. (2003) investigated CF projections from various nuclei of the olive to the ZII stripes in the copula pyramidis and the paramedian lobule of the rat cerebellum. They found that the CFs from the dorsal accessory olive projected to ZII- bands in C1 and C3 zones of the copula pyramidis, the rostral medial accessory olive projected to ZII+ stripes in the C2 zone of the copula pyramidis, and fibre efferent from the principle olive projected to ZII+ stripes of the D zone of the paramedian lobule (Voogd et al.,

2003). Voogd & Ruigrok (2004) studied the organization of CFs from the olive to the ZII stripes in the rat vermis. By injecting various subnuclei in the IO, they saw that CF efferent labelling from each subnuclei was confined to either a ZII+ or ZII- stripe, but not both. Sugihara & Shinoda (2004) injected BDA into various areas of the rat IO and found that ZII- stripes were innervated by the centrocaudal portion of the medial accessory olive, while ZII+ stripes were innervated by CFs from the principal olive, and other medial subnuclei. All three of these studies demonstrate that IO subnuclei show a specificity with regards to the ZII signature of the innervated cerebellar zone.

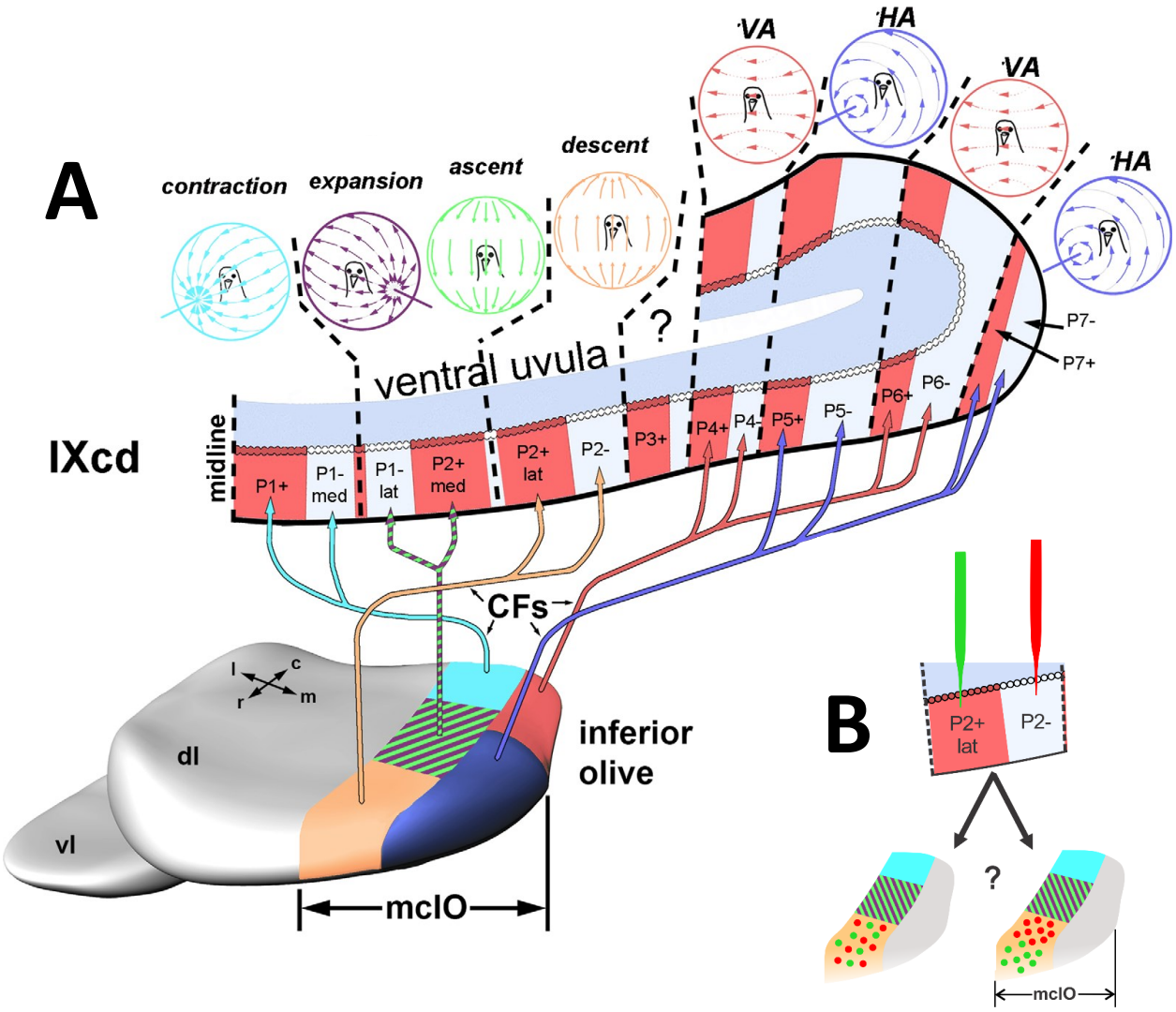

Figure 1.4 Suggested climbing fibre projections to the vestibulocerebellum. **A** depicts a schematic of the climbing fibre (CF) projections from each region of the mcIO to the ZII stripes in the optic flow zones in folium IXcd as proposed by Pakan et al. (2014) and Pakan and Wylie (2008). Note that in this representation, both ZII+ and ZII- stripes are innervated by discreet regions of medial column of the inferior olive (mcIO). **B** depicts the potential patterns of retrograde cell labelling in the mcIO from injections in ZII stripes of the ventral uvula. c, r, m, and l = caudal, rostral, medial, and lateral; dl and vl = dorsal lamella and ventral lamella of the inferior olive. Adapted from Pakan et al. (2014).

To reiterate, these studies have reached different conclusions in terms of olivary input to the cerebellum, varying with the model animal used. Rodent studies have shown that a particular olivary subnucleus will project to either a ZII+ or ZII- stripe, but not to both (Voogd et al., 2003; Sugihara and Shinoda, 2004; Voogd and Ruigrok, 2004; Pijpers et al., 2006; Sugihara and Quy, 2007). Seemingly contrary to what has been proposed with rodent studies, pigeon studies using anterograde tracing methods have demonstrated that discrete regions within the mcIO project CFs to both ZII+ and ZII- stripes, and more specifically to stripes within the same functional pair (Figure 1.4) (Pakan & Wylie, 2008; Pakan et al., 2011, 2014).

With anterograde tracing studies in pigeons, one limitation is the poverty of precision with respect to the injection site. Injection of a tracer into the mcIO results in a multitude of neurons up taking the tracer, and carrying the tracer to the VbC, where both ZII+ and ZII- stripes may end up fluorescing (Pakan & Wylie, 2008; Pakan et al., 2011, 2014). This is not able to predict whether or not ZII+ and ZII- stripes receive differential input from the olive; it in fact leads us toward believing the contrary. Wylie et al. (2017) were the first to address these apparent differences between the avian and mammalian literature in a recent retrograde study that examined olivary projections to the pigeon flocculus (i.e., stripes P4+/- to P6+/-). They found that adjacent regions of the mcIO innervated either a ZII+ or ZII- stripe within a functional pair (Wylie et al., 2017). These data remain in line with the idea of a ZII+/- stipe pair as a functional zone since the CF input originated from adjacent olivary areas, yet still from within a common region of the IO. We did a similar study whereby we injected retrograde tracers into the ZII+ and ZII- stripes of a pairs in the uvula, and visualized the resulting cell labeling pattern in the mcIO (Chapter 2). This study could have resulted in one of two outcomes: one in which the retrograde labelled cells would exist in an intermingled population, or one in which there would

be two separate, but adjacent populations of retrograde labelled cells (Figure 1.4B). The latter result was expected as it aligns with what has been learned from mammalian literature while still remaining in line the idea of a ZII+/ZII- stripe pair being innervated by a similar general olivary region.

1.2 Cerebellar Structures and Circuitry

1.2.1 *Cerebellar Subdivisions*

The cerebellum is highly foliated in birds and mammals, as well as in some fish, where transverse fissures divide the cerebellum into "lobules" (the term generally used for mammals) or "folia" (generally used to refer to avian species). Larsell (1967) named the 10 cerebellar folia from I-X, with I being the anterior-most folium and X being the posterior-most. Folia IX is further divided into IXab and IXcd (Figure 1.2A). IXcd and X are considered to be the VbC. Though the cerebellum has these transverse anatomical separations, the functional divisions of the cerebellum lie in the sagittal plane, as previously elaborated. The uvula and the flocculus are such functional distinctions of folium IXcd. The uvula (responding to translational optic flow) resides in the medial portion of folium IXcd, while the flocculus (responding to rotational optic flow) resides in the lateral portion. These regions are further divided into the various optic flow zones previously described.

1.2.2 *Basic Cerebellar Circuit*

A simple repetitive cerebellar cell circuit has been known since Ramón y Cajal (1911). There are but a few cells that are involved in this circuit: granule cells, Purkinje cells, Golgi

cells, stellate cells, and basket cell, with the latter three comprising the interneurons of the circuit (Ramón y Cajal, 1911). In the circuit, mossy fibres innervate the granule cells in the gcl through synaptic contacts known as rosettes. The granule cell axons travel deep into the mcl and bifurcate into what are called parallel fibres that synapse onto the dendritic arbour of tens of thousands of PCs (Itō, 1984). Therefore, PCs receive indirect input from mossy fibres through this circuit. PCs also receive direct input from the inferior olive by way of climbing fibres (CFs). PCs, the only output cells of the cerebellum, then project to the deep cerebellar and vestibular nuclei. PC activity is also modulated by input from inhibitory cerebellar interneurons. Stellate and basket cells, whose somata reside in the mcl, are examples of such interneurons, and they receive input from parallel fibres as well are from other cerebellar cells such as Lugaro cells (another cerebellar interneuron). Golgi cells, another type of cerebellar interneuron, are found in the gcl, but their dendrites extend into the mcl to receive input from parallel fibres, and provide inhibitory feed back to granule cells (Itō, 1984).

1.2.3 *Lugaro cells*

A cerebellar inhibitory interneuron that isn't always included in descriptions of the basic cerebellar circuit is the Lugaro cell. Lugaro cells are found in the granular layer of the cerebellar cortex, just below or within the Purkinje cell layer (Fox, 1959). These cells are characterized by their fusiform spindle-like shape and dendrites that emerge from opposite ends of their cell bodies (Fox, 1959). Golgi (1874) first described such cells in the human cerebellum, along with another globular type of cell which is now known as a Golgi cell. Lugaro (1894) later described similar fusiform cells, also located right below the Purkinje cell layer in the cat cerebellum and named them "the intermediate cells" as they were a previously unknown cell type. Although

Luagro cells differ from Golgi cells in morphology, they were often classified as Golgi cells as they are also large interneurons in the granular layer. It was Sahin and Hockfield (1990) who determined that Lugaro cells are molecularly distinct from the other large cerebellar cortex cells types, i.e. from the Purkinje cells and the Golgi cells, and as such constitute a distinct cell type. Another characteristic feature of Lugaro cells is their axonal projection patterns. Lugaro cell axons always project into the molecular layer, with axon collaterals traveling parallel to the parallel fibres that arise from granule cells in the cerebellar cortex (Lugaro, 1894; Fox, 1959; Lainé and Axelrad, 1996, 2002). Apart from the typical fusiform Lugaro cell, another globular type of Lugaro cell has been suggested due to their wiring and axonal projection pattern alongside their immunoreactivity for calretinin and innervation by Purkinje axon collaterals (Lainé and Axelrad, 2002; Schilling et al., 2008). Lugaro cells have been described in a diverse array of mammalian species, but there is little evidence for their existence in other vertebrate classes. Based on neurochemistry, Pushchina and Varaksin (2001) suggested their existence in one species of teleost. Similarly, Rogers (1989) postulated they may exist in chickens. Upon investigating calcium binding protein expression in the pigeon VbC, we noticed immunolabelled cells that exhibited Lugaro cell characteristics. Part of this thesis uses immunohistochemistry to suggest that these Lugaro cells do indeed exist in the pigeon cerebellum (Chapter 3). This is an additional piece of evidence to further the conserved nature of the cerebellum across species.

1.3 References

Ahn AH, Dziennis S, Hawkes R, Herrup K (1994) The cloning of zebrin II reveals its identity with aldolase C. *Development* 120:2081–2090.

Apps R, Garwicz M (2005) Anatomical and physiological foundations of cerebellar information processing. *Nat Rev Neurosci* 6:297–311.

Arends JJA, Voogd J (1989) Topographic aspects of the olivocerebellar system in the pigeon. In: Experimental Brain Research Series 17: The olivocerebellar system in motor control (Stata P, ed), pp 52–57.

Armstrong CL, Hawkes R (2000) Pattern formation in the cerebellar cortex. *Biochem Cell Biol* 78:551–562.

Brochu G, Maler L, Hawkes R (1990) Zebrin II: A polypeptide antigen expressed selectively by purkinje cells reveals compartments in rat and fish cerebellum. *J Comp Neurol* 291:538–552.

Bronstein AM (2004) Vision and vertigo: Some visual aspects of vestibular disorders. *J Neurol* 251:381–387.

Corfield JR, Kolominsky J, Craciun I, Mulvany-Robbins BE, Wylie DR (2016) Is cerebellar architecture shaped by sensory ecology in the New Zealand Kiwi (Apteryx mantelli)? *Brain Behav Evol* 87:88–104.

Corfield JR, Kolominsky J, Marin GJ, Craciun I, Mulvany-Robbins BE, Iwaniuk AN, Wylie DR (2015) Zebrin II expression in the cerebellum of a paleognathous bird, the Chilean tinamou (Nothoprocta perdicaria). *Brain Behav Evol* 85:94–106.

Crowder NA, Winship IR, Wylie DRW (2000) Topographic organization of inferior olive cells projecting to translational zones in the vestibulocerebellum of pigeons. *J Comp Neurol* 419:87–95.

Crowder NA, Wylie DR (2001) Fast and slow neurons in the nucleus of the basal optic root in pigeons. *Neurosci Lett* 304:133–136.

Crowder NA, Wylie DR (2002) Responses of optokinetic neurons in the pretectum and accessory optic system of the pigeon to large-field plaids. *J Comp Physiol A* 188:109–119.

Fox CA (1959) The intermediate cells of Lugaro in the cerebellar cortex of the monkey. *J Comp Neurol* 112:39–53.

Gibson JJ (1954) The visual perception of objective motion and subjective movement. *Psychol Rev* 61:304–314.

Giolli RA, Blanks RHI, Lui F (2006) The accessory optic system: basic organization with an update on connectivity, neurochemistry, and function. In: Progress in brain research, pp 407–440.

Golgi C (1903) Sulla fina anatomia del cervelleto umano. In: Opera omnia, pp 99–111. Milan, Italy: Ulrico Hoepli.

Graham DJ, Wylie DR (2012) Zebrin-Immunopositive and -Immunonegative Stripe Pairs Represent Functional Units in the Pigeon Vestibulocerebellum. *J Neurosci* 32:12769–12779.

Hawkes R, Herrup K (1995) Aldolase C/zebrin II and the regionalization of the cerebellum. *J Mol Neurosci* 6:147–158.

Herrup K, Kuemerle B (1997) The compartmentalization of the cerebellum. *Annu Rev Neurosci* 20:61–90.

Ibbotson MR, Price NSC (2001) Spatiotemporal tuning of directional neurons in mammalian and avian pretectum: a comparison of physiological properties. *J Neurophysiol* 86:2621–2624.

Itō M (1984) The cerebellum and neural control. New York : Raven Press.

Iwaniuk AN, Marzban H, Pakan JMP, Watanabe M, Hawkes R, Wylie DR (2009) Compartmentation of the cerebellar cortex of hummingbirds (Aves: Trochilidae) revealed by the expression of zebrin II and phospholipase Cβ4. *J Chem Neuroanat* 37:55–63.

Lainé J, Axelrad H (1996) Morphology of the Golgi-impregnated Lugaro cell in the rat cerebellar cortex: A reappraisal with a description of its axon. *J Comp Neurol* 375:618–640.

Lainé J, Axelrad H (2002) Extending the cerebellar Lugaro cell class. *Neuroscience* 115:363–374.

Lange W (1975) Cell number and cell density in the cerebellar cortex of man and some other mammals. *Cell Tissue Res* 157:115–124.

Larner AJ (1997) The Cerebellum in alzheimer's disease. *Dement Geriatr Cogn Disord* 8:203–209.

Larsell O (1967) The comparative anatomy and histology of the cerebellum: from myxinoids through birds. Minneapolis: University of Minnesota Press.

Leclerc N, Schwarting GA, Herrup K, Hawkes R, Yamamoto M (1992) Compartmentation in mammalian cerebellum: Zebrin II and P-path antibodies define three classes of sagittally organized bands of Purkinje cells. *Proc Natl Acad Sci* 89:5006–5010.

Llinás R, Sasaki K (1989) The Functional Organization of the Olivo-Cerebellar System as Examined by Multiple Purkinje Cell Recordings. *Eur J Neurosci* 1:587–602.

Lugaro E (1894) Sulle connessioni tra gli elementi nervosi della corteccia cerebellare con considerazioni generali sul signifcato fisiologico dei rapporti tra gli elementi nervosi. *Riv Sper Freniatr* 20:297–331.

Marzban H, Chung S-H, Pezhouh MK, Feirabend H, Watanabe M, Voogd J, Hawkes R (2010) Antigenic compartmentation of the cerebellar cortex in the chicken (Gallus domesticus). *J Comp Neurol* 518:2221–2239.

Marzban H, Hawkes R (2011) On the Architecture of the Posterior Zone of the Cerebellum. *The Cerebellum* 10:422–434.

Marzban H, Hoy N, Buchok M, Catania KC, Hawkes R (2015) Compartmentation of the Cerebellar Cortex: Adaptation to Lifestyle in the Star-Nosed Mole Condylura cristata. *The Cerebellum* 14:106–118.

Marzban H, Zahedi S, Sanchez M, Hawkes R (2003) Antigenic compartmentation of the cerebellar cortex in the syrian hamster Mesocricetus auratus. *Brain Res* 974:176–183.

McKenna OC, Wallman J (1985) Accessory optic system and pretectum of birds: Comparisons with those of other vertebrates. *Brain Behav Evol* 26:91–116.

Onodera O (2006) Spinocerebellar ataxia with ocular motor apraxia and DNA repair. In: Neuropathology, pp 361–367.

Ozol K, Hayden JM, Oberdick J, Hawkes R (1999) Transverse zones in the vermis of the mouse cerebellum. *J Comp Neuro*l 412:95–111.

Pakan JMP, Graham DJ, Gutierrez-Ibanez C, Wylie DR (2011) Organization of the cerebellum: correlating zebrin immunochemistry with optic flow zones in the pigeon flocculus. *Vis Neurosci* 28:163–174.

Pakan JMP, Graham DJ, Wylie DR (2014) Climbing fiber projections in relation to Zebrin stripes in the ventral Uvula in Pigeons. *J Comp Neurol* 522:3629–3643.

Pakan JMP, Iwaniuk AN, Wylie DR, Hawkes R, Marzban H (2007) Purkinje cell compartmentation as revealed by Zebrin II expression in the cerebellar cortex of pigeons (Columba livia). *J Comp Neurol* 501:619–630.

Pakan JMP, Wylie DR (2008) Congruence of zebrin II expression and functional zones defined by climbing fiber topography in the flocculus. *Neuroscience* 157:57–69.

Pakan JMPP, Graham DJ, Wylie DR (2010) Organization of visual mossy fiber projections and zebrin expression in the pigeon vestibulocerebellum. *J Comp Neurol* 518:175–198.

Pijpers A, Apps R, Pardoe J, Voogd J, Ruigrok TJH (2006) Precise Spatial Relationships between Mossy Fibers and Climbing Fibers in Rat Cerebellar Cortical Zones. *J Neurosci* 26:12067–12080.

Pijpers A, Voogd J, Ruigrok TJH (2005) Topography of olivo-cortico-nuclear modules in the intermediate cerebellum of the rat. *J Comp Neurol* 492:193–213.

Pushchina E V, Varaksin AA (2001) [Argyrophilic and nitroxydergic bipolar neurons (Lugaro cells) in the cerebellum of Pholidapus dybowskii]. *Zh Evol Biokhim Fiziol* 37:437–441.

Ramón S, Cajal S (1911) Histologie du système nerveux de l'homme et des vertébrés. Paris: Maloine.

Rivkin A, Herrup K (2003) Development of cerebellar modules: Extrinsic control of late-phase Zebrin II pattern and the exploration of rat/mouse species differences. *Mol Cell Neurosci* 24:887–901.

Rogers JH (1989) Immunoreactivity for calretinin and other calcium-binding proteins in cerebellum. *Neuroscience* 31:711–721.

Ruigrok TJH (2003) Collateralization of climbing and mossy fibers projecting to the nodulus and flocculus of the rat cerebellum. *J Comp Neurol* 466:278–298.

Sahin M, Hockfield S (1990) Molecular identification of the lugaro cell in the cat cerebellar cortex. *J Comp Neurol* 301:575–584.

Sanchez M, Sillitoe R V., Attwell PJE, Ivarsson M, Rahman S, Yeo CH, Hawkes R (2002) Compartmentation of the rabbit cerebellar cortex. *J Comp Neurol* 444:159–173.

Schilling K, Oberdick J, Rossi F, Baader SL (2008) Besides Purkinje cells and granule neurons: An appraisal of the cell biology of the interneurons of the cerebellar cortex. *Histochem Cell Biol* 130:601–615.

Seil FJ, Johnson ML, Hawkes R (1995) Molecular compartmentation expressed in cerebellar cultures in the absence of neuronal activity and neuron-glia interactions. *J Comp Neurol* 356:398–407.

Sillitoe R V., Künzle H, Hawkes R (2003) Zebrin II compartmentation of the cerebellum in a basal insectivore, the Madagascan hedgehog tenrec Echinops telfairi. *J Anat* 203:283–296.

Sugihara I, Quy PN (2007) Identification of aldolase C compartments in the mouse cerebellar cortex by olivocerebellar labeling. *J Comp Neurol* 500:1076–1092.

Sugihara I, Shinoda Y (2004) Molecular, Topographic, and Functional Organization of the Cerebellar Cortex: A Study with Combined Aldolase C and Olivocerebellar Labeling. *J Neurosci* 24:8771–8785.

Vibulyaseck S, Luo Y, Fujita H, Oh-Nishi A, Ohki-Hamazaki H, Sugihara I (2015) Compartmentalization of the chick cerebellar cortex based on the link between the striped expression pattern of aldolase C and the topographic olivocerebellar projection. *J Comp Neurol* 523:1886–1912.

Voogd J, Bigaré F (1980) Topographical distribution of olivary and cortico nuclear fibres in the cerebellum: a review. In: The Inferior Olivary Nucleus. (Courville J, de Montigny C, Lamarre Y, eds), pp 207–234. New York: Raven Press.

Voogd J, Glickstein M (1998) The anatomy of the cerebellum. *Trends Cogn Sci* 2:307–313.

Voogd J, Pardoe J, Ruigrok TJH, Apps R (2003) The distribution of climbing and mossy fiber collateral branches from the copula pyramidis and the paramedian lobule: congruence of climbing fiber cortical zones and the pattern of zebrin banding within the rat cerebellum. *J Neurosci* 23:4645–4656.

Voogd J, Ruigrok TJ (1997) Transverse and longitudinal patterns in the mammalian cerebellum. *Prog Brain Res* 114:21–37.

Voogd J, Ruigrok TJH (2004) The organization of the corticonuclear and olivocerebellar climbing fiber projections to the rat cerebellar vermis: The congruence of projection zones and the zebrin pattern. *J Neurocytol* 33:5–21.

Voogd J, Wylie DRW (2004) Functional and Anatomical Organization of Floccular Zones: A Preserved Feature in Vertebrates. *J Comp Neurol* 470:107–112.

Wu HS, Sugihara I, Shinoda Y (1999) Projection patterns of single mossy fibers originating from the lateral reticular nucleus in the rat cerebellar cortex and nuclei. *J Comp Neurol* 411:97–118.

Wylie DR (2001) Projections from the nucleus of the basal optic root and nucleus lentiformis mesencephali to the inferior olive in pigeons (Columba livia). *J Comp Neurol* 429:502–513.

Wylie DR (2013) Processing of visual signals related to self-motion in the cerebellum of pigeons. *Front Behav Neurosci* 7:1–15.

Wylie DR, Frost BJ (1993) Responses of pigeon vestibulocerebellar neurons to optokinetic stimulation. II. The 3-dimensional reference frame of rotation neurons in the flocculus. *J Neurophysiol* 70:2647–2659.

Wylie DR, Frost BJ (1999) Complex spike activity of Purkinje cells in the ventral uvula and nodulus of pigeons in response to translational optic flow. *J Neurophysiol* 81:256–266.

Wylie DR, Gutiérrez-Ibáñez C, Corfield JR, Craciun I, Graham DJ, Hurd PL (2017) Inferior olivary projection to the zebrin II stripes in lobule IXcd of the pigeon flocculus: A retrograde tracing study. *J Comp Neurol* 525:3158–3173.

Wylie DR, Hoops D, Aspden JW, Iwaniuk AN (2016) Zebrin II is expressed in sagittal stripes in the cerebellum of dragon lizards (Ctenophorus sp.). *Brain Behav Evol* 88:177–186.

Wylie DR, Jensen M, Gutierrez-Ibanez C, Graham DJ, Iwaniuk AN (2013) Heterogeneity of calretinin expression in the avian cerebellar cortex of pigeons and relationship with zebrin II. *J Chem Neuroanat* 52:95–103.

Wylie DRW, Brown MR, Barkley RR, Winship IR, Crowder NA, Todd KG (2003a) Zonal Organization of the Vestibulocerebellum in Pigeons (Columba livia): II. Projections of the Rotation Zones of the Flocculus. *J Comp Neurol* 456:140–153.

Wylie DRW, Brown MR, Winship IANR, Crowder NA, Todd KG (2003b) Zonal organization of the vestibulocerebellum in pigeons (Columba livia): III. Projections of the translation zones of the ventral uvula and nodulus. *J Comp Neurol* 465:179–194.

Wylie DRW, Crowder NA (2000) Spatiotemporal properties of fast and slow neurons in the pretectal nucleus lentiformis mesencephali in pigeons. *J Neurophysiol* 84:2529–2540.

Chapter 2: **Inferior Olive Projections to Zebrin II Stripes in the Pigeon Cerebellum**

A version of this chapter has been published:

Craciun, I., Gutiérrez-Ibáñez, C., Corfield, J.R., Hurd, P.L., Wylie, D.R. (2018). Topographic Organization of Inferior Olive Projections to the Zebrin II Stripes in the Pigeon Cerebellar Uvula. *Frontiers in Neuroanatomy*, 12, 18. doi:10.3389/fnana.2018.00018.

The cerebellum exhibits an organization defined by sagittal zones (Voogd and Bigaré, 1980), which is evident with respect to the distribution of afferent input from climbing fibres (CFs) and mossy fibres, the projection patterns of efferent Purkinje cell (PC) outputs, as well as from the response properties and synchronous firing of PCs (Apps and Garwicz, 2005; De Zeeuw et al., 1994; Graham and Wylie, 2012; Llinas and Sasaki, 1989; Pakan et al., 2011, 2014; Pakan and Wylie, 2008; Ruigrok, 2003; Voogd and Glickstein, 1998; Wu et al., 1999). Additionally, several molecular markers exhibit parasagittal expression in the cerebellum. The most extensively studied in this regard is zebrin II (ZII). The ZII antibody recognizes the 36-kDa metabolic isoenzyme aldolase C and is expressed exclusively by PCs (Ahn et al., 1994; Brochu et al., 1990; Hawkes and Herrup, 1995). ZII is expressed heterogeneously such that bands of high ZII expression (ZII+) are interdigitated with bands of little to no ZII expression (ZII-) (Figure 2.1). ZII stripes are seen in several mammalian (Armstrong and Hawkes, 2000; Leclerc et al., 1992; Marzban et al., 2003, 2015; Marzban and Hawkes, 2011; Ozol et al., 1999; Sanchez et al., 2002; Sillitoe et al., 2003a, 2003b) and avian species (Corfield et al., 2015, 2016; Iwaniuk et al., 2009; Marzban et al., 2010; Pakan et al., 2007; Vibulyaseck et al., 2015), as well as in one genus of lizards (Wylie et al., 2016). The prevalence of ZII stripes across various species suggests that the role for ZII is highly conserved and is likely crucial to cerebellar function. Several studies have examined the relationship between ZII stripes and the aforementioned aspects of sagittal cerebellar organization (Akintunde and Eisenman, 1994; Chockkan and Hawkes, 1994; Gao et al., 2006; Gravel and Hawkes, 1990; Hawkes and Gravel, 1991; Ji and Hawkes, 1994; Matsushita et al., 1991; Mostofi et al., 2010; Paukert et al., 2010; Pijpers et al., 2006; Ruigrok et al., 2008; Sugihara, 2011; Sugihara et al., 2007; Sugihara and Quy, 2007; Sugihara and Shinoda, 2004, 2007; Voogd et al., 2003; Voogd and Ruigrok, 2004; Wadiche and

Jahr, 2005; Zhou et al., 2014).

In the pigeon vestibulocerebellum (VbC), we have shown that the ZII stripes coincide with functional properties of PCs and afferent inputs (Graham and Wylie, 2012; Pakan et al., 2010, 2011, 2014; Pakan and Wylie, 2008; Wylie et al., 2013, 2017). The avian VbC, which consists of folia IXcd and X, contains PCs whose complex spike activity (CSA) are responsive to optic flow patterns resulting from self-motion (Wylie and Frost, 1991). Optic flow results from visual motion occurring across the entire retina, and is important for many behaviours such as navigating, controlling posture and locomotion, and perceiving self-motion. The pathways that are involved in optic flow processing originate from retino-recipient nuclei in the pretectum and the accessory optic system and reach the medial column of the inferior olive (mcIO), which innervates the vestibulocerebellar optic flow zones (for review see Wylie 2013). The functional organization of the optic flow zones is shown in Figure 2.1 (Graham and Wylie, 2012; Pakan et al., 2011; Wylie, 2013). There are seven ZII+/- stripe pairs in IXcd (P1+/- to P7+/-), but all PCs in X are ZII+ (Pakan et al., 2007). Nonetheless, the optic flow zones span both folia. In the lateral aspect of the VbC, the flocculus, PC CSA responds best to optic flow resulting from self-rotation about either the vertical axis (VA), or an horizontal axis (HA) (Wylie and Frost, 1993). The flocculus contains two VA zones interdigitated with two HA zones. The VA zones correspond to ZII stripes P4+/– and P6+/-, whereas the HA zones correspond to the P5+/- and P7+/- stripes (Pakan et al., 2011). In the medial VbC, the ventral uvula (IXcd) and nodulus (X), PC CSA responds to patterns of optic flow resulting from self-translation, while the dorsal uvula is not modulated by optic flow stimuli (Wylie et al., 1993, 1998). Within the ventral uvula and nodulus, there are four types of neurons organized into three sagittal zones (Graham and Wylie, 2012). In the most medial zone, which spans P1+ and the medial half of P1- (P1-med), PCs

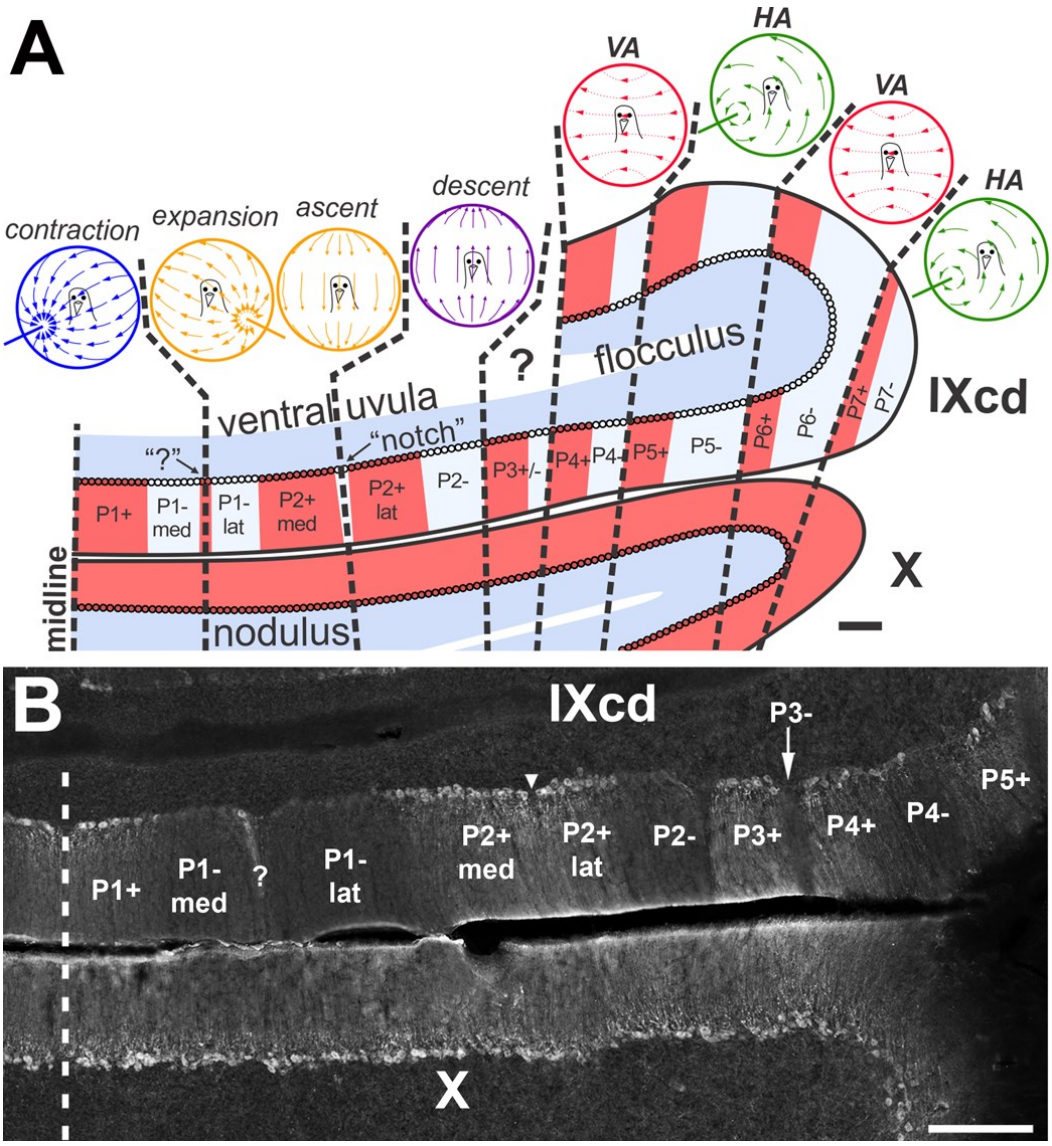

Figure 2.1 Vestibulocerebellar optic flow zones and zebrin II immunolabelling. A shows the optic flow zones and zebrin II (ZII) pattern in the pigeon vestibulocerebellum (VbC). A coronal section through the VbC (folia IXcd and X) is depicted. The alternating ZII+ (red) and ZII- (pale blue) stripes are numbered from P1+/- most medially to P7+/- laterally, with ZII+ and ZII– stripes alternating. **B** is a photomicrograph of ZII immunoreactivity through a caudal section of IXcd showing stripes P1+ through P5+. P1– is bisected by a satellite ZII+ band designated "?", dividing the stripe into medial and lateral halves (P1-med; P1-lat). P2+ is

divided by a ZII– "notch", indicated by the inverted triangle in **B** (Wylie et al., 2007). In the uvula, the optic flow zones from medial to lateral are as follows: contraction zone (P1+/P1–med); expansion/ascent zone (P1–lat/P2+med); descent zone (P2+lat/P2–) (Graham and Wylie, 2012). Purkinje cells (PCs) in the flocculus zones respond optic flow resulting from rotation about either the vertical axis (VA) or an horizontal axis (HA). There are two VA zones, spanning P4+/- and P6+/-, interdigitated with two HA zones, spanning P5+/- and P7+/- (Pakan et al., 2011). PCs in the P3+/- stripe do not respond to optic flow stimuli and their function is unknown (Graham and Wylie, 2012). The sagittal organization of the optic flow zones extend into the nodulus (folia X), although all PCs are ZII+ (Graham and Wylie, 2012; Pakan et al., 2007, 2011, 2014; Pakan and Wylie, 2008). Scale bars = 200 μm in **A**, 300 μm in **B**.

respond to “contraction” optic flow; i.e. optic flow resulting from backward translation. Adjacent to this is a zone that spans the lateral half of the P1- stripe (P1-lat) and the medial half of P2+ (P2+med). (The P1- stripe is bisected by a thin ZII+ stripe 1-3 PCs in width (see “?” in Figure 2.1B). Similarly the P2+ stripe is bisected by a thin a notch that contains no PCs (see inverted triangle in Figure 2.1B)(Pakan et al., 2007). Intermingled in this zone are two types of optic flow PCs: either “expansion” optic flow, or optic flow resulting from “ascent” (i.e. upward translation). Finally, lateral to this and spanning the lateral half of P2+ (P2+lat) and the P2- stripe, is a zone containing neurons responsive to optic flow resulting from “descent”. Previously we have shown that the inputs to the ZII+ and ZII- stipes in the flocculus (i.e., stripes P4+/- to P6+/-) receive climbing fibre input from separate, but adjacent areas of the inferior olive (IO) (Wylie et al., 2017). The ZII+ stipes within the VA zones (P4+ and P6+) receive input from the caudal-most portion of the mcIO while the ZII- stripes of the VA zones (P4- and P6-) are innervated by a slightly more rostral region of the mcIO. Similarly, the ZII+ stripes of the HA zones are innervated by a more caudal region of the mcIO than the ZII- stripes of the HA zone, which are innervated by the rostral-most mcIO (Wylie et al., 2017). Thus, although a ZII+/- stripe pair represents a functional unit in the flocculus whereby all PCs respond to the same pattern of optic flow (either VA or HA), the ZII+ and ZII- stripes receive optic flow from different areas of the IO. In the present study we sought to determine if the same scheme holds true for the ventral uvula.

2.1 Materials and Methods

2.1.1 *Surgical procedure and tracer injection*

The methods used adhere to the guidelines established by the Canadian Council on Animal Care and were approved by the Biosciences Animal Care and Use Committee at the University of Alberta. Twelve rock pigeons (*Coulmba livia*) of either sex, obtained from a local supplier, were anesthetised with an intramuscular injection of a ketamine (65mg/kg) and xylazine (8mg/kg) cocktail. Supplemental doses were administered as necessary. Animals were placed into a stereotaxic device, and their heads stabilized with pigeon ear bars and a beak bar adapter so that the orientation of their skull conformed to the atlas of Karten and Hodos (1967). Sufficient bone and dura were removed to allow access to the uvula with vertical penetrations. To localize the desired ZII stripe for injection of retrograde tracer (CTB; Cholera Toxin Subunit B), responses of PC CSA to visual stimuli were obtained using extracellular recording techniques. Glass micropipettes with tip diameters of 3-5 µm, filled with 2 M NaCl were advanced through the brain into the uvula using a hydraulic microdrive (Frederick Haer). Extracellular signals were then amplified, filtered, and fed through a window discriminator to record isolated PC CSA. The signal from the widow discriminator was fed to an oscilloscope and an audio monitor. The visual stimulation procedure has been described in detail elsewhere (Graham and Wylie, 2012). Briefly, the optic flow preference of the CSA was qualitatively determined by moving a large (90X90°) handheld visual stimulus, consisting of black bars, wavy lines and dots on a white background, in various directions throughout the visual field. Several recording tracts were made such that we could obtain a rough map of the locations of the optic flow zones in the uvula, and thus the presumed locations of the ZII stripes in the uvula (Figure 2.1A). Once the desired ZII stripe was located, the recording electrode was replaced with a

micropipette (tip diameter 20-30 μm) filled with a retrograde tracer: fluorescent Cholera Toxin Subunit B (CTB; 1% in 0.1M PB); either CTB-Alexa Fluor 488 (green) or 594 (red) conjugate (ThermoFisher Scientific). CSA was again recorded with the injection micropipettes to ensure injection in the desired ZII stripe. CTB was iontophoressed over a 7 minute period, at +5 μA, for 7 seconds on, 7 seconds off, and so on. In some cases, we repeated this procedure to inject the adjacent ZII stripe using the CTB opposite in colour to that used in the first injection.

2.1.2 *Post-surgery, recovery and perfusion*

After surgery, the craniotomy was filled with bone wax, and the wound was sutured. An intramuscular injection of buprenorphine (0.012mg/kg) was given as an analgesic. Animals were left to recover for 5 days, allowing the retrograde tracer time to travel to the mcIO. After the recovery period, the animals were deeply anaesthetized with sodium pentobarbital (100mg/kg) and a transcardial perfusion with phosphate buffered saline (PBS; 0.9% NaCl, 0.1 M phosphate buffer) followed by 4% paraformaldehyde in 0.1 M PBS (pH 7.4) was performed. The brains were extracted from the skull and immersed in paraformaldehyde for between 2 to 7 days at 4°C. The brains were then placed in 30% sucrose in 0.1M phosphate buffer until they sank (48-72 hours). They were subsequently embedded in gelatin and cryoprotected in 30% sucrose in 0.1M PBS overnight. The gelatin-embedded brains were frozen and sliced into 40 μm thick coronal sections using a sliding microtome. Sections were collected in three series through the rostro-caudal extent of the cerebellum and the brainstem. Sections were stored in 0.1M PBS (pH 7.4) between sectioning and immunohistochemistry.

2.1.3 *Immunohistochemistry*

ZII immunohistochemistry was used to verify the locations of CTB injections. The sections containing injection sites in the uvula were processed for ZII expression. Tissue was rinsed thoroughly with 0.1 M PBS, then blocked with 10% normal donkey serum (Jackson Immunoresearch Laboratories, West Grove, PA) and 0.4% Triton X-100 in PBS for 1 hour to block non-specific binding of antibody. Tissue was then incubated in PBS containing 0.1% Triton X-100, and the primary antibody, anti-zebrin II/aldolase C (1:1000, goat-polyclonal, sc-12065, Santa Cruz Biotechnologies, Santa Cruz, CA) for 120 hours at 4°C. After primary antibody incubation, sections were rinsed in 0.1 M PBS and incubated in a fluorescent secondary; either AlexaFluor 594 or 488 anti-goat antibody (1:200, Jackson Immunoresearch Laboratories, West Grove, PA) in PBS, 2.5% normal donkey serum, and 0.4% Triton X-100 for 3 hours at room temperature. In cases of a single injection, the secondary antibody used was the color opposite to that of the CTB (i.e., red CTB, green secondary; green CTB, red secondary). In cases where both CTB colors were injected, the red and green secondary was used on alternate sections. The tissue was then rinsed five times in 0.1 M PBS and mounted onto gelatinized slides for viewing.

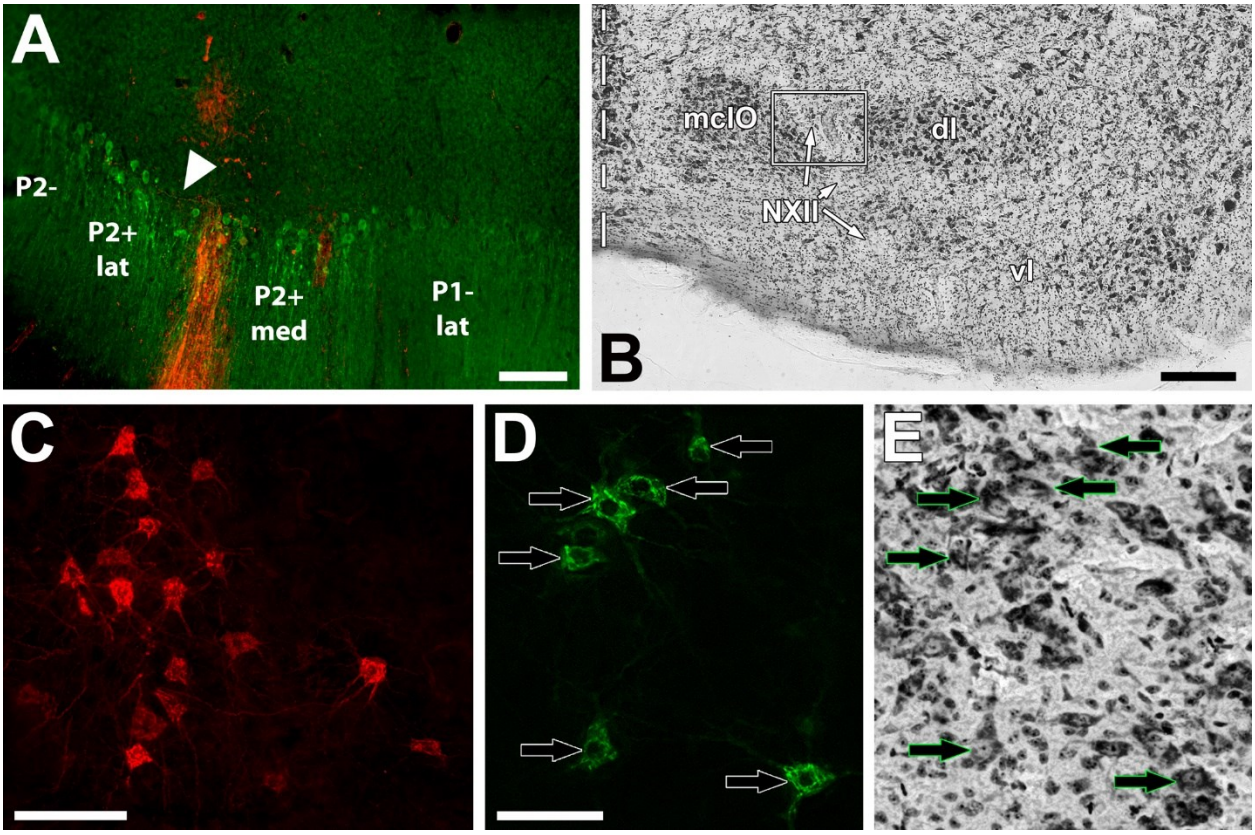

Figure 2.2 CTB injection example and retrograde labelled cells. A shows an example of a CTB injection site (red) in a section immunoprocessed for ZII (green; i.e., Alexafluor 488 secondary antibody). The injection was in the P2+med stripe of the uvula. The triangle indicates the ZII- notch separating the P2+med and P2+. **B** shows a thionine-stained section through the inferior olive showing the three subdivisions: medial column (mcIO), ventral lamella (vl) and dorsal lamella (dl). The course of the twelfth nerve (NXII) is through the lateral part of mcIO. The white box indicates the general region where retrograde labelled cells were found from injections in the uvula. The inset shows a coronal cross section through the medulla and the red box indicates the region where the olive is found. **C** and **D**, respectively, show retrograde labelled cells from red and green CTB injections. **E** shows the same section as in **D** subsequently

stained with thionine. Arrows in **D** and **E** indicate corresponding neurons. Scale bars = 200 μm in **A**; 250 μm in **B**; 100 μm in **C**; 50 μm in **D**.

2.1.4 *Microscopy and image analysis*

Sections were viewed with a compound light microscope (Leica DMRE, Richmond Hill, ON) equipped with TX2 (red) and L5 (green) fluorescence filters. Images were captured with a Retiga EXi *FAST* Cooled Mono 12-bit camera (QImaging, Burnaby, BC) using OpenLAB imaging software (Improvision, Lexington, MA). Adobe Photoshop (San Jose, CA) was used to adjust contrast and brightness.

Injection site location was confirmed using ZII immunohistochemistry and was mapped out to determine the location of tracer within the stripes (Figure 2.2A; Figure 2.3). For two out of three series, we measured the distance from the midline to the borders of each ZII stripe as well as the distance from the midline to the injection site borders. This allowed us to plot the injection site map as seen in Figure 2.3. Using Adobe Photoshop, we calculated the percentage of tracer in each ZII stripe for the cases where the injection spanned different ZII stripe signatures (Table 2.1). To do so, we selected portions of the injection in different stripes from our reconstruction (Figure 2.3) and used a measurement function to provide dimensions for the area selected.

Images were obtained of all sections containing retrogradely labelled IO neurons (Figure 2.2C,D). Subsequently, for one of the three series, the sections were Nissl-stained with thionine to allow visualization of the IO and other nuclei in the brainstem (Figure 2.2E). The thionine-stained sections were imaged, and the respective fluorescent images were overlaid onto the thionine images using Adobe Photoshop, to determine the location of the fluorescing cells within the IO (Figure 2.2D,E). For comparison of the locations of retrograde labelled mcIO cells across cases, sections were overlaid and aligned using several landmarks including: the caudal and rostral tips of the IO, the midline of the brain, the separation point of the ventral and dorsal lamella of the IO, and the course of the hypoglossal nerve (NXII).

Stripe case	P1+	P1-med	P1-lat	P2+med	P2+lat	P2-
Uv01 grn	**G* 61** *(100%)*					
Uv01 red		**R 44** *(100%)*				
Uv12 red	**R* 95** *(100%)*					
Uv12 grn		**G 118** *(63%)*	(*37%)*			
Uv07		*(43%)*	**G 60** *(57%)*			
Uv06 red		*(16%)*	**R 61** *(84%)*			
Uv06 grn				**G 26** *(100%)*		
Uv08			**G 61** *(100%)*			
Un05			**R 19** *(100%)*			
Uv02				**R 29** *(100%)*		
Uv16				**R 61** *(99%)*		
Uv11					**R 57** *(100%)*	
Uv13					**R 88** *(100%)*	
Un07					*(16%)*	**G 88** *(84%)*
Uv04						**R 99** *(100%)*

Table 2.1 Summary of uvular injections by zebrin II stripe. **R** and **G** indicate injections of red and green CTB, respectively. (* indicates bilateral labelling). The number of retrogradely labelled cells in the medial column of the inferior olive (mcIO) is indicated in bold. Beside in parentheses, the proportion (in %) of the area of the injection site in each stripe is indicated.

2.2 Results

The results are based on twelve animals in which we injected red and/or green fluorescent CTB into either a positive or negative stripe of a functional ZII stripe pair. A typical injection site is shown in Figure 2.2A. The location of each injection in relation to the ZII stripes was reconstructed from serial sections and plotted in Figure 2.3. Note that some of these injections extended across the border of a ZII stripe. Using *Adobe Photoshop,* we were able to measure the proportion (in percent) of the injection in the targeted ZII stripe as well as the spread into adjacent stripes. For each case, this is indicated in Table 2.1, along with the total number of retrograde labelled cells in the mcIO. In nine animals, a single CTB injection (red or green) was considered, whereas in three animals, there were two injections of different colours.

The pigeon IO can be divided into three regions; the ventral lamella (vl), the dorsal lamella (dl), and the medical column (mcIO) (Arends and Voogd, 1989) (Figure 2.2B). From all injections, retrograde labelling was found in the lateral margin of contralateral mcIO often within the genu of the XIIth nerve (Crowder et al., 2000; Lau et al., 1998) (Figure 2.2B). This region is immediately lateral to that which provides CF input to stripes P4+/- to P7+/- in the flocculus (Wylie et al., 1999, 2017). The average number of retrograde labelled mcIO cells from each injection was 64.5±7.4 (mean±sem). Photomicrographs of retrograde labelled cells in the mcIO are shown in Figure 2.2C,D. Retrograde labelled olivary cells were confined to separate regions depending on the injection site location (Figures 2.4-2.6). For each optic flow zone, we describe the distribution of retrograde labelled cells in term of their rostro-caudal relationship. Broadly speaking however, labelled cells in the rostral regions of the mcIO are generally located ventrally, while cells in caudal mcIO regions are distributed more dorsally.

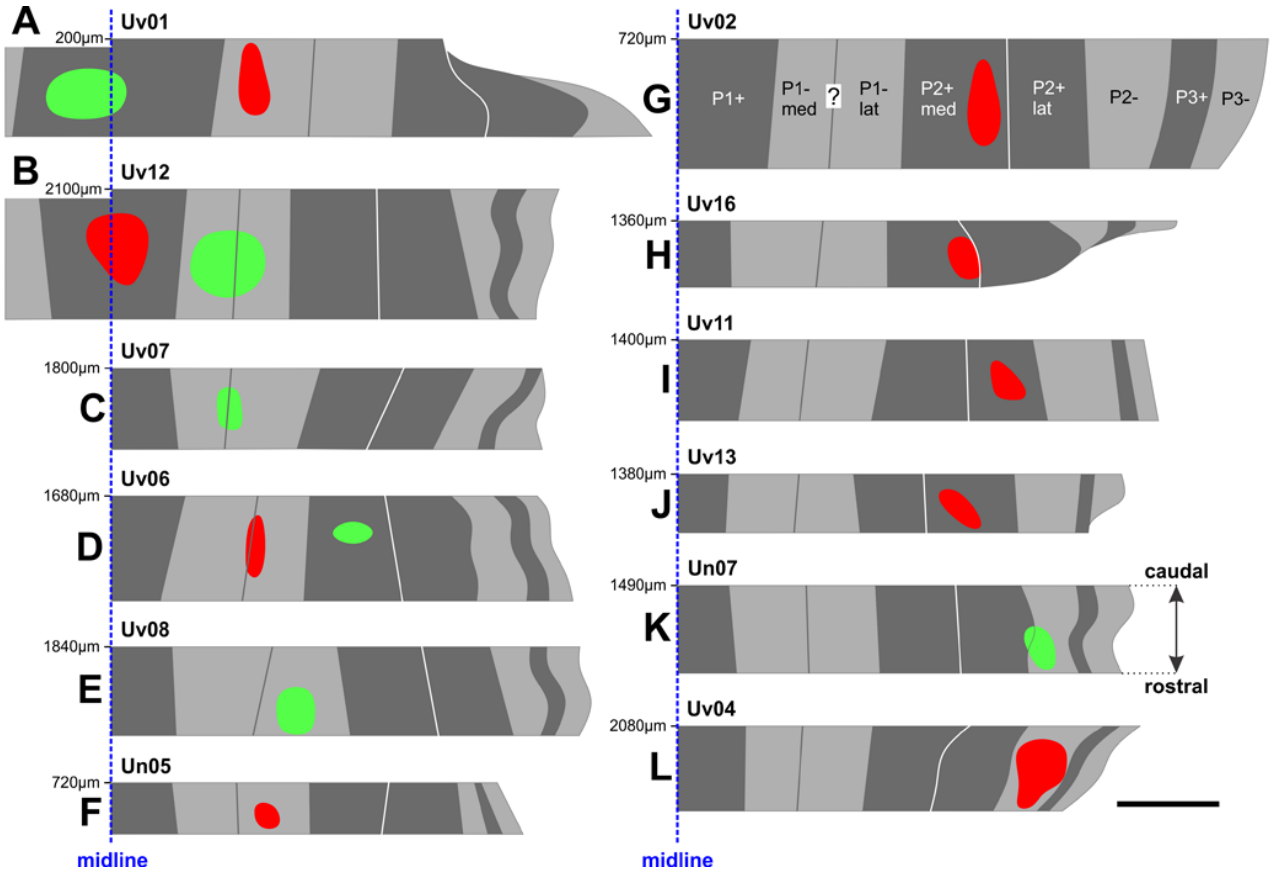

Figure 2.3 Injection site reconstruction. The locations of all CTB injection sites in the ventral uvula were reconstructed from serial coronal sections. The colour of the injection site indicates the colour of CTB injected (red or green). Injection sites are shown from most medial in **A** and **B** (P1+) to most lateral in **K** and **L** (P2–). For each case, the distance (in µm) of the caudal-most section (i.e., top) from the posterior pole of IXcd is indicated. For example, the injections in case Uv01 **(A)** were located about 2 mm posterior to those in case Uv12 **(B)**. The midline is represented as a dashed blue line. See Table 1 for a detailed account of each injection site. Scale bar = 500 µm.

The illustrated sections represent every third collected section and are 120 μm apart. In each section, the locations of retrograde labelled cells from adjacent sections are superimposed. In other words, in each section, the retrograde labelled cells in that section are shown, plus those from the sections 40 μm caudal and 40 μm rostral.

2.2.1 *Contraction zone; P1+ vs. P1–med*

There were two injections in P1+ (Uv01, Uv12; Figure 2.3A,B), both of which crossed the midline and resulted in bilateral labelling in mcIO. There was one injection confined to P1-med (Uv01) and two other cases where P1-med was targeted, but the injection was clearly spread into P1-lat (Uv12, Uv07; Figure 2.3A-C, see also Table 2.1). The resultant retrograde labelling from these cases is shown in Figure 2.4. In this, and subsequent Figures 2.5 and 2.6, the retrograde labelling is shown on ten sections through the caudal-rostral extent of the IO, each 120 μm apart. In each section, the locations of retrograde labelled cells from adjacent sections are also superimposed. In other words, in each section, the retrograde labelled cells in that section are shown, plus those from the sections 40 μm caudal and 40 μm rostral. In Figures 2.4A and B (Uv01, Uv12) the locations of retrograde labelled IO neurons from the P1+ injections are shown as dark blue. As these injections were bilateral, the labelling in the right IO has been superimposed on the left IO. From both cases, most of the labelling was clustered caudally, in sections A_2/B_2, A_3/B_3 and B_4. The retrograde labelling from the P1-med injection (Uv01), shown as light blue, was found more rostrally, mainly in sections A_4 and A_5. Labelling from the two injections that spanned the P1-med and P1-lat stripes (Uv12, Uv07; light blue dots with yellow centres) was also found at this rostro-caudal level ($B_{4,5}/C_{4,5}$), but also spread more rostrally ($B_{6-8}/C_{6,7}$).

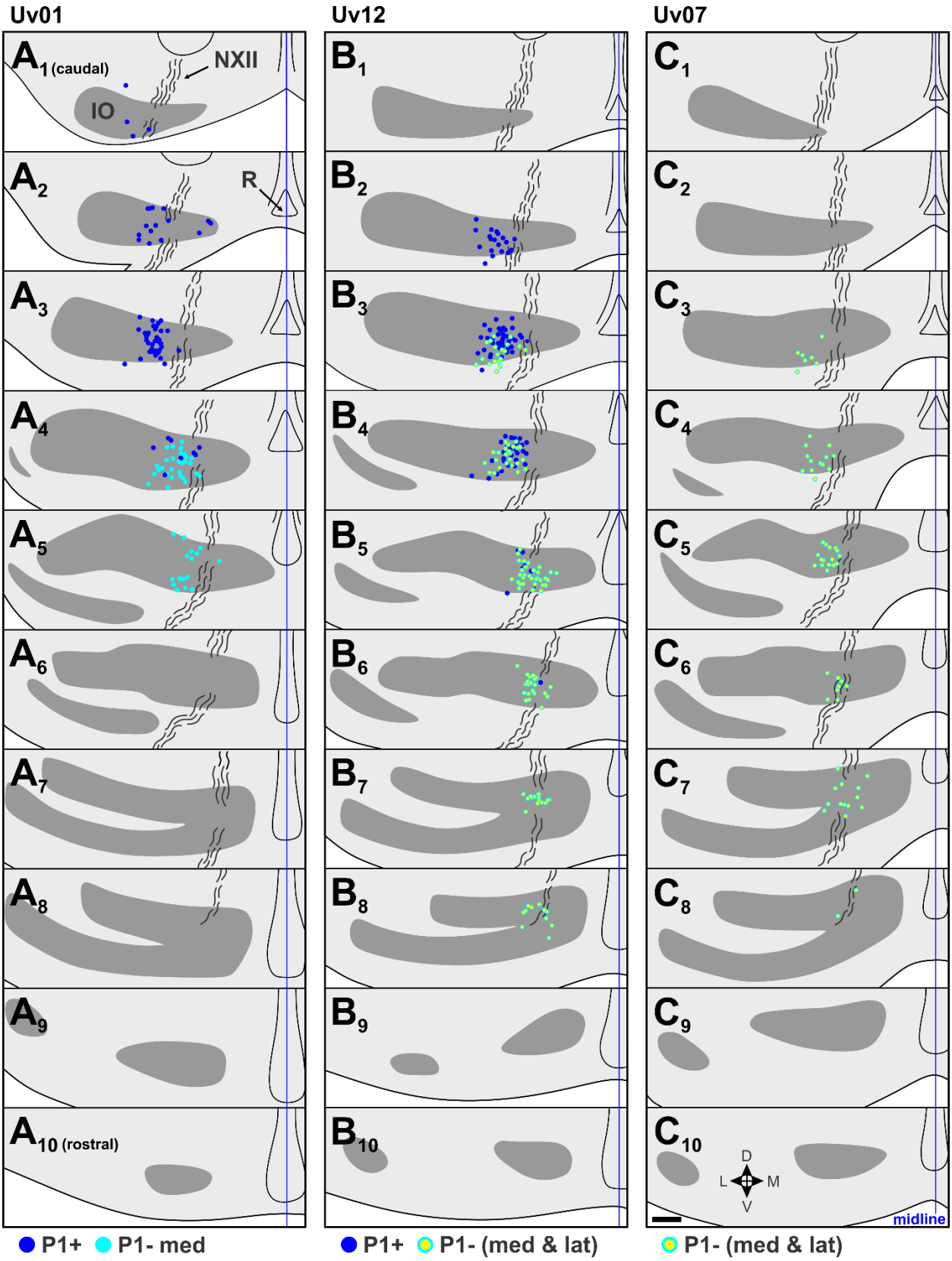
Uv01
Uv12
Uv07
A1 (caudal)
NXII
IO
A2
R
A3
A4
A5
A6
A7
A8
A9
A10 (rostral)
B1
B2
B3
B4
B5
B6
B7
B8
B9
B10
C1
C2
C3
C4
C5
C6
C7
C8
C9
C10
D
L
M
V
midline
P1+
P1- med
P1+
P1- (med & lat)
P1- (med & lat)

Figure 2.4 Retrograde labelling in the inferior olive (IO) from selected P1+ and P1– injections in the contraction zone of the ventral uvula (see Fig. 3). **A**, **B** and **C**, respectively, show the retrograde labelling from cases Uv01, Uv12 and Uv07. For each, 10 coronal sections through the inferior olive from 1 series (of 3) are shown, from caudal (top, **1**) to rostral (bottom, **10**), 120 µm apart. For each section, labelled cells from that section are shown, as well as labelled cells from adjacent sections: i.e., retrograde labelling is superimposed from three consecutive 40µm sections. The IO is represented by grey shading, and the curvy black lines represent the course of the hypoglossal nerve (NXII). Dark blue dots represent retrograde labelled cells from the P1+ injections (**A** and **B**), light blue dots represent those from the P1– med injection **(A)**, and light blue dots with yellow centers represent cells labelled from the injections that included both the medial and lateral halves of P1- (P1-med and P1-lat). d = dorsal, v = ventral, m = medial, l = lateral, R = raphe nucleus. Scale bar = 200 µm.

From these data, we conclude that the IO cells projecting to the P1-med stripe are immediately rostral to those projecting to the P1+ stripe.

2.2.2 *Expansion/ascent zone; P1–lat vs. P2+med*

The location of injection sites in the expansion/ascent zone are shown in Figure 2.3D-H. Case Uv06 included injections in both the P1-lat and P2+med, although the P1-lat injection spread slightly to the P1-med stripe (Table 2.1). Two other cases included a single injection in P1–lat (Uv08, Un05), and two others targeted the P2+med stripe (Uv02, Uv16). There was minimal spread to the P2+lat stripe in case Uv16. The retrograde labelling from case Uv06 is shown in Figure 2.5A, where those cells labeled from the P1-lat and P2+med injections are shown as yellow and orange dots, respectively. Labelling from the P1-lat injection was concentrated in the sections A_6 and A_7. (This is consistent with the labelling in Figure 2.4B,C which spanned the P1-med and P1-lat stripes). We suspect the sparse labelling found caudally may be due to spread of the injection into the P1-med stripe. Cells labelled from the P2+ injection were concentrated more rostrally in the sections A_7 and A_8. In Figure 2.5B, the labelling from all 5 cases involving injections in P1-lat and P2+med has been collapsed onto a single idealized series. Although there is some overlap in section B_7, the labelling from the P1-lat injections is clearly caudal to that from the P2+med injections.

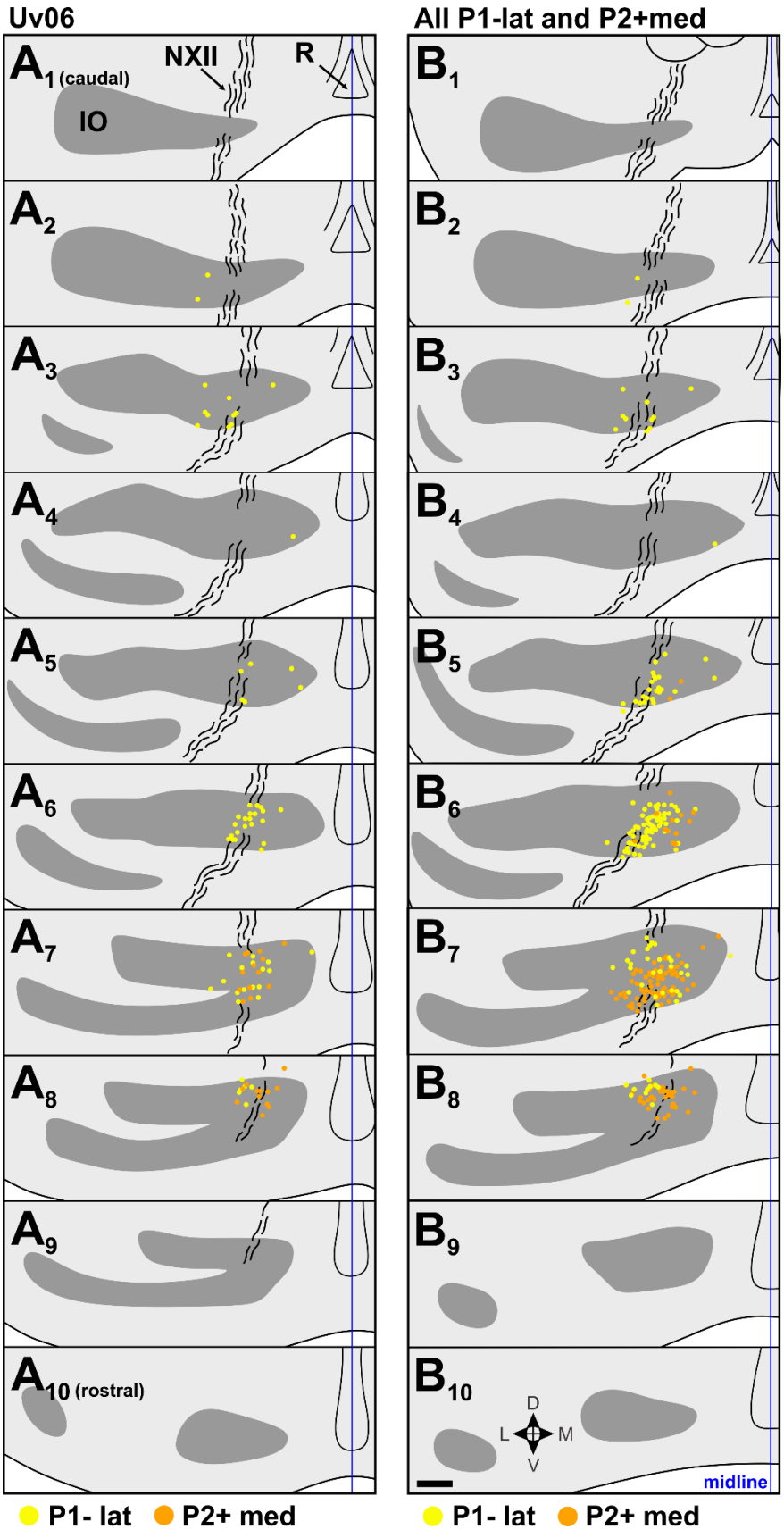
Uv06
All P1-lat and P2+med
A1 (caudal)
NXII
R
IO
A2
A3
A4
A5
A6
A7
A8
A9
A10 (rostral)
B1
B2
B3
B4
B5
B6
B7
B8
B9
B10
D
L
M
V
midline
P1- lat
P2+ med
P1- lat
P2+ med

Figure 2.5 Retrograde inferior olive (IO) labelling from injections in the expansion/ascent optic flow zone. A shows labelled cells from case Uv06, and **B** shows labelling from all injections in P1-lat and P2+med collapsed onto an idealized series (cases Uv06, Uv08, Un05, Uv02, Uv16; see Fig. 3D-H and Table 1). The locations of labelled cells from injections in P1-lat and P2+med are represented by yellow and orange dots, respectively. See caption to Figure 4 for additional details. Scale bar = 200 μm.

2.2.3 ***Descent zone; P2+lat vs. P2–***

Figure 2.3I-L shows the location of injection sites in the descent zone. Two injections were aimed at the P2+lat stripe (cases Uv11, Uv13), and two were aimed at the P2- stripe (cases Uv04, Un07). The injection in Un07 was the only one of these that showed spread to an adjacent stripe (84% in P2-, 16% in P2+lat; Table 2.1). Retrograde labelling (dark purple dots) from case Uv13 (P2+lat) is shown in Figure 2.6A, where the bulk of the labelled cells lie in sections A_7-A_9. The retrograde labelling (light purple) from the Un07 injection (P2-) is shown in Figure 2.6B, with the bulk of the labelling in sections B_8-B_{10}. Figure 2.6C depicts the retrograde cell labelling involving all injections in P2+lat and P2- collapsed onto a single series, showing that labelling from the P2+lat injection is caudal to that from the P2- injection. Note that the cells labelled from the P2- cells tended to lie ventral to that from the P2+lat injections (Figure 2.6C_8,C_9).

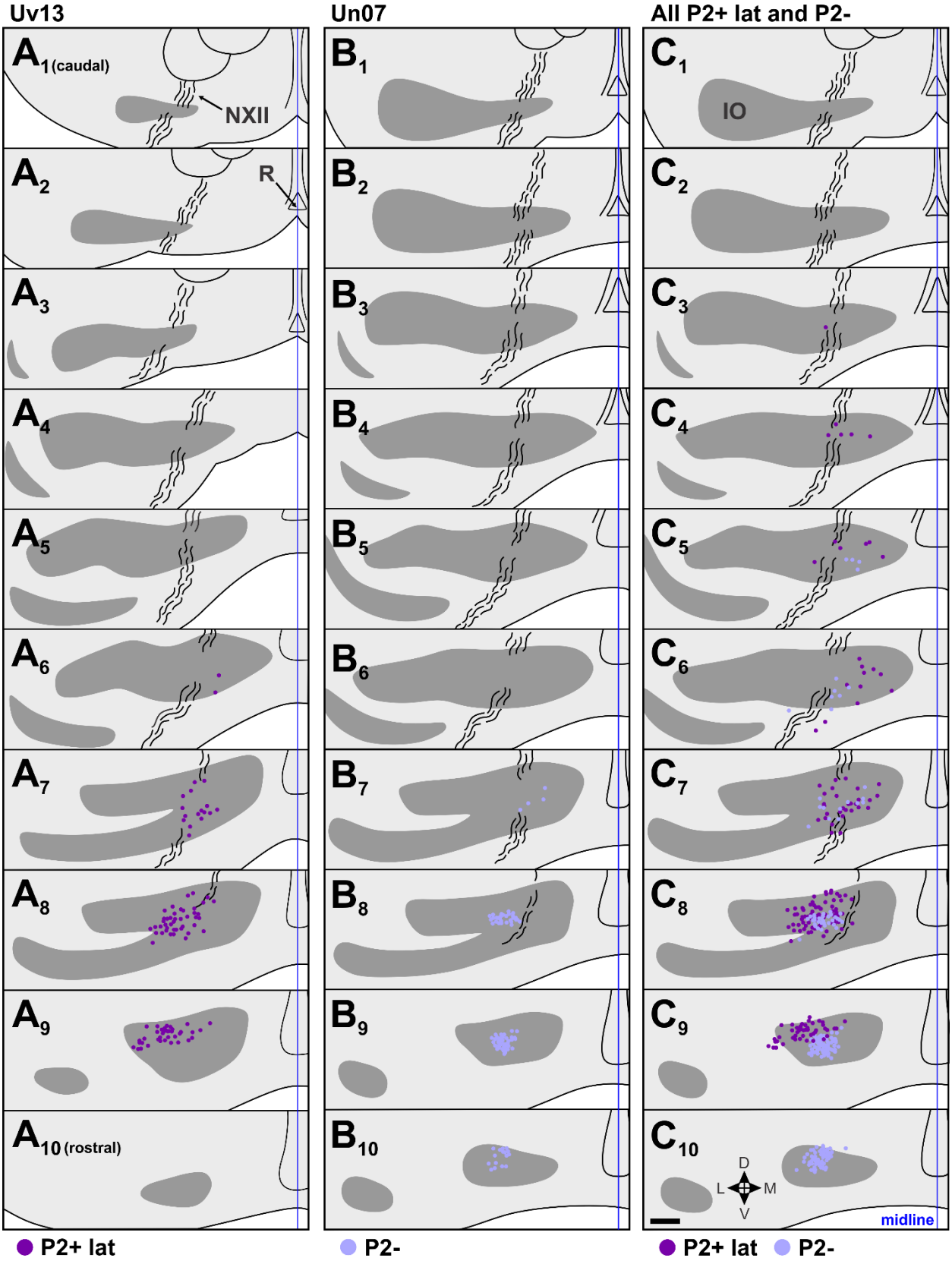
Uv13
Un07
All P2+ lat and P2-
A1 (caudal)
NXII
A2
R
A3
A4
A5
A6
A7
A8
A9
A10 (rostral)
B1
B2
B3
B4
B5
B6
B7
B8
B9
B10
C1
IO
C2
C3
C4
C5
C6
C7
C8
C9
C10
D
L
M
V
midline
P2+ lat
P2-
P2+ lat
P2-

Figure 2.6 Retrograde inferior olive (IO) labelling from injections in the descent optic flow zone. A and **B** show the locations of retrogradely labelled cells in the IO from cases Uv13 and Un07, respectively. **C** shows the labelling from all injections in P2+lat and P2- collapsed onto an idealized series (cases Uv11, Uv13, Un07, Uv04; see Fig. 3I-L and Table 1). The locations of labelled cells from injections in P2+lat and P2- are represented by dark purple and light purple dots, respectively. See caption to Figure 4 for additional details. Scale bar = 200 μm.

2.2.4 *Analysis of rostro-caudal differences of retrograde labelled cell distribution in the mcIO*

The data illustrated in Figures 2.4-2.6 suggest that there are rostro-caudal differences in retrograde labelling from injections in each of the ZII+ and ZII- stripes in the uvula. Figure 2.7 shows quantitative support for this claim, where the location of retrograde labelled cells in mcIO are projected onto an horizontal plane for all injections except for the two injections that spanned both P1-med and P1-lat (i.e., green injections in Uv12 and Uv07; Figure 2.3B,C). The bulk of the labelling from the P1+stripe was located 700-1000 μm lateral to the midline and 100-300 μm from the caudal tip of mcIO. The labelling from the P1-med injection was rostral and slightly medial to this (350-450 μm from the caudal tip; 600-800 μm from the midline; Figure 2.7A). The bulk of the retrograde labelling from the P1-lat stripe was 500-750 μm from the midline and 500-750 μm from the caudal tip, whereas that from the P2+med injections was rostral to this, 700-800 μm from the caudal-tip (Figure 2.7B). Finally, shown in Figure 2.7C, the bulk of the labelling from the P2+lat injections was found 650-950 μm from the midline, 750-1000 μm from the caudal tip, whereas the labelling from the P2- stripe was slightly rostral to this, 900-1100 μm from the caudal tip. All of these data are summarized in Figure 2.7D, where 80% confidence ellipses were fit to these distributions using the *ggplot2* package in R (v 3.3.2; R core Team, 2016). Included in this are the distributions of the mcIO cells projecting to the ZII stripes in the flocculus (P4+/- to P7+/-, from Wylie et al., 2017).

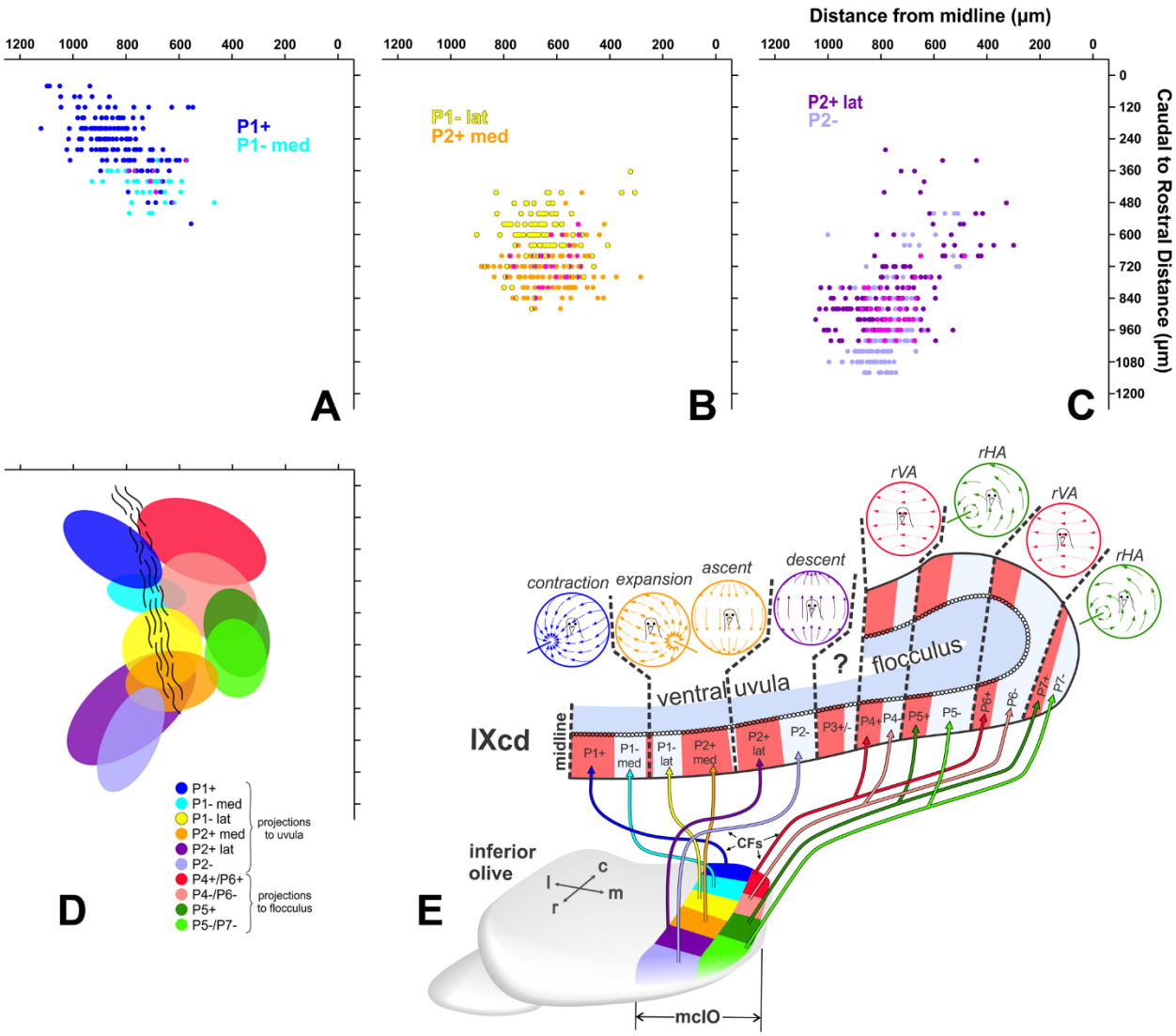

Figure 2.7 Retrograde labelled cell distribution and CF projections to the VbC.

A-D: Reconstructions of retrograde labelling in the medial column of the inferior olive (mcIO) as projected onto the horizontal plane. These were reconstructed from serial sections 40 µm apart in the rostro-caudal dimension (y-axes) and the distance of each retrogradely labelled cell from the midline was measured (x-axes). **A** shows retrograde labelled olive cells from injections in P1+ (dark blue; cases Uv01 green CTB injection, Uv12 red CTB injection; see Fig. 3) and P1– med (light blue; Uv01 red injection) stripes. **B** shows retrograde labelling from injections in P1–

lat (yellow; Uv06 red, Uv08, Un05) and P2+med (orange; Uv06 green, Uv02, Uv16). **(C)** shows retrograde labelling from injections in P2+lat (dark purple; Uv11, Uv13) and P2– (light purple; Un07, Uv04). The magenta in **A-C** represents overlap. **D** shows 80% confidence ellipses that fit these six distributions. In addition, the regions that project to the ZII stripes in the flocculus (P4+/- to P7+/-) are shown based on data from Wylie et al. (2017). **E** shows a schematic of the climbing fibre (CFs) projections from each region of the mcIO to the ZII stripes in the optic flow zones in folium IXcd. d = dorsal, v = ventral, m = medial, l = lateral.

2.3 Discussion

Studies of the pigeon VbC have previously shown that a ZII+/- stripe pair represents a functional unit insofar as the response of PC CSA to optic flow stimuli is consistent within a ZII+/- stripe pair (Graham and Wylie, 2012; Pakan et al., 2011) (see Figure 2.7E). In the present study we showed that ZII+ and ZII- stripes within each functional unit in the uvula receive input from different, although adjacent areas of the mcIO. This is depicted in the schematic in Figure 2.7E. The projection to the uvula arises from the lateral mcIO, which can be divided into six rostro-caudal regions. The contraction zone receives input from the caudal-most lateral mcIO en masse, but the P1+ zone receives input from the most caudal end (dark blue), while the P1–med zone receives input from a slightly more rostral region (light blue), as well as slightly more medial region (Figures 2.4,2.7A). The expansion/ascent zone is innervated by the middle lateral mcIO en mass, but the region projecting to the P1–lat stripe (yellow) is caudal to that projecting to the P2+med stripe (orange). Finally, the descent zone is innervated by the rostral lateral mcIO en mass, but the projections to P2+lat arises from a region of the mcIO (dark purple) that is slightly more caudal to that region innervating the P2- stripe (light purple). Note that the region innervating the P2- stripe is slightly ventral to that innervating the P2+lat stripe (Figure 2.6C_8, C_9). Also included in the schematic in Figure 2.7E is the projection from the medial mcIO to the ZII stripes in the flocculus (Wylie et al., 2017). It is similar insofar as the input to the ZII- and ZII+ functional zones arises from adjacent rostro-caudally separated regions in the mcIO. However, each of these regions innervates two stripes. For example, there are two VA zones in the flocculus, spanning stripes P4+/- and P6+/-. The most caudal region of the medial mcIO (red) innervates both the P4+ and P6+ stripes, whereas an area immediately rostral to this (pink) innervates the P4- and P6- stripes.

From work mostly in rodents, it is generally stated that that a particular olivary subnucleus innervates either ZII+ or ZII- stripes, but not both (Pijpers et al., 2006; Sugihara and Quy, 2007; Sugihara and Shinoda, 2004; Voogd et al., 2003; Voogd and Ruigrok, 2004). However, it is often adjacent subnuclei that project to adjacent ZII+ and ZII- stripes. For instance, Sugihara and Shinoda (2004) found that ZII+ stripes a+ and 2+ of the rat anterior vermis receive CF afferents from subnucleus c of the caudal medial accessory olive, while ZII- stripes a- and 2- receive input from the immediately adjacent subnucleus b. As olivary projections to ZII+ and ZII- regions arise from adjacent olivary nuclei in rodents, our scheme in which projections to different ZII stripe signatures arise from adjacent olivary regions is quite similar. It is possible that our six mcIO regions could exhibit different neurochemical properties and therefore be considered separate subnuclei (Vibulyaseck et al., 2015), but such divisions were not apparent in our thionine stained pigeon sections. Comparisons between the pigeon and mammalian IO must be approached with caution as the mammalian IO is complex and has more subdivisions than the avian IO. However, there are very clear comparisons that can be made between IO projections to the flocculus of mammals and pigeons. Floccular organization is strikingly similar in mammals and pigeons. As in pigeon, in rabbits, VA and HA zones interdigitate, and are innervated by separate olivary subnuclei (Voogd et al., 1996; Voogd and Wylie, 2004). In rats, rabbits, and cats, the caudal dorsal cap of the principal olive projects to the VA zones and the ventral lateral outgrowth and the rostral dorsal cap to HA zones (for review see Voogd et al., 1996). As such, these two areas in the IO of mammals can been considered analogous to the pigeon medial caudal mcIO and dorsal mcIO respectively, particularly as they also receive similar optic flow information and project to interdigitating floccular zones (For review, see Voogd and Wylie, 2004). Comparing the pigeon uvula to the mammalian uvula is not

as clear. In pigeons, the lateral caudal and rostral mcIO project to the lateral and medial uvula, respectively. In mammals, the β-nucleus and the dorsomedial cell column of the medial accessory olive project to the medial and lateral uvula, respectively. In this regard, these structures could be considered analogous in terms of their projection patters. However, the mammalian and avian uvula differ in terms of their optic flow response property organization. PC CSA in the pigeon uvula responds to translational patterns of optic flow (Graham and Wylie, 2012), while in rabbits, PC CSA responds vestibular sensory information (Shojaku et al., 1991; Barmack and Shojaku, 1992, 1995). As such, the seemingly analogous olivary structures between pigeons and mammals process different types of sensory information, and so are not analogous in this regard.

Not only do the ZII+ and ZII- stripes within a functional unit receive different olivary inputs, there is also some evidence showing that they have functional differences, despite the fact the CSA responds best to the same pattern of optic flow. First, PCs in ZII+ stripes likely project to different areas within the cerebellar and vestibular nuclei than PCs in ZII- stripes (Sugihara, 2011; Wylie et al., 2012). Second, it is likely that mossy fibres project to ZII+ and ZII- stripes differentially. Pakan et al. (2010) showed that mossy fibres from two retinorecipient nuclei in pigeons, the nucleus of the basal optic root and the nucleus lentiformis mesencephali, generally terminated adjacent to ZII+ stripes in the VbC, including the ventral uvula. Therefore, ZII+ cells are likely receiving more visual input via the mossy fibre pathways. It is not known if mossy fibre inputs from other sensory systems project preferentially to ZII- stripes in the pigeon, but it is possible that ZII+ and ZII- stripes are processing different sensory information. In addition to visual inputs, the VbC receives secondary vestibular inputs (Pakan et al., 2008) as well as spinal

inputs (Necker, 1994; Okado et al., 1987). It is possible that these preferentially target ZII- zones, but this remains to be seen.

Finally, several studies in rodents have suggested that ZII+ and ZII− PCs differ with respect to the mechanism of synaptic plasticity during motor learning: ZII+ cells rely more on long term potentiation (LTP), whereas ZII- cells rely more on long term depression (LTD) (Ebner et al., 2012; Hawkes, 2014; Paukert et al., 2010; Wadiche and Jahr, 2005; Wang et al., 2011; Zhou et al., 2014). The VbC is involved in the plasticity of the vestibulo-ocular response (VOR)(du Lac et al. 1995), a reflex that is responsible for mediating retinal image stabilization. VOR enhancement is associated with LTD, while VOR suppression is associated with LTD (Broussard et al., 2011), so within a functional unit of the pigeon VbC, it is possible that the ZII+ stripe is primary involved in VOR suppression while the ZII- stipes is involved in VOR enhancement. Thus, each functional unit consists of a stripe of ZII+ PCs and a stripe of ZII- that: (i) receive different CF inputs, (ii) receive mossy inputs from different sensory systems, (iii) project to different areas of the vestibular and cerebellar nuclei, and (iv) use LTP and LTD, respectively.

2.4 References

Ahn, A. H., Dziennis, S., Hawkes, R., and Herrup, K. (1994). The cloning of zebrin II reveals its identity with aldolase C. *Development* 120, 2081–90.

Akintunde, A., and Eisenman, L. M. (1994). External cuneocerebellar projection and Purkinje cell zebrin II bands: A direct comparison of parasagittal banding in the mouse cerebellum. *J. Chem. Neuroanat.* 7, 75–86.

Apps, R., and Garwicz, M. (2005). Anatomical and physiological foundations of cerebellar information processing. *Nat. Rev. Neurosci.* 6, 297–311.

Arends, J. J. A., and Voogd, J. (1989). "Topographic aspects of the olivocerebellar system in the pigeon," in *Experimental Brain Research Series 17: The olivocerebellar system in motor control*, ed. P. Stata, 52–57.

Armstrong, C. L., and Hawkes, R. (2000). Pattern formation in the cerebellar cortex. *Biochem. Cell Biol.* 78, 551–62.

Brochu, G., Maler, L., and Hawkes, R. (1990). Zebrin II: A polypeptide antigen expressed selectively by purkinje cells reveals compartments in rat and fish cerebellum. *J. Comp. Neurol.* 291, 538–552. doi:10.1002/cne.902910405.

Broussard, D. M., Titley, H. K., Antflick, J., and Hampson, D. R. (2011) Motor learning in the VOR: the cerebellar component. *Exp Brain Res.* 210, 451-463. doi: 10.1007/s00221-011-2589-z.s

Chockkan, V., and Hawkes, R. (1994). Functional and antigenic maps in the rat cerebellum: Zebrin compartmentation and vibrissal receptive fields in lobule IXa. *J. Comp. Neurol.* 345, 33–45. doi:10.1002/cne.903450103.

Corfield, J. R., Kolominsky, J., Craciun, I., Mulvany-Robbins, B. E., and Wylie, D. R. (2016). Is cerebellar architecture shaped by sensory ecology in the New Zealand Kiwi (Apteryx mantelli) ? *Brain. Behav. Evol.* 87, 88–104. doi:10.1159/000445315.

Corfield, J. R., Kolominsky, J., Marin, G. J., Craciun, I., Mulvany-Robbins, B. E., Iwaniuk, A. N., et al. (2015). Zebrin II expression in the cerebellum of a paleognathous bird, the Chilean tinamou (Nothoprocta perdicaria). *Brain. Behav. Evol.* 85, 94–106. doi:10.1159/000380810.

Crowder, N. A., Winship, I. R., and Wylie, D. R. W. (2000). Topographic organization of inferior olive cells projecting to translational zones in the vestibulocerebellum of pigeons. *J. Comp. Neurol.* 419, 87–95.

De Zeeuw, C. I., Wylie, D. R., Digiorgi, P. L., and Simpson, J. I. (1994). Projections of individual purkinje cells of identified zones in the flocculus to the vestibular and cerebellar nuclei in the rabbit. *J. Comp. Neurol.* 349, 428–447. doi:10.1002/cne.903490308.

du Lac, S., Raymond, J. L., Sejnowski, T. J., and Lisberger, S. G. (1995) Learning and memory in the vestibulo-ocular reflex. *Annu. Rev. Neurosci.* 18, 409-441. doi: 10.1146/annurev.ne.18.030195.002205.

Ebner, T. J., Wang, X., Gao, W., Cramer, S. W., and Chen, G. (2012). Parasagittal Zones in the Cerebellar Cortex Differ in Excitability, Information Processing, and Synaptic Plasticity. *The Cerebellum* 11, 418–419. doi:10.1007/s12311-011-0347-1.

Gao, W., Chen, G., Reinert, K. C., and Ebner, T. J. (2006). Cerebellar cortical molecular layer inhibition is organized in parasagittal zones. *J. Neurosci.* 26, 8377–8387. doi:10.1523/JNEUROSCI.2434-06.2006.

Graham, D. J., and Wylie, D. R. (2012). Zebrin-Immunopositive and -Immunonegative Stripe Pairs Represent Functional Units in the Pigeon Vestibulocerebellum. *J. Neurosci.* 32, 12769–12779. doi:10.1523/JNEUROSCI.0197-12.2012.

Gravel, C., and Hawkes, R. (1990). Parasagittal organization of the rat cerebellar cortex: Direct comparison of purkinje cell compartments and the organization of the spinocerebellar projection. *J. Comp. Neurol.* 291, 79–102. doi:10.1002/cne.902910107.

Hawkes, R. (2014). Purkinje cell stripes and long-term depression at the parallel fibre-Purkinje cell synapse. *Front. Syst. Neurosci.* 8, 41. doi:10.3389/fnsys.2014.00041.

Hawkes, R., and Gravel, C. (1991). The modular cerebellum. *Prog. Neurobiol.* 36, 309–327. doi:10.1016/0301-0082(91)90004-K.

Hawkes, R., and Herrup, K. (1995). Aldolase C/zebrin II and the regionalization of the cerebellum. *J. Mol. Neurosci.* 6, 147–158. doi:10.1007/BF02736761.

Iwaniuk, A. N., Marzban, H., Pakan, J. M. P., Watanabe, M., Hawkes, R., and Wylie, D. R. (2009). Compartmentation of the cerebellar cortex of hummingbirds (Aves: Trochilidae) revealed by the expression of zebrin II and phospholipase Cβ4. *J. Chem. Neuroanat.* 37, 55–63. doi:10.1016/j.jchemneu.2008.10.001.

Ji, Z., and Hawkes, R. (1994). Topography of purkinje cell compartments and mossy fibre terminal fields in lobules ii and iii of the rat cerebellar cortex: Spinocerebellar and cuneocerebellar projections. *Neuroscience* 61, 935–954. doi:10.1016/0306-4522(94)90414-6.

Karten, H. J., and Hodos, W. (1967). *A Stereotaxic Atlas of the Brain of the Pigeon (Columbia livia)*. Baltimore Md.: Johns Hopkins Press doi:10.2307/1421283.

Lau, K. L., Glover, R. G., Linkenhoker, B., and Wylie, D. R. (1998). Topographical organization of inferior olive cells projecting to translation and rotation zones in the vestibulocerebellum of pigeons. *Neuroscience* 85, 605–614.

Leclerc, N., Schwarting, G. A., Herrup, K., Hawkes, R., and Yamamoto, M. (1992). Compartmentation in mammalian cerebellum: Zebrin II and P-path antibodies define three classes of sagittally organized bands of Purkinje cells. *Proc. Natl. Acad. Sci. U. S. A.* 89, 5006–10. doi:10.1073/pnas.89.11.5006.

Llinás, R., and Sasaki, K. (1989). The functional organization of the olivo-cerebellar system as examined by multiple Purkinje cell recordings. *Eur. J. Neurosci.* 1, 587–602. doi:10.1111/j.1460-9568.1989.tb00365.x.

Marzban, H., Chung, S.-H., Pezhouh, M. K., Feirabend, H., Watanabe, M., Voogd, J., et al. (2010). Antigenic compartmentation of the cerebellar cortex in the chicken (Gallus domesticus). *J. Comp. Neurol.* 518, 2221–2239. doi:10.1002/cne.22328.

Marzban, H., and Hawkes, R. (2011). On the Architecture of the Posterior Zone of the Cerebellum. *The Cerebellum* 10, 422–434. doi:10.1007/s12311-010-0208-3.

Marzban, H., Hoy, N., Buchok, M., Catania, K. C., and Hawkes, R. (2015). Compartmentation of the Cerebellar Cortex: Adaptation to Lifestyle in the Star-Nosed Mole Condylura cristata. *The Cerebellum* 14, 106–118. doi:10.1007/s12311-014-0618-8.

Marzban, H., Zahedi, S., Sanchez, M., and Hawkes, R. (2003). Antigenic compartmentation of the cerebellar cortex in the syrian hamster Mesocricetus auratus. *Brain Res.* 974, 176–83.

Matsushita, M., Ragnarson, B., and Grant, G. (1991). Topographic relationship between sagittal Purkinje cell bands revealed by a monoclonal antibody to zebrin I and spinocerebellar projections arising from the central cervical nucleus in the rat. *Exp. Brain Res.* 84, 133–41.

Mostofi, A., Holtzman, T., Grout, A. S., Yeo, C. H., and Edgley, S. A. (2010). Electrophysiological Localization of Eyeblink-Related Microzones in Rabbit Cerebellar Cortex. *J. Neurosci.* 30, 8920–8934. doi:10.1523/JNEUROSCI.6117-09.2010.

Necker, R. (1994). Sensorimotor aspects of flight control in birds: specializations in the spinal cord. *Eur. J. Morphol.* 32, 207–11.

Okado, N., Ito, R., and Homma, S. (1987). The terminal distribution pattern of spinocerebellar fibres. An anterograde labelling study in the posthatching chick. *Anat. Embryol. (Berl).* 176, 175–82.

Ozol, K., Hayden, J. M., Oberdick, J., and Hawkes, R. (1999). Transverse zones in the vermis of the mouse cerebellum. *J. Comp. Neurol.* 412, 95–111. doi:10.1002/(SICI)1096-9861(19990913)412:1<95::AID-CNE7>3.0.CO;2-Y.

Pakan, J. M. P., Graham, D. J., Gutierrez-Ibanez, C., and Wylie, D. R. (2011). Organization of the cerebellum: correlating zebrin immunochemistry with optic flow zones in the pigeon flocculus. *Vis. Neurosci.* 28, 163–174. doi:10.1017/S0952523810000532.

Pakan, J. M. P., Graham, D. J., Iwaniuk, A. N., and Wylie, D. R. (2008). Differential projections from the vestibular nuclei to the flocculus and uvula-nodulus in pigeons (Columba livia). *J. Comp. Neurol.* 508, 402–417. doi:10.1002/cne.21623.

Pakan, J. M. P., Graham, D. J., and Wylie, D. R. (2010). Organization of visual mossy fibre projections and zebrin expression in the pigeon vestibulocerebellum. *J. Comp. Neurol.* 518, 175–198. doi:10.1002/cne.22192.

Pakan, J. M. P., Graham, D. J., and Wylie, D. R. (2014). Climbing fibre projections in relation to Zebrin stripes in the ventral Uvula in Pigeons. *J. Comp. Neurol.* 522, 3629–3643. doi:10.1002/cne.23626.

Pakan, J. M. P., Iwaniuk, A. N., Wylie, D. R., Hawkes, R., and Marzban, H. (2007). Purkinje cell compartmentation as revealed by Zebrin II expression in the cerebellar cortex of pigeons (Columba livia). *J. Comp. Neurol.* 501, 619–630. doi:10.1002/cne.21266.

Pakan, J. M. P., and Wylie, D. R. (2008). Congruence of zebrin II expression and functional zones defined by climbing fibre topography in the flocculus. *Neuroscience* 157, 57–69. doi:10.1016/j.neuroscience.2008.08.062.

Paukert, M., Huang, Y. H., Tanaka, K., Rothstein, J. D., and Bergles, D. E. (2010). Zones of Enhanced Glutamate Release from Climbing Fibers in the Mammalian Cerebellum. *J. Neurosci.* 30, 7290–7299. doi:10.1523/JNEUROSCI.5118-09.2010.

Pijpers, A., Apps, R., Pardoe, J., Voogd, J., and Ruigrok, T. J. H. (2006). Precise Spatial Relationships between Mossy Fibers and Climbing Fibers in Rat Cerebellar Cortical Zones. *J. Neurosci.* 26, 12067–12080. doi:10.1523/JNEUROSCI.2905-06.2006.

Ruigrok, T. J. H. (2003). Collateralization of climbing and mossy fibres projecting to the nodulus and flocculus of the rat cerebellum. *J. Comp. Neurol.* 466, 278–298. doi:10.1002/cne.10889.

Ruigrok, T. J. H., Pijpers, A., Goedknegt-Sabel, E., and Coulon, P. (2008). Multiple cerebellar zones are involved in the control of individual muscles: a retrograde transneuronal tracing study with rabies virus in the rat. *Eur. J. Neurosci.* 28, 181–200. doi:10.1111/j.1460-9568.2008.06294.x.

Sanchez, M., Sillitoe, R. V., Attwell, P. J. E., Ivarsson, M., Rahman, S., Yeo, C. H., et al. (2002). Compartmentation of the rabbit cerebellar cortex. *J. Comp. Neurol.* 444, 159–73.

Sillitoe, R. V., Hulliger, M., Dyck, R., and Hawkes, R. (2003). Antigenic compartmentation of the cat cerebellar cortex. *Brain Res.* 977, 1–15.

Sillitoe, R. V., Künzle, H., and Hawkes, R. (2003). Zebrin II compartmentation of the cerebellum in a basal insectivore, the Madagascan hedgehog tenrec Echinops telfairi. *J. Anat.* 203, 283–96. doi:10.1046/j.1469-7580.2003.00216.x.

Sugihara, I. (2011). Compartmentalization of the deep cerebellar nuclei based on afferent projections and aldolase C expression. *Cerebellum* 10, 449–463. doi:10.1007/s12311-010-0226-1.

Sugihara, I., Marshall, S. P., and Lang, E. J. (2007). Relationship of complex spike synchrony bands and climbing fibre projection determined by reference to aldolase C compartments in crus IIa of the rat cerebellar cortex. *J. Comp. Neurol.* 501, 13–29. doi:10.1002/cne.21223.

Sugihara, I., and Quy, P. N. (2007). Identification of aldolase C compartments in the mouse cerebellar cortex by olivocerebellar labeling. *J. Comp. Neurol.* 500, 1076–1092. doi:10.1002/cne.21219.

Sugihara, I., and Shinoda, Y. (2004). Molecular, Topographic, and Functional Organization of the Cerebellar Cortex: A Study with Combined Aldolase C and Olivocerebellar Labeling. *J. Neurosci.* 24, 8771–8785. doi:10.1523/JNEUROSCI.1961-04.2004.

Sugihara, I., and Shinoda, Y. (2007). Molecular, Topographic, and Functional Organization of the Cerebellar Nuclei: Analysis by Three-Dimensional Mapping of the Olivonuclear Projection and Aldolase C Labeling. *J. Neurosci.* 27, 9696–9710. doi:10.1523/JNEUROSCI.1579-07.2007.

Vibulyaseck, S., Luo, Y., Fujita, H., Oh-Nishi, A., Ohki-Hamazaki, H., and Sugihara, I. (2015). Compartmentalization of the chick cerebellar cortex based on the link between the striped expression pattern of aldolase C and the topographic olivocerebellar projection. *J. Comp. Neurol.* 523, 1886–1912. doi:10.1002/cne.23769.

Voogd, J., and Bigaré, F. (1980). "Topographical distribution of olivary and cortico nuclear fibres in the cerebellum: a review," in *The Inferior Olivary Nucleus.*, eds. J. Courville, C. de Montigny, and Y. Lamarre (New York: Raven Press), 207–234.

Voogd, J., Gerrits, N. M., and Ruigrok, T. J. H. (1996) Organization of the Vestibulocerebellum. *Ann. N. Y. Acad. Sci.* 781, 553-579. doi: 10.1111/j.1749-6632.1996.tb15728.x.

Voogd, J., and Glickstein, M. (1998). The anatomy of the cerebellum. *Trends Cogn. Sci.* 2, 307–313. doi:10.1016/S1364-6613(98)01210-8.

Voogd, J., Pardoe, J., Ruigrok, T. J. H., and Apps, R. (2003). The distribution of climbing and mossy fibre collateral branches from the copula pyramidis and the paramedian lobule: congruence of climbing fibre cortical zones and the pattern of zebrin banding within the rat cerebellum. *J. Neurosci.* 23, 4645–56. doi:23/11/4645 [pii].

Voogd, J., and Ruigrok, T. J. H. (2004). The organization of the corticonuclear and olivocerebellar climbing fibre projections to the rat cerebellar vermis: The congruence of projection zones and the zebrin pattern. *J. Neurocytol.* 33, 5–21. doi:10.1023/B:NEUR.0000029645.72074.2b.

Voogd, J., and Wylie, D. R. (2004) Functional and Anatomical Organization of Floccular Zones: A Preserved Feature in Vertebrates. *J. Comp. Neurol.* 470, 107-112. doi: 10.1002/cne.11022

Wadiche, J. I., and Jahr, C. E. (2005). Patterned expression of Purkinje cell glutamate transporters controls synaptic plasticity. *Nat. Neurosci.* 8, 1329–1334. doi:10.1038/nn1539.

Wang, X., Chen, G., Gao, W., and Ebner, T. J. (2011). Parasagittally aligned, mGluR1-dependent patches are evoked at long latencies by parallel fibre stimulation in the mouse cerebellar cortex in vivo. *J. Neurophysiol.* 105, 1732–1746. doi:10.1152/jn.00717.2010.

Wu, H. S., Sugihara, I., and Shinoda, Y. (1999). Projection patterns of single mossy fibres originating from the lateral reticular nucleus in the rat cerebellar cortex and nuclei. *J. Comp. Neurol.* 411, 97–118.

Wylie, D. R. (2013). Processing of visual signals related to self-motion in the cerebellum of pigeons. *Front. Behav. Neurosci.* 7, 4. doi:10.3389/fnbeh.2013.00004.

Wylie, D. R., Bischof, W. F., and Frost, B. J. (1998). Common reference frame for neural coding of translational and rotational optic flow. *Nature* 392, 278–282. doi:10.1038/32648.

Wylie, D. R., and Frost, B. J. (1991). Purkinje cells in the vestibulocerebellum of the pigeon respond best to either translational or rotational wholefield visual motion. *Exp. Brain Res.* 86, 229–232. doi:10.1007/BF00231059.

Wylie, D. R., and Frost, B. J. (1993). Responses of pigeon vestibulocerebellar neurons to optokinetic stimulation. II. The 3-dimensional reference frame of rotation neurons in the flocculus. *J. Neurophysiol.* 70, 2647–2659.

Wylie, D. R., Gutiérrez-Ibáñez, C., Corfield, J. R., Craciun, I., Graham, D. J., and Hurd, P. L. (2017). Inferior olivary projection to the zebrin II stripes in lobule IXcd of the pigeon flocculus: A retrograde tracing study. *J. Comp. Neurol.* 525, 3158–3173. doi:10.1002/cne.24270.

Wylie, D. R., Hoops, D., Aspden, J. W., and Iwaniuk, A. N. (2016). Zebrin II is expressed in sagittal stripes in the cerebellum of dragon lizards (Ctenophorus sp.). *Brain. Behav. Evol.* 88, 177–186. doi:10.1159/000452857.

Wylie, D. R., Jensen, M., Gutierrez-Ibanez, C., Graham, D. J., and Iwaniuk, A. N. (2013). Heterogeneity of calretinin expression in the avian cerebellar cortex of pigeons and relationship with zebrin II. *J. Chem. Neuroanat.* 52, 95–103. doi:10.1016/j.jchemneu.2013.07.005.

Wylie, D. R., Kripalani, T., and Frost, B. J. (1993). Responses of pigeon vestibulocerebellar neurons to optokinetic stimulation. I. Functional organization of neurons discriminating between translational and rotational visual flow. *J. Neurophysiol.* 70, 2632–2646.

Wylie, D. R., Pakan, J. M. P., Elliot, C. A., Graham, D. J., and Iwaniuk, A. N. (2007). Projections of the nucleus of the basal optic root in pigeons (Columba livia): A comparison of the morphology and distribution of neurons with different efferent projections. *Vis. Neurosci.* 24, 691–707. doi:10.1017/S0952523807070599.

Wylie, D. R., Pakan, J. M. P., Huynh, H., Graham, D. J., and Iwaniuk, A. N. (2012). Distribution of zebrin-immunoreactive Purkinje cell terminals in the cerebellar and vestibular nuclei of birds. *J. Comp. Neurol.* 520, 1532–1546. doi:10.1002/cne.22810.

Wylie, D. R., Winship, I. R., and Glover, R. G. (1999). Projections from the medial column of the inferior olive to different classes of rotation-sensitive Purkinje cells in the flocculus of pigeons. *Neurosci. Lett.* 268, 97–100. doi:10.1016/S0304-3940(99)00390-0.

Zhou, H., Lin, Z., Voges, K., Ju, C., Gao, Z., Bosman, L. W. J., et al. (2014). Cerebellar modules operate at different frequencies. *Elife* 3, e02536. doi:10.7554/eLife.02536.

Chapter 3: **Characterization of the Avian Lugaro Cell**

The mammalian cerebellar cortex consists of numerous cell types including Purkinje cells (PCs), basket and stellate cells in the molecular cell layer (mcl), and granule cells in the granular cell layer (gcl) (Figure 3.1). Also in the gcl are large inhibitory interneurons including Golgi cells and Lugaro cells. Lugaro cells, the subject of the study, are mainly located in the gcl just below the PCs, or sometimes within the Purkinje cell layer (pcl) itself (Fox, 1959). These cells are characterized by their fusiform spindle-like shape and dendrites that emerge from opposite ends of their cell bodies (Fox, 1959). Initially, it seems that Lugaro cells and Golgi cells were grouped together (Golgi, 1874; Ramón and Cajal, 1911). Lugaro (1894) later distinguished smaller fusiform cells, also located right below the pcl in the cat cerebellum, as separate from larger globular (Golgi) cells, and named the former as "intermediate cells". In addition to this morphological difference between Lugaro and Golgi cells, Sahin and Hockfield (1990) showed that Lugaro cells are molecularly distinct from the other large cerebellar cortex cells types, including Golgi cells. More recent evidence has blurred the morphological distinction between Golgi and Lugaro cells as the existence of a globular Lugaro cell type has been proposed. Both globular and fusiform Lugaro cells, but not Golgi cells, are immunoreactive for calretinin, and are innervated by Purkinje axon collaterals (Lainé and Axelrad, 2002; Singec et al., 2003; Simat et al., 2007; Schilling et al., 2008). Additionally, Golgi cells express metabotropic glutamate receptor 2 (mGluR2) and neurogranin while Lugaro cells do not (Singec et al., 2003; Simat et al., 2007). In terms of their projection pattern, Lugaro cell axons always project into the molecular cell layer (mcl), with axon collaterals traveling alongside parallel fibres that arise from granule cells in the cerebellar cortex (Figure 3.1) (Lugaro, 1894; Fox, 1959; Lainé and Axelrad, 1996). Golgi cells on the other hand exhibit a very thin and profuse axonal plexus that remains in the granular cell layer (gcl), whereas their dendrites radiate into the mcl (Lainé and Axelrad, 2002).

With respect to circuitry, Lugaro cells receive inhibitory inputs from PC axon collaterals (Larramendi and Lemkey-Johnston, 1970; Palay and Chan-Palay, 1974), and their axons project into the mcl to innervate stellate cells and basket cells, which in turn inhibit PCs (Figure 3.1) (Lainé and Axelrad, 1996). Lugaro cells have also been found to inhibit Golgi cells through axons projecting in the coronal plane (Dieudonné and Dumoulin, 2000). An additional feature that distinguishes Lugaro cells from the other cerebellar cells is that they are selectively excited by serotonin axons (Dieudonné and Dumoulin, 2000).

Lugaro cells have been described in a broad array of mammalian species (e.g. Equidna; Ashwell et al., 2007; Rat: Lainé and Axelrad, 1996; Cat: Sahin and Hockfield, 1990; Human: Braak, 1974, but evidence for the existence of Lugaro cells in other vertebrates is scarce. Pushchina and Varaksin (2001), based only on histochemistry against nitric oxidase, described Lugaro-like cells in the cerebellum of a teleost. In chickens, Rogers (1989), based solely on the location near the Purkinje cells layer, suggested that some weakly calretinin positive cells could be either basket or Lugaro cells. (We previously found no calretinin positive cells in the molecular layer of the pigeon cerebellum (Wylie et al., 2013)). While this evidence suggests that Lugaro cells could exist in vertebrates other than mammals, solid evidence is needed.

Upon investigating the expression of secretagogin (SCGN), a recently discovered calcium binding protein (reviewed in Alpár et al., 2012), we noted secretagogin-labelling of large cells throughout the gcl in the pigeon cerebellum. In this report, based on cell morphology, local connectivity, and immunohistochemistry, we argue that at least some of the SCGN-labelled cells correspond to Lugaro cells in the pigeon cerebellum.

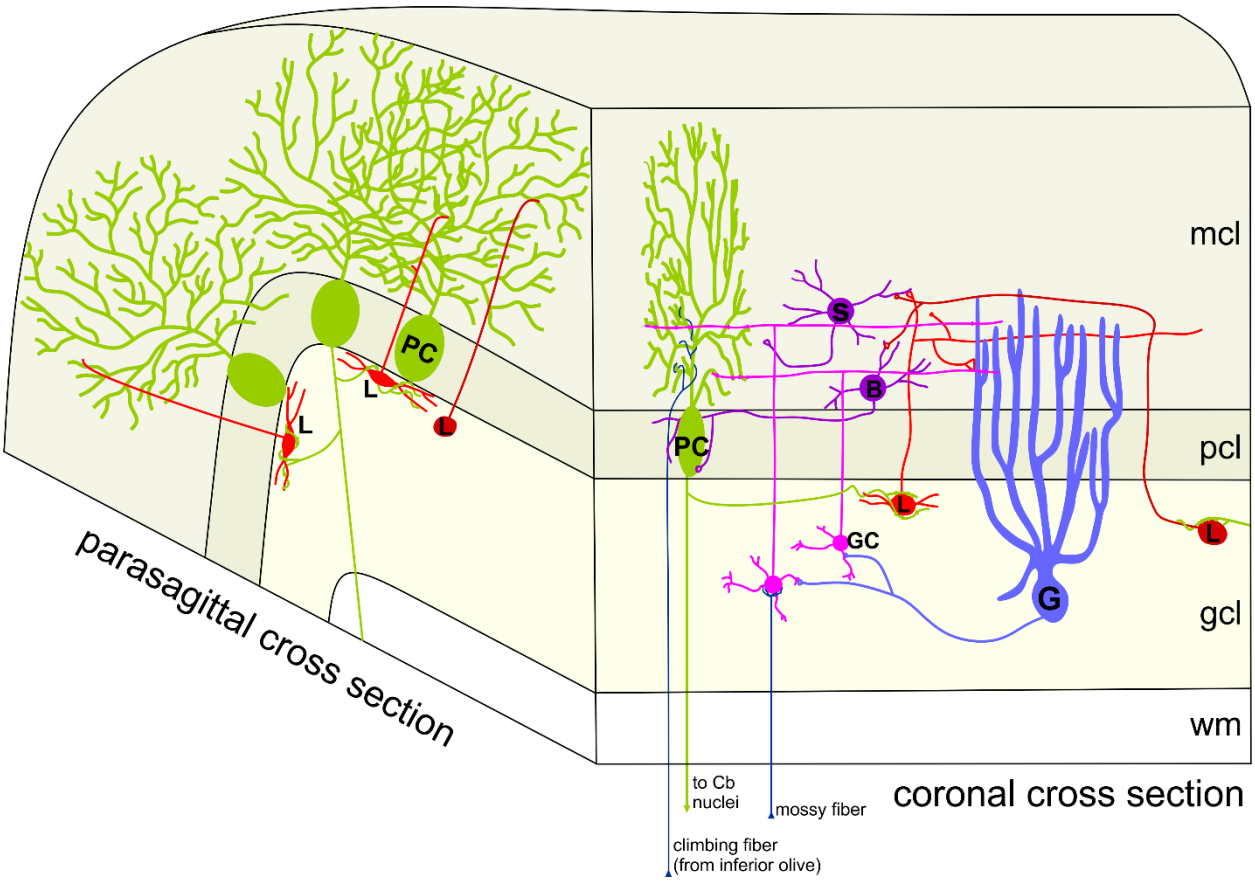

Figure 3.1 Simplified cerebellar circuitry. The schematic shows simple cerebellar connectivity, and a view of a cerebellar folium in the parasagittal and coronal planes. Climbing fibres (CFs; navy) and mossy fibres (mFs; navy) are the two main inputs into the cerebellum. CFs come from the inferior olive and synapse directly onto the Purkinje cells (PCs; green) while mFs terminate on granule cells (GC; magenta) and Golgi cells (G; blue) in the granular cell layer (gcl). Granule cells project their axons into the molecular cell layer (mcl) and bifurcate to send off parallel fibres that synapse extensively onto the PCs. Lugaro cells (L; red) also project their axons into the mcl, and their axons travel through the coronal plane alongside granule cell parallel fibres to synapse on basket (B) and stellate (S) cells (purple). Basket and stellate cells in turn synapse on PCs, and PC collaterals synapse on Lugaro cells. Lugaro cells also synapse onto

Golgi cells. Note both fusiform (bright red) and globular (dark red) types of Lugaro cells. The fusiform somata are only noticeable in parasagittal cross sections. pcl = Purkinje cell layer; wm = white matter.

3.1 Materials and Methods

3.1.1 *Perfusion and brain processing*

The methods used adhere to the guidelines established by the Canadian Council on Animal Care and were approved by the Biosciences Animal Care and Use Committee at the University of Alberta. Three rock pigeons (*Coulmba livia*) of either sex, obtained from a local supplier, were anesthetised with an intramuscular injection of a ketamine (65mg/kg) and xylazine (8mg/kg) cocktail, followed by sodium pentobarbital (100 mg/kg). A transcardial perfusion with phosphate buffered saline (PBS; 0.9% NaCl, 0.1 M phosphate buffer) followed by 4% paraformaldehyde in 0.1 M PBS (pH 7.4) was then performed. The brains were extracted from the skull and immersed in paraformaldehyde for 3-4 hours at 4°C, then immersed in 30% sucrose in 0.1 M phosphate buffer until they sank (48 hours). Brains were subsequently embedded in gelatin, post-fixed in 4% PFA and 30% sucrose in 0.1 phosphate buffer for 5 hours, and cryoprotected in 30% sucrose in 0.1 M PBS overnight. The gelatin-embedded brains were then frozen and sliced into 40 µm thick sections (coronal or sagittal) using a sliding microtome. Sections were collected in four series throughout the extent of the cerebellum. Two rat cerebella (archival tissue) were also processed. One was cut in the parasagittal plane and the other in the coronal plane. Sections were stored in 0.1M PBS (pH 7.4) between sectioning and immunohistochemistry.

3.1.2 *Antigen Retrieval*

Secretagogin expression was only observed in the pigeon cerebellum if antigen retrieval or amplification was used. For the sections that were subject to antigen retrieval, prior to

processing the tissue using the immunohistochemical procedures below, well plates filled with 10 mM sodium citrate buffer (pH 8) were placed in a hot water bath (80˚C) for 15 minutes to allow the buffer to reach 80˚C. Sections were rinsed fives times for five minutes in 0.1 M phosphate buffer after which they were placed in 10 mM sodium citrate buffer (pH 8) for thirty minutes at 80˚C. The well plate containing the tissue was removed from the water bath and left to cool for fifteen minutes with the lid removed. The tissue was rinsed another five times for five minutes in 0.1 M phosphate buffer.

3.1.3 *Immunohistochemistry*

The immunohistochemistry protocols differed for each antibody, but the general protocol was as outlined here. Tissue was rinsed thoroughly with 0.1 M PBS (with the exception of the tissue that had undergone antigen retrieval). Sections were then blocked with 10% normal donkey serum (Jackson Immunoresearch Laboratories, West Grove, PA) and 0.4% Triton X-100 in PBS for 1 hour. Tissue was then incubated in PBS containing 0.1% Triton X-100, 2.5% normal donkey serum, and the primary antibody for 24-48 hours at 4°C. After primary antibody incubation, sections were rinsed five times in 0.1 M PBS and incubated with animal host appropriate fluorescent secondary antibodies AlexaFluor 594 or 488 (either anti-mouse, -goat or -rabbit; 1:200, Jackson Immunoresearch Laboratories, West Grove, PA) in PBS, 2.5% normal donkey serum, and 0.4% Triton X-100 for 3 hours at room temperature. In some cases, two secondary fluorescent antibodies (one of each colour) were used. The tissue was then rinsed five times for five minutes in 0.1 M PBS and mounted onto gelatinized slides for viewing. Although SCGN expression was the focus of this study, several other antibodies were also used. (See Table 3.1). The specificity of the antibodies against secretagogin has previously been tested in an

avian species (chicken) and recognizes a band of 32 kDa in both the chicken and rat (Gáti et al., 2014).

Primary antibody	Source	Host	IH dilution	Time incubated
Secretagogin	R&D Systems	goat	1:500	48 hours
Secretagogin	Atlas Antibodies	rabbit	1:5000	72 hours
Calretinin	SWant	rabbit	1:2000	48 hours
Calbindin D-28k	SWant	rabbit	1:2000	48 hours
GAD	Millipore Sigma	rabbit	1:1000	24 hours
Zebrin II/aldolase C	Santa Cruz Biotech	goat	1:1000	48 hours

Table 3.1 List of markers used for immunohistochemistry (IH). The different primary antibodies we used require specific incubation protocols that differ in the dilution concentration of antibody used and time incubated.

In some cases, we used an amplification protocol requiring a biotin tyramide reaction. In these cases, after primary antibody incubation, tissue was rinsed 5 times for 5 minutes, then incubated with a biotin secondary (1:1000) for 2 hours at room temperature. Sections were then rinsed 5 times for 5 minutes. After rinsing, sections were incubated in avidin- biotin peroxidase complex (ABC; Vectastain Elite ABC Kit, Vector Laboratories Inc., Burlingame, CA, USA; 3.2 µl/ml in PBS- Tx 0.5%/4% NaCl) for 1 hour. Sections were again rinsed 5 times. This was followed by tyramide signal amplification where sections were incubated in 0.0001% biotin- tyramide (IRIS Biotech GmbH, Marktredwitz, Germany; Cat# LS- 3500, Lot. 1407008) and 0.003% H_2O_2 in 0.05M borate buffer (pH 8.5) for 1 hour. Sections were once again rinsed 5 times for 5 minutes. Last, sections were incubated for 1 hour with Streptavidin- Alexa594 (Streptavidin Alexa Fluor 594 conjugate, Thermo Fisher Scientific, Waltham, MA, USA) diluted 1:500 in 0.5% Triton X-100 in PBS.

3.1.4 *NADPH-d staining*

Because Lugaro and Golgi cells sometimes contain nitric oxide synthase (i.e., in the rabbit cerebellum; Okhotin and Kalinichenko, 2000), the tissue was stained for nicotinamide adenine dinucleotide phosphate-diaphorase (NADPH-d) according to the protocol of Fischer and Stell (1999). Sections were mounted on the slides and left to dry for 2-3 days. The slides were washed in 0.1 M Tris buffer (pH 8.0) for 5 minutes. The NADPH-d staining solution (1 mM NADPH, 18 mM CaCl2, 0.5 nM nitrotetrazolium blue (NTB) and 0.3% Triton-X) was applied directly to the slides. The slides were then covered with a large petri dish to avoid evaporation of the staining solution during incubation. The different slides were incubated between 20-60

minutes at 37 °C. After the incubation period, the slides were rinsed 5 times for 5 minutes with 0.1M phosphate buffered saline (pH 7.4).

3.1.5 *Microscopy*

Sections were viewed with a compound light microscope (Leica DM6B, Concord, ON) equipped with TX2 (red) and L5 (green) fluorescence filters. Images were captured with a DFC7000 T camera using Leica Application Suite X imaging software (Leica Microsystems, Concord, ON). Adobe Photoshop CC (San Jose, CA) was used to adjust contrast and brightness.

3.2 Results

3.2.1 *Secretagogin Labelling in the Cerebellum*

As previously mentioned, we visualized SCGN labelling in the cerebellum with the following techniques: 1) classic immunohistochemistry, 2) using amplification with biotin tyramide and streptavidin, and 3) using an antigen retrieval protocol prior to immunohistochemistry. Figure 3.2 shows SCGN immunoreactivity (SCGN-ir) from each of these protocols in coronal sections through the cerebellum (A-C, E-F, and H-J) and the optic tectum (D, G, and K). Although SCGN-ir was apparent in the optic tectum without amplification or antigen retrieval (Figure 3.2D), immunoreactivity in the cerebellum was very faint (Figure 3.2A-C). Upon treatment of the tissue with amplification or antigen retrieval, SCGN immunolabelling in the cerebellum became clearly apparent, particularly with the latter (Figure 3.2 A-C, E-F). Immunoreactivity was apparent in the somata, proximal dendrites, and axons or neurons in the gcl. Most of these cells appeared near the pcl. Generally, in coronal sections, the

somata of these neurons appear round (Figure 3.2I). We also noted SCGN-labelled fibres traveling through the mcl in the coronal plane (Figure 3.2H). SCGN cloned in a rabbit host is particularly effective at labelling Lugaro cell axons, as shown in Figure 3.5, while SCGN cloned in a goat host is not. Finally, labelled mossy fibre rosettes were occasionally apparent (Figure 3.3D,E).

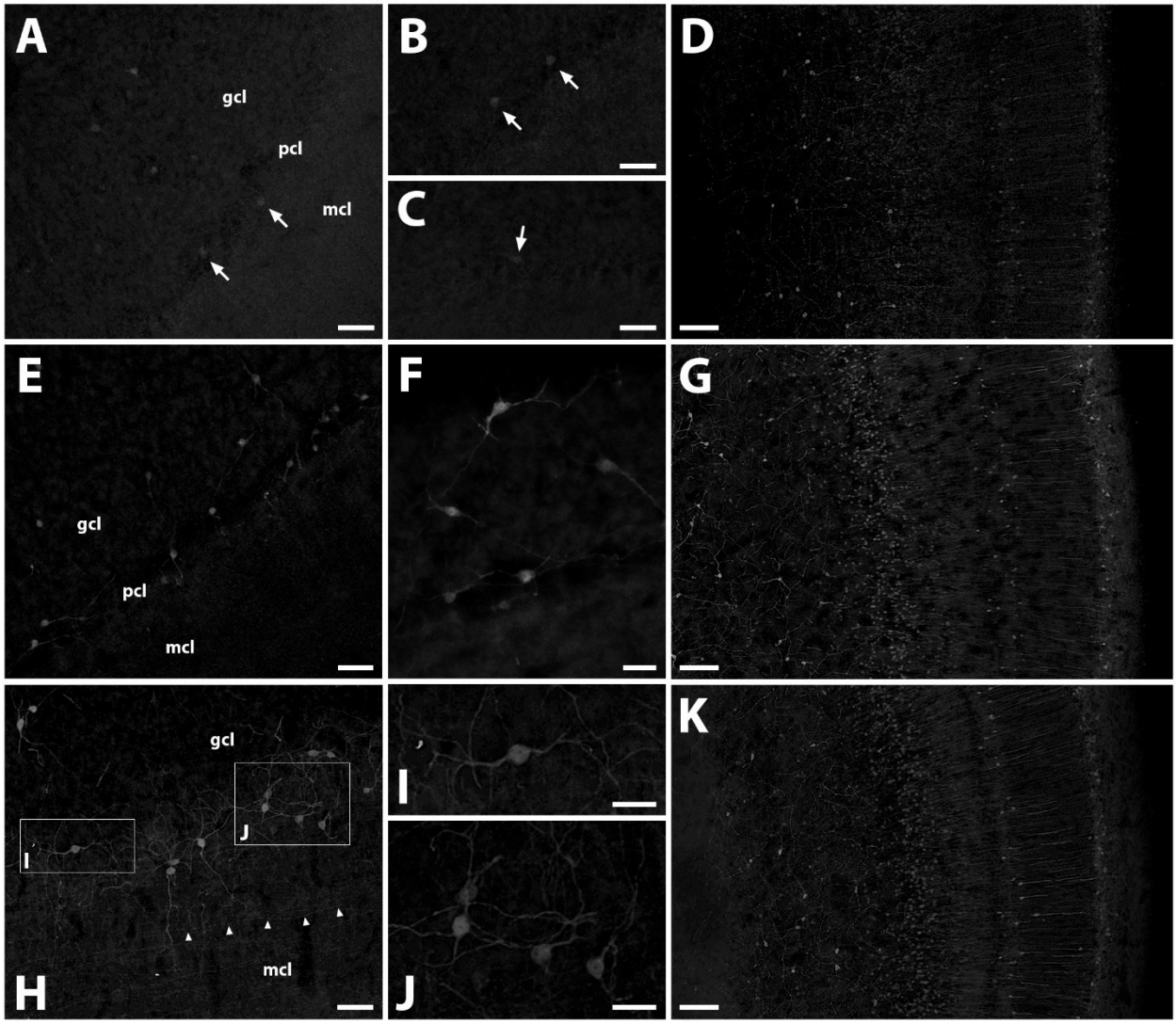

Figure 3.2 Secretagogin (SCGN) labelling in the pigeon cerebellum and optic tectum. A-D show SCGN labelling without any enhancement methods for sections cut in the coronal plane. **A-C** show labelling in the cerebellum, and **D** shows labelling in the optic tectum for comparison. In the cerebellum, cells in the granular cell layer were very faintly labelled (arrows). With amplification (**E,F)** and antigen retrieval **(H-J)**, these cells showed strong SCGN immunoreactivity. Note SCGN immunoreactive fibres in the mcl in **H**. **G** and **K**, respectively, show SCGN immunoreactivity in the optic tectum with amplification and antigen revival. The

SCGN used in these sections was cloned in rabbit. mcl = molecular cell layer; pcl = Purkinje cell layer; gcl = granular cell layer. Scale bars = 25 μm **F,I,J**, 50 μm in **A-C,E,H**, 100 μm in **D,G,K**.

To show the proximity of SCGN-ir cells to the pcl, some sections were immunoprocessed for CB, which is expressed by all PCs. Figures 3.3 and 3.4 both show SCGN (red) and CB (green) labelling in sagittal cerebellar sections. SCGN-labelled cells consistently appeared in the gcl both close to the PCs, and deeper within the gcl (Figure 3.3A,3.4A). Moreover, some of these cells were clearly within the pcl (e.g., Figure 3.4B). The somata of the SCGN-immunoreactive cells nearest the pcl were smaller, and often fusiform, compared to those deeper in the gcl (e.g., Figure 3.3A,3.4B,F). We also noted SCGN-immunoreactive cells at the border of the gcl and white matter (figure 3.3B).

In sagittal sections, some of the SCGN-ir cells closest to the pcl resembled the morphology of Lugaro cells described in mammals (Figure 3.4B-I). The cell bodies were fusiform in shape, with dendrites emerging from both poles parallel to the pcl (e.g., Figure 3.4F). Some of the cells were more globular in shape, but these were situated slightly further away from the pcl than those fusiform cells (e.g., Figure 3.4D,H,I). Often the SCGN-labelled cells were encapsulated by CB-labelled varicosities (e.g., Figure 3.4D,F). Presumably these arise from PC axon collaterals.

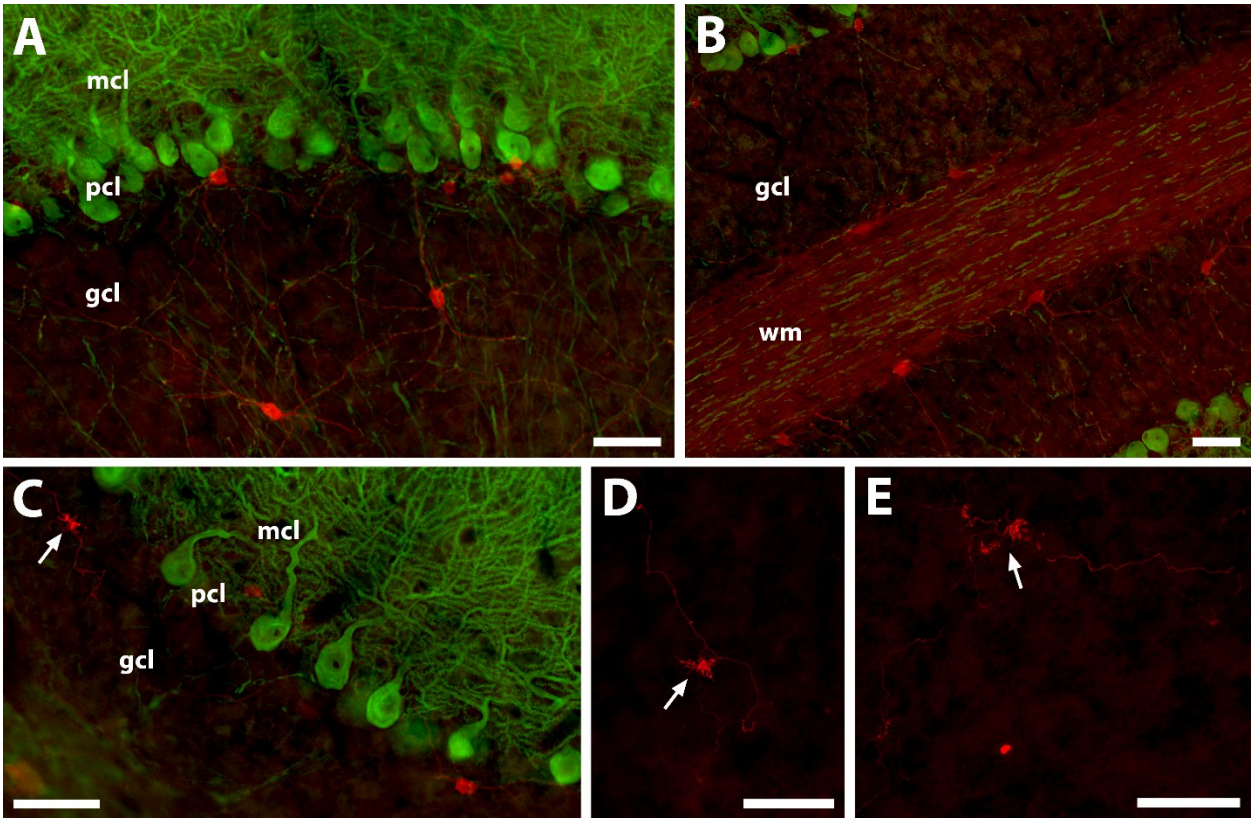

Figure 3.3 Secretagogin (SCGN) labelling in the cerebellum. Tissue was immunoprocessed for secretagogin (SCGN; red) and Calbindin-D28k (CB; green). Purkinje cells (PCs) are CB immunopositive. **A** shows different types of SCGN-labelled cells: smaller ones closer to the Purkinje cell layer (pcl) and larger ones deeper in the granular cell layer (gcl). PCs are labelled by CB in green. **B** shows SCGN-labelled cells in the gcl adjacent to the white matter (wm). **C-E** show mossy fibre rosettes labelled by SCGN (arrows). mcl = molecular cell layer. Scale bars = 50 μm in **A-E**.

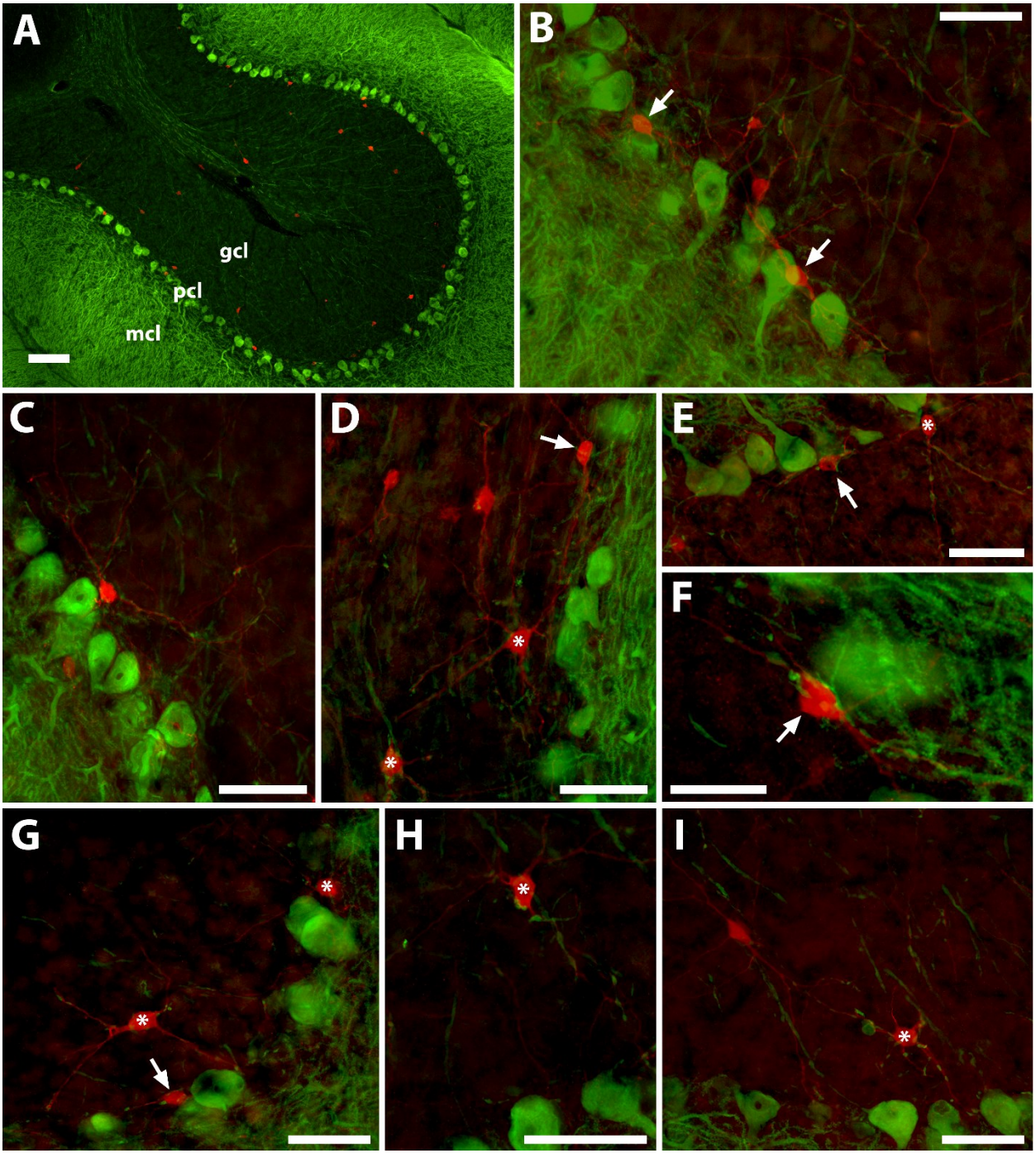
A
gcl
pcl
mcl
B
C
D
E
F
G
H
I

Figure 3.4 SCGN-labelled cells near the Purkinje cell layer (pcl). Sagittal sections were immunoprocessed with secretagogin (SCGN; red) and Calbindin-D28k (CB; green). Purkinje cells (PCs) are CB-immunoreactive. **A** shows SCGN-labelled cells in a low-power photomicrograph of the pigeon cerebellum. **B-I** show high magnification images of various SCGN-labelled cells near the PCs. Note the CB-immunopositive varicosities surrounding a both fusiform (arrows) and globular (asterisks) cells. This is clearest for the cells in **F**, on the left in **D**, and in **H,I**. mcl = molecular cell layer; gcl = granular cell layer. Scale bars = 25 μm **F**, 50 μm in **B-E,G-I**, 100 μm in **A**.

An additional characteristic of mammalian Lugaro cells is the existence of parallel-fibre-like axonal projections through the mcl. When viewing SCGN labelling in coronal sections, we noted similar parallel-fibre-like projections (Figure 3.5). The white arrow in Figure 3.5 highlights a single SCGN immunopositive fibre (arrow heads) projecting into the mcl, making an abrupt turn (empty arrowhead), and traveling in the same plane as parallel fibres of granule cells.

3.2.2 *Glutamic Acid Decarboxylase Labelling in the Cerebellum*

As Lugaro cells are inhibitory, we examined the co-expression of SCGN and GAD (Figure 3.6). SCGN immunopositive cells in the gcl co-expressed GAD.

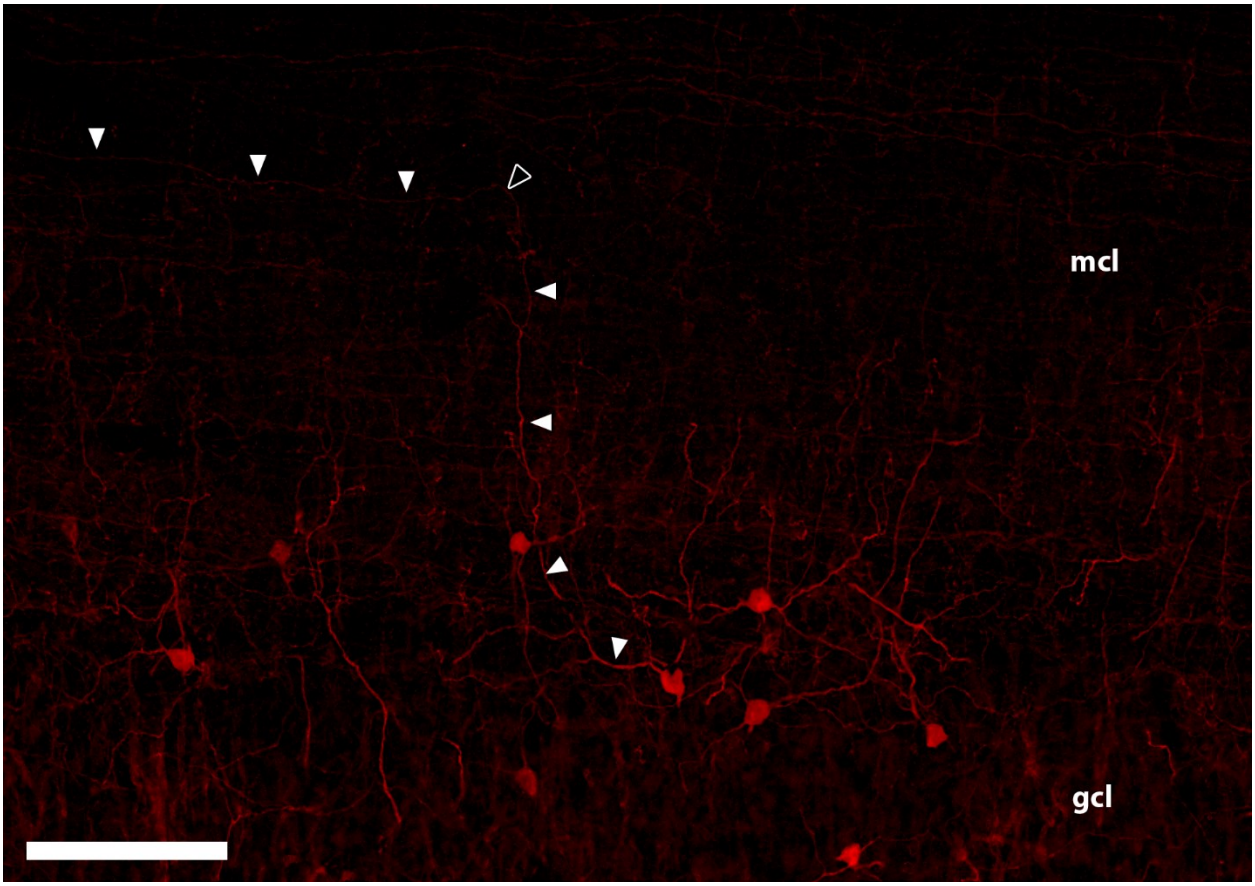

Figure 3.5 Coronal section through the pigeon cerebellum. Cell bodies, dendrites, and axons are labelled by SCGN. The labelled cells exhibit axons that project into the molecular cell layer (mcl) and traverse alongside parallel fibres, which is a characteristic of Lugaro cells. White arrowheads follow along a single axon as it ascends into the mcl. The empty arrowhead points out the abrupt turn taken by the axon before projecting transversely along the folium. gcl = granular cell layer. Scale bar = 100 µm.

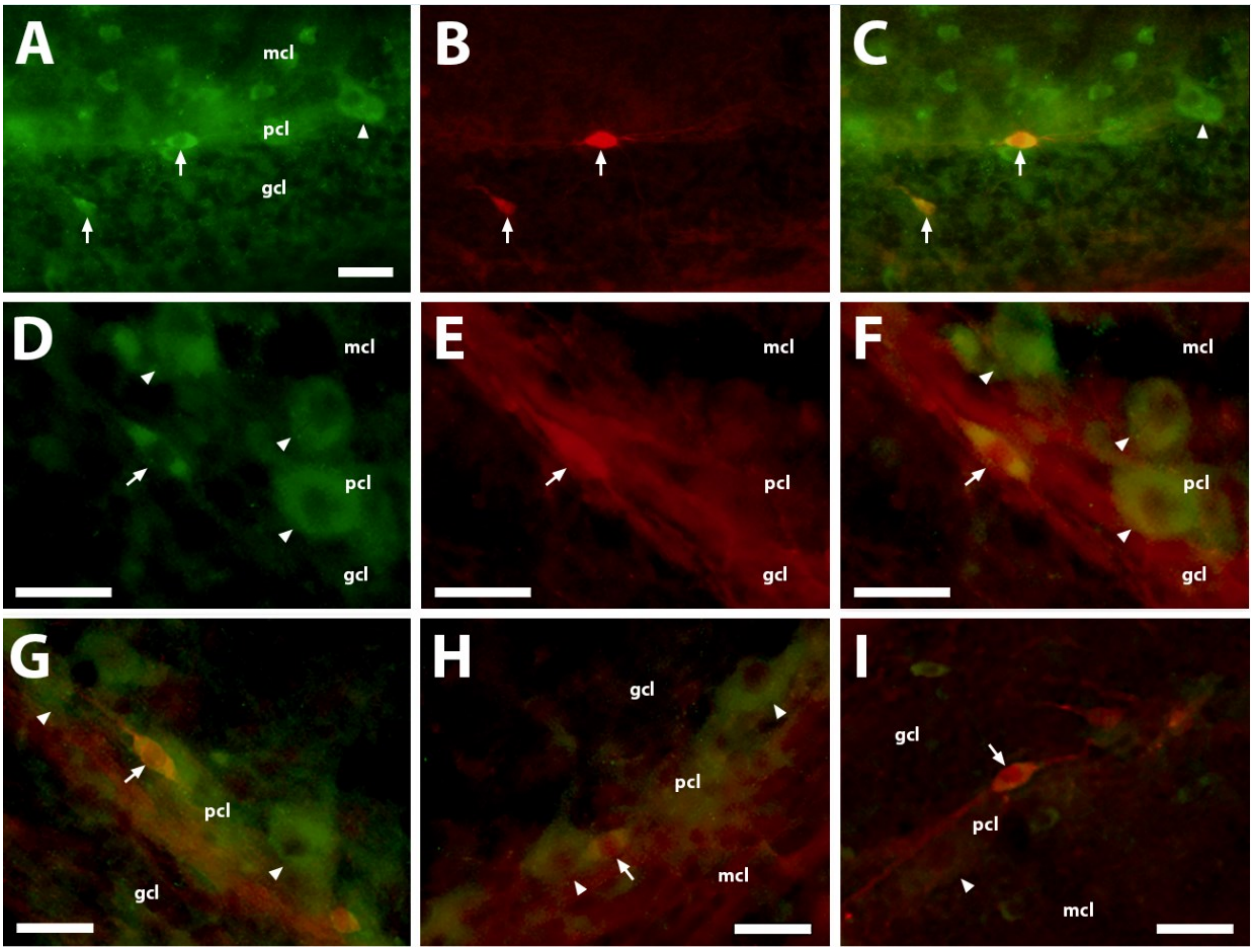

Figure 3.6 GAD and SCGN labelling in the cerebellum. A-C and **D-F** are shown as triptychs: GAD (**A,D**; green), secretagogin (**B,E**; SCGN; red) and the overlays (**C,F**). The yellow cells in **C** and **F** indicate that SCGN-immunopositive cells co-express GAD. In all others **(G-I)**, only the overlay is shown. Arrows indicated double-labelled cells whereas arrowheads indicate some Purkinje cells. mcl = molecular cell layer; pcl = Purkinje cell layer; gcl = granular cell layer. Scale bars = 25 μm in **A-I**.

3.2.3 *Calretinin and SCGN Labelling in Rat v. Pigeon*

As apparent Lugaro cells express SCGN in pigeons, we used the same immunohistochemical techniques to see whether SCGN is expressed by Lugaro cells in rats. Figure 3.7A,B shows a section through the rat cerebellum immunoprocessed for SCGN (red) and as well as CB (green) to visualize the PCs. There was no trace whatsoever of SCGN labelling in the cerebellum. However, this was not due to failure of the antibody as SCGN-expressing cells were seen in the central grey of the rat mesencephalon (Figure 3.7C). For comparison, pigeon CB and SCGN labelling is shown in Figure 3.7D.

Because Lugaro cells in the rat cerebellum express CR (Rogers, 1989; Lainé and Axelrad, 2002), we examined whether the apparent Lugaro cells that express SCGN in pigeons also expressed CR. Immunolabelling for CR is shown in the rat cerebellum (Figure 3.7E-J). We noted many fusiform cells in the gcl below the pcl, which were likely Lugaro cells (arrows in Figure3.7F-J). In coronal rat cerebellar sections, we noted CR-immunopositive parallel-like fibres coursing through the mcl (Figure 3.7E). In pigeons, the SCGN-immunolabelled cells did not express CR (Figure 7K-M).

3.2.4 *NADPH-diaphorase Staining*

NADPH-diaphorase (NADPH-d) selectively stains cells that contain nitric oxide synthase and thus nitric oxide. Lugaro cells in the rabbit cerebellum are known to contain nitric oxide and thus stain for NADPH-d (Okhotin and Kalinichenko, 2000), though in humans and cats they do not. We did not see any NADPH-d stained cell bodies in the pigeon cerebellum (Figure 3.8A), though we noted differential staining of the separate cerebellar layers, which has been previously

reported in the pigeon (Atoji et al., 2001). Some cells in the optic tectum were stained for NADPH-d (Figure 3.8B) indicating that the procedure was reliable.

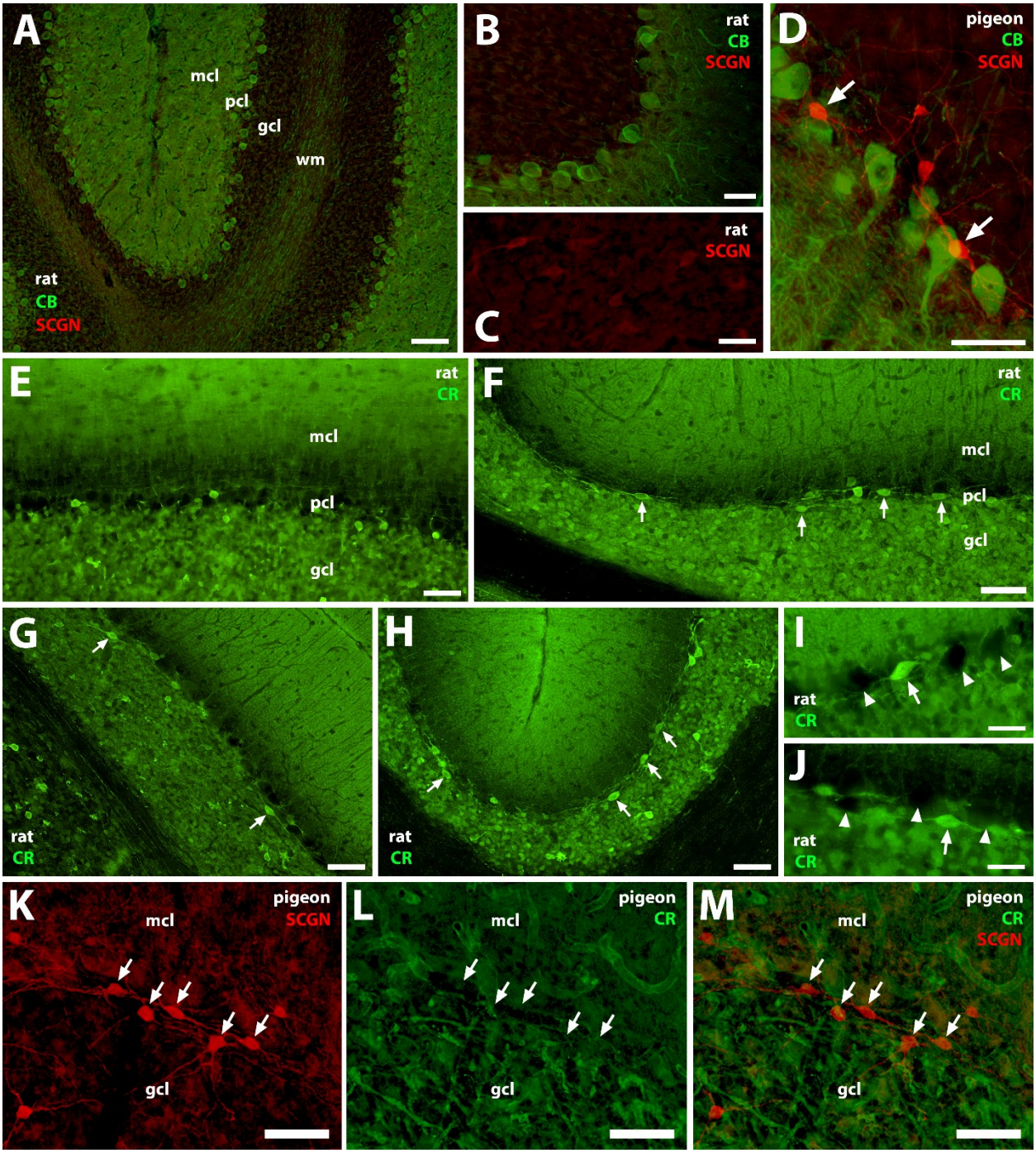

Figure 3.7 Calretinin (CR) and secretagogin (SCGN) labelling in rat and pigeon cerebellum. A,B show a coronal section through the rat cerebellum immunoprocessed for secretagogin (SCGN; red) and Calbindin-D28k (CB; green). Purkinje cells (PCs) express CB. There were no SCGN-immunopositive cells in the rat cerebellum. **C** shows SCGN

immunoreactive cells in the central grey of the rat mesencephalon. **D** shows SCGN and CB immunoreactivity in the pigeon cerebellum. **E-J** show calretinin (CR) immunoreactivity in the rat cerebellum. In the sagittal sections **(F-J)**, note the many fusiform Lugaro cells in the granular cell layer (gcl) below the Purkinje cell layer (pcl) (arrows). **E** is a coronal section where parallel-fibre-like axons can be seen in the molecular cell layer (mcl). **K-M** is a triptych of a sagittal pigeon section immunolabelled with SCGN (red) and CR (green). The SCGN-expressing cells in the pigeon cerebellum do not express CR. Arrows indicate supposed Lugaro cells; arrowheads indicate holes where PCs would be found. Scale bars = 25 μm **I,J**, 50 μm in **B-H,K-M**, 100 μm in **A**.

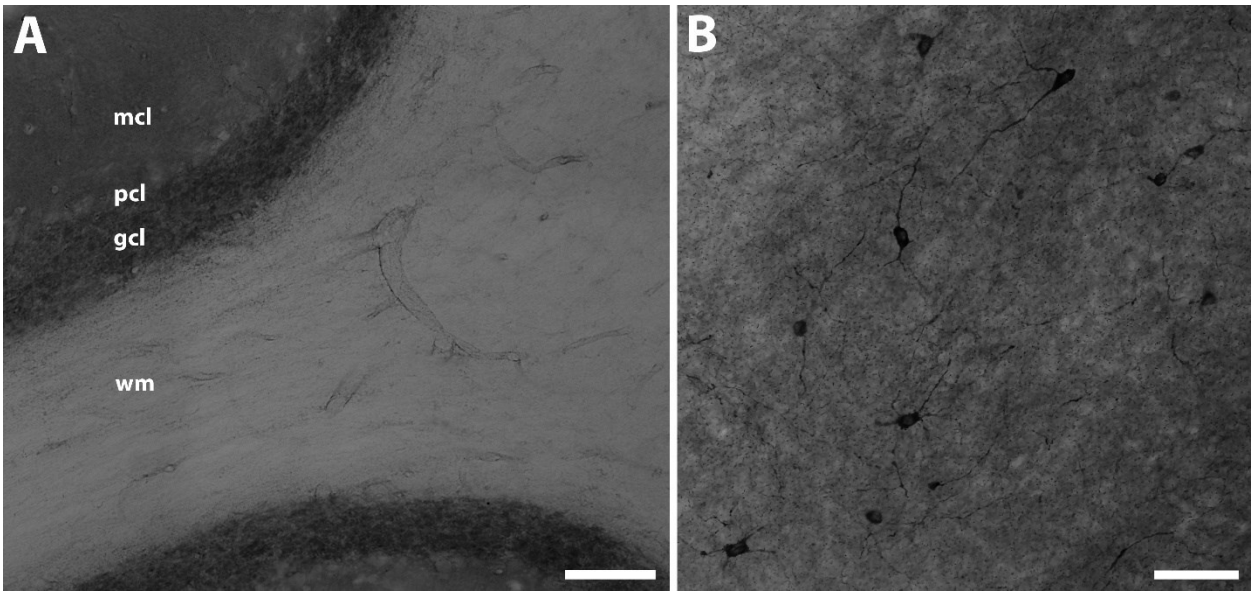

Figure 3.8 NADHP-diaphorase (NADPH-d) labelling in the pigeon optic tectum and cerebellum. **A** shows staining for nicotinamide adenine dinucleotide phosphate-diaphorase (NADPH-d) in a sagittal section of the pigeon cerebellum. **B** shows staining for NADPH-d in the optic tectum of the pigeon. There were no apparent NADPH-d-stained cells in the cerebellum, while the optic tectum did exhibit staining. mcl = molecular cell layer; plc = Purkinje cell layer; gcl = granular cell layer; wm = white matter. Scale bars 50 μm in **B**, 100 μm in **A**.

3.3 Discussion

Because calcium binding proteins parvalbumin (PV), CR and CB are expressed in the avian cerebellum (Bastianelli, 2003; Pakan et al., 2007; Wylie et al., 2011, 2013), we were interested in investigating the expression another calcium binding protein, SCGN. Classic immunohistochemical protocols failed to reveal SCGN immunolabelling in the cerebellum, as only a very faint trace of expression was noted (Figure 3.2A-C). However, after implementing an antigen retrieval protocol prior to immunoprocessing, SCGN immunoreactive cells became apparent (Figure 3.2H-J). We also used an amplification protocol requiring a biotin tyramide reaction and streptavidine as a fluorescent tag. In these cases, we noted a similar density of cerebellar labelling as with antigen retrieval (Figure 3.2E,F), so we are confident that the SCGN primary antibody was labelling SCGN-immunoreactive cells with antigen retrieval and not simply binding with miscellaneous antigens. Whereas PV is expressed mainly in PCs and mcl interneurons (Wylie et al., 2011), CB is expressed mainly in PCs (Bastianelli, 2003), and CR is expressed mainly in mossy fibres (Wylie et al., 2013), we found the SCGN was mainly expressed in large cells in the gcl.

3.3.1 *Characterization of SCGN-immunopositive cells*

When large SCGN-immunopositive cells in the gcl of the pigeon cerebellum were first noticed, we assumed them to be Golgi cells as given their size and location in the gcl, and the existence of Golgi cells in the pigeon cerebellum has long been known (Ramón y Cajal, 1911). Upon closer inspection, these cells exhibited a striking similarity to mammalian Lugaro cells in terms of both morphology and circuitry. Morphological similarities included fusiform somata

and bipolar dendrites extending parallel to the pcl in sagittal sections. Similarities in circuitry were also apparent as the SCGN-immunoreactivity revealed parallel-fibre-like axons in the mcl in coronal sections, which is characteristic of mammalian Lugaro cells (Lugaro, 1894; Fox, 1959; Lainé and Axelrad, 1996). Presumably, these axonal projections originated from the SCGN-labelled Lugaro cells and not from granule cells, as granule cells themselves were not immunoreactive for SCGN. Additionally, PC axon collaterals are known to synapse on mammalian Lugaro cells (Larramendi and Lemkey-Johnston, 1970; Lainé and Axelrad, 2002). Immunoprocessing for CB in the pigeon cerebellum showed CB-labelled varicosities on the SCGN-labelled somata near the pcl (Figure 3.4D,F,H). Presumably, these were PC axon collaterals as CB is mainly expressed in PCs.

Additionally, we found that SCGN labelled other large cells in the granular cells layer of the pigeon's cerebellum. These large cells did not resemble mammalian Lugaro cells as they either lacked the classic fusiform cells morphology and/or resided deeper in the molecular layer (Figure 3.3 and 3.4). It is possible that these correspond to Golgi cells, but could also correspond to a more recently described subtype of mammalian Lugaro cells described by Lainé and Axelrad (2002) in the rat cerebellum. These cells morphologically resemble Golgi cells, as they have globular somata, three to four long radiating dendrites, and are located at variable depths in the granular layer. However, these are thought to be Lugaro cells as they have axons that travel in to the molecular layer in similar fashion to fusiform Lugaro cells, and also receive axon collaterals from Purkinje cells. At least some of the SCGN-ir cells in the pigeon's cerebellum further from the Purkinje cells closely resemble this description (asteriks in Figure 3.4) and in several cases, CB positive varicosities can be seen in close proximity of the cell body (Figure 3.4G-I). This suggests that like calretinin in mammals, SCGN labels all types Lugaro cells in the pigeon

cerebellum. There are several SCGN-ir cells in the gcl, including on the border of the white matter, which do not appear to be innervated from PC axon collaterals. As such, we assume these to be Golgi cells (Palay and Chan-Palay, 1974).

3.3.2 *Comparison of Mammalian and Avian Lugaro cell Characteristics*

Though there were many striking similarities between the proposed avian Lugaro cells and their mammalian counterparts, there were some noted differences (resumed in Table 3.2). First, mammalian Lugaro cells are known to express CR, whereas pigeon Lugaro cells, however, do not (Figure 3.7K-M). Conversely, pigeon Lugaro cells express SCGN while rat Lugaro cells do not. In fact, there was no SCGN immunoreactivity noted in the rat cerebellum (Figure 3.7A,B). Finally, mammalian Lugaro cells may either contain nitric oxide or not, depending on the species in which they reside. In the cases that the cells contain nitric oxide, they are stained with NADPH-d. Interestingly, Lugaro cells in rabbits are stained by NADPH-d, while they are not stained in rats, cats, and humans. The Lugaro cells described in the one species of teleost were detected by NADPH-d staining (Pushchina and Varaksin, 2001). In the pigeon, although we noted differential staining of the neuropil in the cerebellar layers, there were no somata stained by NADPH-d (Figure 8A). This was not surprising as Atoji et al. (2001) described similar NADPH-d stain in the pigeon cerebellum. Thus, despite the striking similarities in circuitry and morphology, the putative Lugaro cells in pigeon cerebellum have clear neurochemical differences to those described in other vertebrates (Table 3.2).

The existence of Lugaro cells in aves is not surprising as the basic structure and circuitry of the cerebellar cortex is highly conserved among vertebrates (Ramón y Cajal, 1911). This

includes the connectivity among PCs, granule cells, and Golgi cells, basket and stellate cells, as well as unipolar brush cells (UBCs). Indeed, UBCs were first described in mammals (Mugnaini and Floris, 1994), and then were subsequently reported in an avian species (Takács et al., 1999). Interestingly, as with Lugaro cells, UBCs in mammalian and avian species are similar in their structure and circuitry, but different in terms neurochemistry. For example, mammalian UBCs express PLCB4, while their avian counterparts do not.

Table 3.2 Lugaro cell characteristics in different vertebrates.

Characteristic	Mammals	Pigeons	Teleosts
Calretinin-ir	+	–	?
Secretagogin-ir	–	+	?
GAD-ir	+	+	?
NADPH-diaphorase	+ / –*	–	+
Neurogranin-ir	–	–	?
mGluR2/3-ir	–		?
Fusiform somata	+	+	+
Bilateral horizontally oriented dendrites	+	+	+
Parallel-fiber-like axons	+	+	?
Innervation by Purkinje cell collaterals	+	+	?
Located in the gcl below the pcl	+	+	+

* Lugaro cells express NADPH-d in rabbits but not in rats, cats, or humans
ir = immunoreactivity; gcl = granular cell layer; pcl = Purkinje cell layer
+, present; –, absent; ?, unknown

3.3.3 *Calcium Binding Proteins in Lugaro cells*

Although they have several functions, a major task of calcium binding proteins (CBPs) is to regulate the amount of intracellular calcium by either sensing intracellular calcium levels, and/or by acting as cytosolic buffers to dissipate local calcium, as an overabundance of calcium results in neuronal death from excessive neuronal excitation (Alpár et al., 2012). Parvalbumin and Calbindin-D28k (CB) for instance, acts to buffer cytosolic calcium, while SCGN has been suggested to act as an intracellular calcium sensor as it undergoes structural changes upon binding calcium (Alpár et al., 2012). Similarly to SCGN, CR may also have calcium-sensing properties as it also undergoes conformational changes when binding calcium (Palczewska et al., 2005), but unlike SCGN it has also been reported to act as a calcium buffer (Billing-Marczak and Kuźnicki, 1999).

CBPs are particularly prevalent in the cerebellum as PCs are at risk for glutamate excitotoxicity (Slemmer et al., 2004). As previously discussed, pigeon Lugaro cells do not express CR, but express SCGN, whereas the contrary is true for their mammalian counterparts. It may be that CR has been replaced by SCGN in avian Lugaro cells, as both of these proteins have the ability to function in sensing intracellular calcium levels (Alpár et al., 2012). It is possible that calcium buffering in the pigeon Lugaro cells is not as important as in their mammalian counterparts, as SCGN shows evidence for function as a calcium sensor and not a buffer, whereas CR may also able to buffer (Palczewska et al., 2005; Alpár et al., 2012). It is also possible that pigeon Lugaro cells use a different mechanism to fulfill the calcium buffering role.

3.3.4 *Evolution of Mammalian and Avian Lugaro cells*

As Lugaro cells seem to be present in both aves and mammals, it begs the question as to whether their presence is a case of convergent evolution or homology. If it is a case of homology, it may be that mammalian and avian Lugaro cells have retained the morphological characteristics and connections, but evolved different neurochemical profiles. Alternatively, it is possible that this cell type and circuitry is an example of convergent evolution. In this case, neurochemically different cells evolved to have common morphology and connectivity. Because the presence of Lugaro cells has also seen suggested in one species of teleost (Pushchina and Varaksin, 2001), we would argue that Lugaro cells are homologous in different species. It is unlikely that they would have evolved similarly in three separate instances, and the neurochemical profiles are likely derivative (Striedter, 2005).

3.3.5 *Conclusion*

Lugaro cells, a characteristic feature of the mammalian cerebellar cortex, have not been described in the cerebellum of birds or non-avian reptiles. In the present study, using SCGN expression in the avian cerebellum, we observed inhibitory cells in the gcl near the pcl that exhibit the morphological features and connectivity of mammalian Lugaro cells. They are characterised by a fusiform cell body with bipolar dendrites projecting in the sagittal plane, parallel-fibre-like axons projecting transversely through the mcl, and theses cells are innervated by PC axon collaterals. We argue that these are Lugaro cells although they have a different neurochemical profile than mammalian Lugaro cells. The presence of Lugaro cells in the avian

cerebellum provides an additional piece of evidence towards cerebellar conservation in vertebrate species.

3.4 References

Alpár A, Attems J, Mulder J, Hökfelt T, Harkany T (2012) The renaissance of Ca2+-binding proteins in the nervous system: secretagogin takes center stage. Cell Signal 24:378–387.

Ashwell KWS, Paxinos G, Watson CRR (2007) Cyto- and Chemoarchitecture of the Cerebellum of the Short-Beaked Echidna *(Tachyglossus aculeatus)*. Brain Behav Evol 70:71–89.

Atoji Y, Yamamoto Y, Suzuki Y (2001) Distribution of NADPH diaphorase-containing neurons in the pigeon central nervous system. J Chem Neuroanat 21:1–22.

Bastianelli E (2003) Distribution of calcium-binding proteins in the cerebellum. Cerebellum 2:242–262.

Billing-Marczak K, Kuźnicki J (1999) Calretinin - Sensor or buffer - Function still unclear. Pol J Pharmacol 51:173–178.

Braak H (1974) On the intermediate cells of lugaro within the cerebellar cortex of man - A pigmentarchitectonic study. Cell Tissue Res 149:399–411.

Dieudonné S, Dumoulin A (2000) Serotonin-driven long-range inhibitory connections in the cerebellar cortex. J Neurosci 20:1837–1848.

Fischer AJ, Stell WK (1999) Nitric oxide synthase-containing cells in the retina, pigmented epithelium, choroid, and sclera of the chick eye. J Comp Neurol 405:1–14.

Fox CA (1959) The intermediate cells of Lugaro in the cerebellar cortex of the monkey. J Comp Neurol 112:39–53.

Gáti G, Lendvai D, Hökfelt T, Harkany T, Alpár A (2014) Revival of calcium-binding proteins for neuromorphology: Secretagogin typifies distinct cell populations in the avian brain. Brain Behav Evol 83:82–92.

Golgi C (1903) Sulla fina anatomia del cervelleto umano. In: Opera omnia, pp 99–111. Milan, Italy: Ulrico Hoepli.

Lainé J, Axelrad H (1996) Morphology of the Golgi-impregnated Lugaro cell in the rat cerebellar cortex: A reappraisal with a description of its axon. J Comp Neurol 375:618–640.

Lainé J, Axelrad H (2002) Extending the cerebellar Lugaro cell class. Neuroscience 115:363–374.

Larramendi LMH, Lemkey-Johnston N (1970) The distribution of recurrent purkinje collateral synapses in the mouse cerebellar cortex: An electron microscopic study. J Comp Neurol 138:451–482.

Lugaro E (1894) Sulle connessioni tra gli elementi nervosi della corteccia cerebellare con considerazioni generali sul signifcato fisiologico dei rapporti tra gli elementi nervosi. Riv Sper Freniatr Med Leg Alien Ment 20:297–331.

Mugnaini E, Floris A (1994) The unipolar brush cell: A neglected neuron of the mammalian cerebellar cortex. J Comp Neurol 339:174–180.

Okhotin VE, Kalinichenko SG (2000) Localization of NO synthase in Lugaro cells and the mechanisms of NO-ergic interaction between inhibitory interneurons in the rabbit cerebellum. Neurosci Behav Physiol 30:525–533.

Pakan JMP, Iwaniuk AN, Wylie DR, Hawkes R, Marzban H (2007) Purkinje cell compartmentation as revealed by Zebrin II expression in the cerebellar cortex of pigeons (Columba livia). J Comp Neurol 501:619–630.

Palay SL, Chan-Palay V (1974) Cerebellar Cortex: cytology and organization.

Palczewska M, Batta G, Groves P, Linse S, Kuznicki J (2005) Characterization of calretinin I-II as an EF-hand, Ca2+, H+-sensing domain. Protein Sci 14:1879–1887.

Pushchina E V, Varaksin AA (2001) Argyrophilic and nitroxydergic bipolar neurons (Lugaro cells) in the cerebellum of Pholidapus dybowskii. Zh Evol Biokhim Fiziol 37:437–441.

Ramón S, Cajal S (1911) Histologie du système nerveux de l'homme et des vertébrés. Paris: Maloine.

Rogers JH (1989) Immunoreactivity for calretinin and other calcium-binding proteins in cerebellum. Neuroscience 31:711–721.

Sahin M, Hockfield S (1990) Molecular identification of the lugaro cell in the cat cerebellar cortex. J Comp Neurol 301:575–584.

Schilling K, Oberdick J, Rossi F, Baader SL (2008) Besides Purkinje cells and granule neurons: An appraisal of the cell biology of the interneurons of the cerebellar cortex. Histochem Cell Biol 130:601–615.

Simat M, Parpan F, Fritsch JM (2007) Heterogeneity of glycinergic and gabaergic interneurons in the granule cell layer of mouse cerebellum. J Comp Neurol 500:71–83.

Singec I, Knoth R, Ditter M, Frotscher M, Volk B (2003) Neurogranin expression by cerebellar neurons in rodents and non-human primates. J Comp Neurol 459:278–289.

Slemmer JE, De Zeeuw CI, Weber JT (2004) Don't get too excited: Mechanisms of glutamate-mediated Purkinje cell death. Prog Brain Res 148:367–390.

Striedter GF (2005) Priciples of brain evolution.

Takács J, Markova L, Borostyánköi Z, Görcs TJ, Hámori J (1999) Metabotrop glutamate receptor type 1a expressing unipolar brush cells in the cerebellar cortex of different species: A comparative quantitative study. J Neurosci Res 55:733–748.

Wylie DR, Gutierrez-Ibanez C, Graham DJ, Kreuzer MB, Pakan JMP, Iwaniuk AN (2011) Heterogeneity of parvalbumin expression in the avian cerebellar cortex and comparisons with zebrin II. Neuroscience 185:73–84.

Wylie DR, Jensen M, Gutierrez-Ibanez C, Graham DJ, Iwaniuk AN (2013) Heterogeneity of calretinin expression in the avian cerebellar cortex of pigeons and relationship with zebrin II. J Chem Neuroanat 52:95–103.

Chapter 4: **Summary and Future Direction**

Though highly conserved among species, there are still differences in avian and mammalian cerebella, and as such, the pigeon cerebellum has been questioned as a useful model. Here, we were able to show that two apparent differences between mammalian and avian cerebella were somewhat false. First, mammalian cerebellar regions denoted by ZII+ and ZII- immunohistochemistry are innervated by discreet olivary subnuclei, whereas it has been suggested that some ZII+/- stripe pairs receive input form the same olivary subregions in pigeons. Second, the existence of Lugaro cells has only been confirmed in the mammalian cerebellum (refs). To address the first apparent discrepancy, we were able to build on the study by Wylie et al. (2017) on olivary input to ZII stripes in the flocculus and investigate olivary-cerebellar connections in the uvula. We confirmed that ZII+ and ZII- stripes receive input from discreet regions in the mcIO. This aligns with what has been reported in mammalian literature, being that an olivary subnucleus innervate either a ZII+ or ZII- stripe, but never both (Voogd et al., 2003; Sugihara and Shinoda, 2004; Voogd and Ruigrok, 2004; Pijpers et al., 2006; Sugihara and Quy, 2007). Towards the second discrepancy, we argue for the presence of Lugaro cells in the pigeon cerebellum. Taken together, these projects demonstrate further concordance between mammalian and avian cerebellar systems.

4.1 Summary of Chapters

In Chapter 2, we took advantage of the well-defined description of the cerebellar optic flow zones in pigeons, and the fact that they coincide with ZII stripes, to investigate the organization of olivary inputs into the ventral uvula. The cerebellar pattern of ZII expression is highly conserved and exhibits seven pairs of interdigitated ZII+ and ZII- stripes from P1+/- to P7+/- (for review see Hawkes and Herrup, 1995). It has been determined from previous research that the medial-most ZII stripes (P1+/- to P2+/-) correspond to the translational optic flow zones responding to *contraction, expansion, ascent,* and *descent* patterns of optic flow (Wylie and Frost, 1991,1993; Wylie et al., 1998; Graham and Wylie, 2012). A recent paper from our lab has shown that inputs into the ZII+ and ZII- stripes of the floccular optic flow zones (P4+/- to P7+/-) receive differential input from adjacent areas of mcIO (Wylie et al., 2017). Wylie et al. (2017) found that the inputs to the ZII+ and ZII− stipes in the flocculus receive CF input from separate, but adjacent areas of the inferior olive. The ZII+ stripes of the VA zones (P4+ and P6+) receive input from the caudal-most portion of the mcIO while the ZII− stripes of the VA zones (P4− and P6−) are innervated by a slightly more rostral region. Similarly, the region of the mcIO projecting to the ZII+ stripes of the HA zones is located caudal to the mcIO region projecting to the ZII− stripes of the HA zones (Wylie et al., 2017). Thus, although a ZII+/− stripe pair represents a functional unit in the flocculus whereby all PCs respond to the same pattern of optic flow (either VA or HA), the ZII+ and ZII− stripes received optic flow from different areas of the IO. We wanted to investigate whether this same pattern holds true for the uvula.

To do so, we injected different colours of CTB (red and green; anterograde tracer) into adjacent ZII+ and ZII- stripes. We used a handheld stimulus to simulate optic flow in the anesthetised pigeon and recorded electrophysiological responses to determine the approximate

location of our electrode (i.e., from which ZII stripe we were recording). We used immunohistochemistry to label ZII and confirm the location of our injection sites. We were also able to examine the retrograde labelled cells from each CTB injection and compare the results from injections in the different ZII stripes. We found that the contraction zone (P1+/P1-med) was innervated by the caudal-most lateral mcIO en masse, but the P1+ zone received input from the most caudal end while the P1–med zone received input from a slightly more rostral region. The expansion/ascent zone received projections from the middle lateral mcIO en masse, but the region projecting to the P1–lat stripe was caudal to that projecting to the P2+med stripe. Finally, the descent zone was innervated by the rostral lateral mcIO en masse, but the projections to P2+lat came from a region of the mcIO that was slightly more caudal to that region innervating the P2− stripe. These data suggested that discreet, yet adjacent regions of the inferior olive innervate neighbouring ZII stripes of a functional pair. These results mirror those of Wylie et al. 2017, and also align with the mammalian literature stating that discreet olive subnuclei project to either a ZII+ or ZII- stripe (Voogd et al., 2003; Sugihara & Shinoda, 2004; Voogd & Ruigrok, 2004; Pijpers et al., 2006; Sugihara & Quy, 2007).

In Chapter 3, we suggest that Lugaro cells, inhibitory cerebellar interneurons, are found in the pigeon cerebellum, although previously theses have only been described in several mammalian species and in one species of teleost (ref). Lugaro cells are found in the granular cell layer, just below the Purkinje cell layer (Fox, 1959). They are characterized by a multitude of features including a fusiform somata, horizontally projecting dendrites, proximity to the pcl, long axonal projections into the mcl running parallel to granule cell parallel fibres, and innervation by PC axon collaterals. A newer, globular type of Lugaro cell has also been decribed based on their immunoreactivity for calretinin, their axonal projection pattern and wiring, and their innervation

by Purkinje axon collaterals (Lainé and Axelrad, 2002). Upon investigating the expression of the calcium binding protein SCGN in the pigeon VbC, we noticed a novel type of cell that was SCGN-immunoreactive. Many of these cells exhibited similar charchterics to mammalian Lugaro cells indluding a fusiform shape, horizontally projecting dendrites, proximity to the pcl, and long axons coursing parallel to parallel fibres in the mcl (Fox, 1959; Lugaro, 1894; Lainé and Axelrad, 1996). Other SCGN-ir cells resembled the globular Lugaro cells described by Lainé and Axelrad (2002). To proble the molecular characteristics of these proposed avian Lugaro cells, we immunoreacted pigeon cerebellar sections with various antibodies known to label Lugaro cells in mammals. Calretinin is known to be expressed by mammalian Lugaro cells (Rogers, 1989), however, it did not label Luagaro cells in pigeons. We also treated sections of rat cerebellum with anti-SCGN antibodies, but there were no SCGN-labelled cells in the rat cerebellum. Another discrepancy between the mammalian and avian Lugaro cells is the apparent lack of nitric oxide synthase-expressing cells in pigeons. GAD labelling confirmed that the pigeon Lugaro cells are inhibitory, while Calbindin-D28k labelling confirmed the presence of Lugaro cell innervation by PC axon collaterals, which has been established to also be the case in mammals (Larramendi and Lemkey-Johnston, 1970; Lainé and Axelrad, 2002). Although there appear to be some key differences in the molecular characteristics between mammalian Lugaro cells and SCGN-labelled avian cells, we propose that the SCGN-expressing cells are of the Lugaro cell class based on their morphological characteritics, location in the gcl (proximity to the pcl), their parallel-fibre-like axons projecting though the mcl, and their innervation by PC axon collaterals.

4.2 Future Directions

Many interesting questions can be addressed in extending the work presented in this thesis. While in Chapter 2 we focused on discerning the input into ZII+ and ZII- stripes of a functional pair, the next natural step would be to investigate the nature of the efferent projections from the ZII stripes to the vestibular and cerebellar nuclei. As the projections into the separate ZII stripes originated from discreet regions of the inferior olive, we would expect discreet regions of the vestibular and cerebellar nuclei to be innervated by PCs in either ZII stripe. There is evidence that this is the case in both birds and mammals (Wylie et al., 2012; Look for info on ZII stripes to nuclei in mammals to compare). Moreover, there is some evidence that the ZII+ and ZII- terminals innervate different types of cerebellar circuits (Long et al., 2018). Long et al. (2018) showed that ZII+ PCs are more sensitive to optic flow and project to areas of the vestibular nuclei that provide inhibitory feedback to the inferior olive, while ZII- PCs do not.

Though we used a host of immunohistochemical protocols to argue for the presence of Lugaro cells in the avian cerebellum (Chapter 3), we plan to immunolabel for additional markers to further our evidence. Dieudonné and Dumoulin (2000) suggest that serotonin-driven inhibition of Golgi cells arises through the excitation of Lugaro cells. Lugaro cells are thought to be the intermediate cells in this circuit as Purkinje cells and Golgi cells do not contact Goligi cells, and Lugaro cells appear to be selectively excited by serotonin in a slice. Immunolabelling for serotonergic terminals on the proposed Lugaro cells in the pigeon cerebellum would provide further evidence for these cells being of the Lugaro cell class. Additionally, mammalian Golgi and Lugaro cells can be distinguished from one another in their expression of mGluR2 and neurogranin. Golgi cells have been found to express either or both of these two markers, while Lugaro cells lack both (Simat et al., 2007). Immunoprocessing of pigeon cerebellar tissue for

mGluR2, neurogranin, and SCGN would help to differentiate between Lugaro and Golgi cells in the pigeon cerebellar cortex.

As in Chapter 3 we suggest the presence of Lugaro cells in the avian cerebellum, it would also be of interest to investigate the presence of other cerebellar cell types in the pigeon. Candelabrum cells are another type or cerebellar interneuron that have not been described in an avian species, but their existence is probable as cerebellar circuitry is highly conserved and we have seen evidence for the many other cells types that exist.

It may also be of interest to compare the SCGN-ir in other reptilian species such as alligators and lizards. Should SCGN-ir reveal Lugaro-like cells, this would provide additional evidence for the existence of Lugaro cells in non-mammalian vertebrates. This would also lend towards the idea of reptilian Lugaro cells as homologous to their mammalian counter parts and not a result of convergent evolution.

4.3 Conclusion

While there are many similarities between the avian and mammalian cerebellum, there are also some apparent differences. In this thesis, we addressed two of these apparent differences, namely the difference in olivary projections to zebrin II stripes in the cerebellum and the existence of Lugaro cells in the mammals but not in aves. We showed that the connectivity from the olive to the cerebellum in mammals and pigeons is more similar than was previously thought. Based on a multitude of shared characteristics, we also propose that Lugaro cells do exist in avian species. Taken together, these data offer additional evidence towards the conserved

nature of the cerebellum across species, and further aid in the validation of the pigeon as an animal model for cerebellar processes.

4.4 References

Fox CA (1959) The intermediate cells of Lugaro in the cerebellar cortex of the monkey. J Comp Neurol 112:39–53.

Graham DJ, Wylie DR (2012) Zebrin-Immunopositive and -Immunonegative Stripe Pairs Represent Functional Units in the Pigeon Vestibulocerebellum. J Neurosci 32:12769–12779.

Hawkes R, Herrup K (1995) Aldolase C/zebrin II and the regionalization of the cerebellum. J Mol Neurosci 6:147–158.

Lainé J, Axelrad H (1996) Morphology of the Golgi-impregnated Lugaro cell in the rat cerebellar cortex: A reappraisal with a description of its axon. J Comp Neurol 375:618–640.

Lainé J, Axelrad H (2002) Extending the cerebellar Lugaro cell class. Neuroscience 115:363–374.

Larramendi LMH, Lemkey-Johnston N (1970) The distribution of recurrent purkinje collateral synapses in the mouse cerebellar cortex: An electron microscopic study. J Comp Neurol 138:451–482.

Long RM, Pakan JMP, Graham DJ, Hurd PL, Gutierrez-Ibanez C, Wylie DR. (2018) Modulation of complex spike activity differs between zebrin positive and negative Purkinje cells in the pigeon cerebellum. J Neurophysiol. doi: 10.1152/jn.00797.2017

Lugaro E (1894) Sulle connessioni tra gli elementi nervosi della corteccia cerebellare con considerazioni generali sul signifcato fisiologico dei rapporti tra gli elementi nervosi. Riv Sper Freniatr Med Leg Alien Ment 20:297–331.

Pijpers A, Apps R, Pardoe J, Voogd J, Ruigrok TJH (2006) Precise Spatial Relationships between Mossy Fibers and Climbing Fibers in Rat Cerebellar Cortical Zones. J Neurosci 26:12067–12080

Rogers JH (1989) Immunoreactivity Calcium-Binding for Calretinin and Other Proteins in Cerebellum. 31:711–721.

Sugihara I, Quy PN (2007) Identification of aldolase C compartments in the mouse cerebellar cortex by olivocerebellar labeling. J Comp Neurol 500:1076–1092

Sugihara I, Shinoda Y (2004) Molecular, Topographic, and Functional Organization of the Cerebellar Cortex: A Study with Combined Aldolase C and Olivocerebellar Labeling. J Neurosci 24:8771–8785

Voogd J, Pardoe J, Ruigrok TJH, Apps R (2003) The distribution of climbing and mossy fibre collateral branches from the copula pyramidis and the paramedian lobule: congruence of climbing fibre cortical zones and the pattern of zebrin banding within the rat cerebellum. J Neurosci 23:4645–4656

Voogd J, Ruigrok TJH (2004) The organization of the corticonuclear and olivocerebellar climbing fibre projections to the rat cerebellar vermis: The congruence of projection zones and the zebrin pattern. J Neurocytol 33:5–21.

Wylie DR, Bischof WF, Frost BJ (1998) Common reference frame for neural coding of translational and rotational optic flow. Nature 392:278–282

Wylie DR, and Frost BJ (1991) Purkinje cells in the vestibulocerebellum of the pigeon respond best to either translational or rotational wholefield visual motion. Exp Brain Res 86: 229–232. doi:10.1007/BF00231059.

Wylie DR, Frost BJ (1993) Responses of pigeon vestibulocerebellar neurons to optokinetic stimulation. II. The 3-dimensional reference frame of rotation neurons in the flocculus. J Neurophysiol 70:2647–2659

Wylie DR, Gutiérrez-Ibáñez C, Corfield JR, Craciun I, Graham DJ, Hurd PL (2017) Inferior olivary projection to the zebrin II stripes in lobule IXcd of the pigeon flocculus: A retrograde tracing study. J Comp Neurol 525:3158–3173.

Wylie DR, Pakan JMP, Huynh H, Graham DJ, Iwaniuk AN (2012) Distribution of zebrin-immunoreactive Purkinje cell terminals in the cerebellar and vestibular nuclei of birds. J Comp Neurol 520:1532–1546. doi:10.1002/cne.22810.

5.1 Bibliography

Ahn AH, Dziennis S, Hawkes R, Herrup K (1994) The cloning of zebrin II reveals its identity with aldolase C. *Development* 120:2081–2090.

Akintunde A, Eisenman LM (1994) External cuneocerebellar projection and Purkinje cell zebrin II bands: A direct comparison of parasagittal banding in the mouse cerebellum. *J. Chem. Neuroanat* 7:75–86.

Alpár A, Attems J, Mulder J, Hökfelt T, Harkany T (2012) The renaissance of Ca2+-binding proteins in the nervous system: secretagogin takes center stage. *Cell Signal* 24:378–387.

Apps R, Garwicz M (2005) Anatomical and physiological foundations of cerebellar information processing. *Nat Rev Neurosci* 6:297–311.

Arends JJA, Voogd J (1989) Topographic aspects of the olivocerebellar system in the pigeon. In: Experimental Brain Research Series 17: The olivocerebellar system in motor control (Stata P, ed), pp 52–57.

Armstrong CL, Hawkes R (2000) Pattern formation in the cerebellar cortex. *Biochem Cell Biol* 78:551–562.

Ashwell KWS, Paxinos G, Watson CRR (2007) Cyto- and Chemoarchitecture of the Cerebellum of the Short-Beaked Echidna *(Tachyglossus aculeatus)*. *Brain Behav Evol* 70:71–89.

Atoji Y, Yamamoto Y, Suzuki Y (2001) Distribution of NADPH diaphorase-containing neurons in the pigeon central nervous system. *J Chem Neuroanat* 21:1–22.

Bastianelli E (2003) Distribution of calcium-binding proteins in the cerebellum. *Cerebellum* 2:242–262.

Billing-Marczak K, Kuźnicki J (1999) Calretinin - Sensor or buffer - Function still unclear. *Pol J Pharmacol* 51:173–178.

Braak H (1974) On the intermediate cells of lugaro within the cerebellar cortex of man - A pigmentarchitectonic study. *Cell Tissue Res* 149:399–411.

Brochu G, Maler L, Hawkes R (1990) Zebrin II: A polypeptide antigen expressed selectively by purkinje cells reveals compartments in rat and fish cerebellum. *J Comp Neurol* 291:538–552.

Bronstein AM (2004) Vision and vertigo: Some visual aspects of vestibular disorders. *J Neurol* 251:381–387.

Broussard DM, Titley HK, Antflick J, Hampson DR (2011) Motor learning in the VOR: the cerebellar component. *Exp Brain Res* 210:451–463. doi: 10.1007/s00221-011-2589-z.s

Chockkan V, Hawkes R (1994) Functional and antigenic maps in the rat cerebellum: Zebrin compartmentation and vibrissal receptive fields in lobule IXa. *J Comp Neurol* 345:33–45. doi:10.1002/cne.903450103.

Corfield JR, Kolominsky J, Craciun I, Mulvany-Robbins BE, Wylie DR (2016) Is cerebellar architecture shaped by sensory ecology in the New Zealand Kiwi (Apteryx mantelli)? *Brain Behav Evol* 87:88–104.

Corfield JR, Kolominsky J, Marin GJ, Craciun I, Mulvany-Robbins BE, Iwaniuk AN, Wylie DR (2015) Zebrin II expression in the cerebellum of a paleognathous bird, the Chilean tinamou (Nothoprocta perdicaria). *Brain Behav Evol* 85:94–106.

Crowder NA, Winship IR, Wylie DRW (2000) Topographic organization of inferior olive cells projecting to translational zones in the vestibulocerebellum of pigeons. *J Comp Neurol* 419:87–95.

Crowder NA, Wylie DR (2001) Fast and slow neurons in the nucleus of the basal optic root in pigeons. *Neurosci Lett* 304:133–136.

Crowder NA, Wylie DR (2002) Responses of optokinetic neurons in the pretectum and accessory optic system of the pigeon to large-field plaids. *J Comp Physiol A* 188:109–119.

De Zeeuw CI, Wylie DR, Digiorgi PL, Simpson JI (1994) Projections of individual purkinje cells of identified zones in the flocculus to the vestibular and cerebellar nuclei in the rabbit. *J Comp Neurol* 349:428–447. doi:10.1002/cne.903490308.

Dieudonné S, Dumoulin A (2000) Serotonin-driven long-range inhibitory connections in the cerebellar cortex. *J Neurosci* 20:1837–1848.

du Lac S, Raymond JL, Sejnowski TJ, Lisberger SG (1995) Learning and memory in the vestibulo-ocular reflex. *Annu Rev Neurosci* 18:409-441.

Ebner TJ, WangX, Gao W, Cramer SW, Chen G (2012) Parasagittal Zones in the Cerebellar Cortex Differ in Excitability, Information Processing, and Synaptic Plasticity. *The Cerebellum* 11:418–419.

Fischer AJ, Stell WK (1999) Nitric oxide synthase-containing cells in the retina, pigmented epithelium, choroid, and sclera of the chick eye. *J Comp Neurol* 405:1–14.

Fox CA (1959) The intermediate cells of Lugaro in the cerebellar cortex of the monkey. *J Comp Neurol* 112:39–53.

Gao W, Chen G, Reinert KC, Ebner TJ (2006) Cerebellar cortical molecular layer inhibition is organized in parasagittal zones. *J Neurosci* 26:8377–8387. doi:10.1523/JNEUROSCI.2434-06.2006.

Gáti G, Lendvai D, Hökfelt T, Harkany T, Alpár A (2014) Revival of calcium-binding proteins for neuromorphology: Secretagogin typifies distinct cell populations in the avian brain. *Brain Behav Evol* 83:82–92.

Gibson JJ (1954) The visual perception of objective motion and subjective movement. *Psychol Rev* 61:304–314.

Giolli RA, Blanks RHI, Lui F (2006) The accessory optic system: basic organization with an update on connectivity, neurochemistry, and function. In: Progress in brain research, pp 407–440.

Golgi C (1903) Sulla fina anatomia del cervelleto umano. In: Opera omnia, pp 99–111. Milan, Italy: Ulrico Hoepli.

Graham DJ, Wylie DR (2012) Zebrin-Immunopositive and -Immunonegative Stripe Pairs Represent Functional Units in the Pigeon Vestibulocerebellum. *J Neurosci* 32:12769–12779.

Gravel C, Hawkes R. (1990) Parasagittal organization of the rat cerebellar cortex: Direct comparison of purkinje cell compartments and the organization of the spinocerebellar projection. *J Comp Neurol* 291:79–102. doi:10.1002/cne.902910107.

Hawkes R (2014) Purkinje cell stripes and long-term depression at the parallel fibre-Purkinje cell synapse. *Front Syst Neurosci* 8:41. doi:10.3389/fnsys.2014.00041.

Hawkes R, Gravel C (1991) The modular cerebellum. *Prog Neurobiol* 36:309–327. doi:10.1016/0301-0082(91)90004-K.

Hawkes R, Herrup K (1995) Aldolase C/zebrin II and the regionalization of the cerebellum. *J Mol Neurosci* 6:147–158.

Herrup K, Kuemerle B (1997) The compartmentalization of the cerebellum. *Annu Rev Neurosci* 20:61–90.

Ibbotson MR, Price NSC (2001) Spatiotemporal tuning of directional neurons in mammalian and avian pretectum: a comparison of physiological properties. *J Neurophysiol* 86:2621–2624.

Itō M (1984) The cerebellum and neural control. New York : Raven Press.

Iwaniuk AN, Marzban H, Pakan JMP, Watanabe M, Hawkes R, Wylie DR (2009) Compartmentation of the cerebellar cortex of hummingbirds (Aves: Trochilidae) revealed by the expression of zebrin II and phospholipase Cβ4. *J Chem Neuroanat* 37:55–63.

Ji Z, and Hawkes R (1994) Topography of purkinje cell compartments and mossy fibre terminal fields in lobules ii and iii of the rat cerebellar cortex: Spinocerebellar and cuneocerebellar projections. *Neuroscience* 61:935–954. doi:10.1016/0306-4522(94)90414-6.

Karten HJ, Hodos W (1967) *A Stereotaxic Atlas of the Brain of the Pigeon (Columbia livia)*. Baltimore Md.: Johns Hopkins Press doi:10.2307/1421283.

Lainé J, Axelrad H (1996) Morphology of the Golgi-impregnated Lugaro cell in the rat cerebellar cortex: A reappraisal with a description of its axon. *J Comp Neurol* 375:618–640.

Lainé J, Axelrad H (2002) Extending the cerebellar Lugaro cell class. *Neuroscience* 115:363–374.

Lange W (1975) Cell number and cell density in the cerebellar cortex of man and some other mammals. *Cell Tissue Res* 157:115–124.

Larner AJ (1997) The Cerebellum in alzheimer's disease. *Dement Geriatr Cogn Disord* 8:203–209.

Larramendi LMH, Lemkey-Johnston N (1970) The distribution of recurrent purkinje collateral synapses in the mouse cerebellar cortex: An electron microscopic study. *J Comp Neurol* 138:451–482.

Larsell O (1967) The comparative anatomy and histology of the cerebellum: from myxinoids through birds. Minneapolis: University of Minnesota Press.

Lau KL, Glover RG, Linkenhoker B, and Wylie DR (1998) Topographical organization of inferior olive cells projecting to translation and rotation zones in the vestibulocerebellum of pigeons. *Neuroscience* 85:605–614.

Leclerc N, Schwarting GA, Herrup K, Hawkes R, Yamamoto M (1992) Compartmentation in mammalian cerebellum: Zebrin II and P-path antibodies define three classes of sagittally organized bands of Purkinje cells. *Proc Natl Acad Sci* 89:5006–5010.

Llinás R, Sasaki K (1989) The Functional Organization of the Olivo-Cerebellar System as Examined by Multiple Purkinje Cell Recordings. *Eur J Neurosci* 1:587–602.

Long RM, Pakan JMP, Graham DJ, Hurd PL, Gutierrez-Ibanez C, Wylie DR. (2018) Modulation of complex spike activity differs between zebrin positive and negative Purkinje cells in the pigeon cerebellum. J Neurophysiol. doi: 10.1152/jn.00797.2017

Lugaro E (1894) Sulle connessioni tra gli elementi nervosi della corteccia cerebellare con considerazioni generali sul signifcato fisiologico dei rapporti tra gli elementi nervosi. *Riv Sper Freniatr* 20:297–331.

Marzban H, Chung S-H, Pezhouh MK, Feirabend H, Watanabe M, Voogd J, Hawkes R (2010) Antigenic compartmentation of the cerebellar cortex in the chicken (Gallus domesticus). *J Comp Neurol* 518:2221–2239.

Marzban H, Hawkes R (2011) On the Architecture of the Posterior Zone of the Cerebellum. *The Cerebellum* 10:422–434.

Marzban H, Hoy N, Buchok M, Catania KC, Hawkes R (2015) Compartmentation of the Cerebellar Cortex: Adaptation to Lifestyle in the Star-Nosed Mole Condylura cristata. *The Cerebellum* 14:106–118.

Marzban H, Zahedi S, Sanchez M, Hawkes R (2003) Antigenic compartmentation of the cerebellar cortex in the syrian hamster Mesocricetus auratus. *Brain Res* 974:176–183.

Matsushita M, Ragnarson B, and Grant G (1991) Topographic relationship between sagittal Purkinje cell bands revealed by a monoclonal antibody to zebrin I and spinocerebellar projections arising from the central cervical nucleus in the rat. *Exp Brain Res* 84:133–41.

Mostofi A, Holtzman T, Grout AS, Yeo CH, Edgley SA (2010) Electrophysiological Localization of Eyeblink-Related Microzones in Rabbit Cerebellar Cortex. *J Neurosci* 30:8920–8934. doi:10.1523/JNEUROSCI.6117-09.2010.

McKenna OC, Wallman J (1985) Accessory optic system and pretectum of birds: Comparisons with those of other vertebrates. *Brain Behav Evol* 26:91–116.

Mugnaini E, Floris A (1994) The unipolar brush cell: A neglected neuron of the mammalian cerebellar cortex. *J Comp Neurol* 339:174–180.

Necker R (1994) Sensorimotor aspects of flight control in birds: specializations in the spinal cord. *Eur J Morphol* 32:207–11.

Okado N, Ito R, Homma S (1987) The terminal distribution pattern of spinocerebellar fibres. An anterograde labelling study in the posthatching chick. *Anat Embryol (Berl)* 176:175–82.

Okhotin VE, Kalinichenko SG (2000) Localization of NO synthase in Lugaro cells and the mechanisms of NO-ergic interaction between inhibitory interneurons in the rabbit cerebellum. *Neurosci Behav Physiol* 30:525–533.

Onodera O (2006) Spinocerebellar ataxia with ocular motor apraxia and DNA repair. In: Neuropathology, pp 361–367.

Ozol K, Hayden JM, Oberdick J, Hawkes R (1999) Transverse zones in the vermis of the mouse cerebellum. *J Comp Neuro*l 412:95–111.

Pakan JMP, Graham DJ, Gutierrez-Ibanez C, Wylie DR (2011) Organization of the cerebellum: correlating zebrin immunochemistry with optic flow zones in the pigeon flocculus. *Vis Neurosci* 28:163–174.

Pakan, JMP, Graham DJ., Iwaniuk AN, and Wylie DR (2008) Differential projections from the vestibular nuclei to the flocculus and uvula-nodulus in pigeons (Columba livia). *J Comp Neurol* 508:402–417. doi:10.1002/cne.21623.

Pakan JMP, Graham DJ, Wylie DR (2014) Climbing fiber projections in relation to Zebrin stripes in the ventral Uvula in Pigeons. *J Comp Neurol* 522:3629–3643.

Pakan JMP, Iwaniuk AN, Wylie DR, Hawkes R, Marzban H (2007) Purkinje cell compartmentation as revealed by Zebrin II expression in the cerebellar cortex of pigeons (Columba livia). *J Comp Neurol* 501:619–630.

Pakan JMP, Wylie DR (2008) Congruence of zebrin II expression and functional zones defined by climbing fiber topography in the flocculus. *Neuroscience* 157:57–69.

Pakan JMP, Graham DJ, Wylie DR (2010) Organization of visual mossy fiber projections and zebrin expression in the pigeon vestibulocerebellum. *J Comp Neurol* 518:175–198.

Palay SL, Chan-Palay V (1974) Cerebellar Cortex: cytology and organization.

Palczewska M, Batta G, Groves P, Linse S, Kuznicki J (2005) Characterization of calretinin I-II as an EF-hand, Ca2+, H+-sensing domain. *Protein Sci* 14:1879–1887.

Paukert M, Huang YH, Tanaka K, Rothstein JD, Bergles DE (2010) Zones of Enhanced Glutamate Release from Climbing Fibers in the Mammalian Cerebellum. *J Neurosci* 30:7290–7299. doi:10.1523/JNEUROSCI.5118-09.2010.

Pijpers A, Apps R, Pardoe J, Voogd J, Ruigrok TJH (2006) Precise Spatial Relationships between Mossy Fibers and Climbing Fibers in Rat Cerebellar Cortical Zones. *J Neurosci* 26:12067–12080.

Pijpers A, Voogd J, Ruigrok TJH (2005) Topography of olivo-cortico-nuclear modules in the intermediate cerebellum of the rat. *J Comp Neurol* 492:193–213.

Pushchina E V, Varaksin AA (2001) Argyrophilic and nitroxydergic bipolar neurons (Lugaro cells) in the cerebellum of Pholidapus dybowskii. *Zh Evol Biokhim Fiziol* 37:437–441.

Ramón S, Cajal S (1911) Histologie du système nerveux de l'homme et des vertébrés. Paris: Maloine.

Rogers JH (1989) Immunoreactivity for calretinin and other calcium-binding proteins in cerebellum. *Neuroscience* 31:711–721.

Rivkin A, Herrup K (2003) Development of cerebellar modules: Extrinsic control of late-phase Zebrin II pattern and the exploration of rat/mouse species differences. *Mol Cell Neurosci* 24:887–901.

Rogers JH (1989) Immunoreactivity for calretinin and other calcium-binding proteins in cerebellum. *Neuroscience* 31:711–721.

Ruigrok TJH (2003) Collateralization of climbing and mossy fibers projecting to the nodulus and flocculus of the rat cerebellum. *J Comp Neurol* 466:278–298.

Ruigrok TJH, Pijpers A, Goedknegt-Sabel E, and Coulon P (2008) Multiple cerebellar zones are involved in the control of individual muscles: a retrograde transneuronal tracing study with rabies virus in the rat. *Eur J Neurosci* 28:181–200. doi:10.1111/j.1460-9568.2008.06294.x.

Sanchez M, Sillitoe RV, Attwell PJE, Ivarsson M, Rahman S, Yeo CH, et al. (2002) Compartmentation of the rabbit cerebellar cortex. *J Comp Neurol* 444:159–73.

Sahin M, Hockfield S (1990) Molecular identification of the lugaro cell in the cat cerebellar cortex. *J Comp Neurol* 301:575–584.

Sanchez M, Sillitoe R V., Attwell PJE, Ivarsson M, Rahman S, Yeo CH, Hawkes R (2002) Compartmentation of the rabbit cerebellar cortex. *J Comp Neurol* 444:159–173.

Schilling K, Oberdick J, Rossi F, Baader SL (2008) Besides Purkinje cells and granule neurons: An appraisal of the cell biology of the interneurons of the cerebellar cortex. *Histochem Cell Biol* 130:601–615.

Seil FJ, Johnson ML, Hawkes R (1995) Molecular compartmentation expressed in cerebellar cultures in the absence of neuronal activity and neuron-glia interactions. *J Comp Neurol* 356:398–407.

Sillitoe RV, Hulliger M, Dyck R, and Hawkes R (2003) Antigenic compartmentation of the cat cerebellar cortex. *Brain Res* 977:1–15.

Sillitoe RV, Künzle H, Hawkes R (2003) Zebrin II compartmentation of the cerebellum in a basal insectivore, the Madagascan hedgehog tenrec Echinops telfairi. *J Anat* 203:283–296.

Simat M, Parpan F, Fritsch JM (2007) Heterogeneity of glycinergic and gabaergic interneurons in the granule cell layer of mouse cerebellum. *J Comp Neurol* 500:71–83.

Singec I, Knoth R, Ditter M, Frotscher M, Volk B (2003) Neurogranin expression by cerebellar neurons in rodents and non-human primates. *J Comp Neurol* 459:278–289.

Slemmer JE, De Zeeuw CI, Weber JT (2004) Don't get too excited: Mechanisms of glutamate-mediated Purkinje cell death. *Prog Brain Res* 148:367–390.

Striedter GF (2005) Priciples of brain evolution.

Sugihara I (2011) Compartmentalization of the deep cerebellar nuclei based on afferent projections and aldolase C expression. *Cerebellum* 10:449–463. doi:10.1007/s12311-010-0226-1.

Sugihara I, Marshall SP, Lang EJ (2007) Relationship of complex spike synchrony bands and climbing fibre projection determined by reference to aldolase C compartments in crus IIa of the rat cerebellar cortex. *J Comp Neurol* 501:13–29. doi:10.1002/cne.21223.

Sugihara I, Quy PN (2007) Identification of aldolase C compartments in the mouse cerebellar cortex by olivocerebellar labeling. *J Comp Neurol* 500:1076–1092.

Sugihara I, Shinoda Y (2004) Molecular, Topographic, and Functional Organization of the Cerebellar Cortex: A Study with Combined Aldolase C and Olivocerebellar Labeling. *J Neurosci* 24:8771–8785.

Sugihara I, Shinoda Y (2007) Molecular, Topographic, and Functional Organization of the Cerebellar Nuclei: Analysis by Three-Dimensional Mapping of the Olivonuclear Projection and Aldolase C Labeling. *J Neurosci* 27:9696–9710. doi:10.1523/JNEUROSCI.1579-07.2007.

Takács J, Markova L, Borostyánköi Z, Görcs TJ, Hámori J (1999) Metabotrop glutamate receptor type 1a expressing unipolar brush cells in the cerebellar cortex of different species: A comparative quantitative study. *J Neurosci Res* 55:733–748.

Vibulyaseck S, Luo Y, Fujita H, Oh-Nishi A, Ohki-Hamazaki H, Sugihara I (2015) Compartmentalization of the chick cerebellar cortex based on the link between the striped expression pattern of aldolase C and the topographic olivocerebellar projection. *J Comp Neurol* 523:1886–1912.

Voogd J, Bigaré F (1980) Topographical distribution of olivary and cortico nuclear fibres in the cerebellum: a review. In: The Inferior Olivary Nucleus. (Courville J, de Montigny C, Lamarre Y, eds), pp 207–234. New York: Raven Press.

Voogd J, Gerrits NM, Ruigrok TJH (1996) Organization of the Vestibulocerebellum. *Ann N. Y. Acad Sci* 781:553-579. doi: 10.1111/j.1749-6632.1996.tb15728.x.

Voogd J, Glickstein M (1998) The anatomy of the cerebellum. *Trends Cogn Sci* 2:307–313.

Voogd J, Pardoe J, Ruigrok TJH, Apps R (2003) The distribution of climbing and mossy fiber collateral branches from the copula pyramidis and the paramedian lobule: congruence of climbing fiber cortical zones and the pattern of zebrin banding within the rat cerebellum. *J Neurosci* 23:4645–4656.

Voogd J, Ruigrok TJ (1997) Transverse and longitudinal patterns in the mammalian cerebellum. *Prog Brain Res* 114:21–37.

Voogd J, Ruigrok TJH (2004) The organization of the corticonuclear and olivocerebellar climbing fiber projections to the rat cerebellar vermis: The congruence of projection zones and the zebrin pattern. *J Neurocytol* 33:5–21.

Voogd J, Wylie DRW (2004) Functional and Anatomical Organization of Floccular Zones: A Preserved Feature in Vertebrates. *J Comp Neurol* 470:107–112.

Wadiche JI, Jahr CE (2005) Patterned expression of Purkinje cell glutamate transporters controls synaptic plasticity. *Nat Neurosci* 8:1329–1334. doi:10.1038/nn1539.

Wang X, Chen G, Gao W, and Ebner TJ (2011) Parasagittally aligned, mGluR1-dependent patches are evoked at long latencies by parallel fibre stimulation in the mouse cerebellar cortex in vivo. *J Neurophysiol* 105:1732–1746. doi:10.1152/jn.00717.2010.

Wu HS, Sugihara I, Shinoda Y (1999) Projection patterns of single mossy fibers originating from the lateral reticular nucleus in the rat cerebellar cortex and nuclei. *J Comp Neurol* 411:97–118.

Wylie DR (2001) Projections from the nucleus of the basal optic root and nucleus lentiformis mesencephali to the inferior olive in pigeons (Columba livia). *J Comp Neurol* 429:502–513.

Wylie DR (2013) Processing of visual signals related to self-motion in the cerebellum of pigeons. *Front Behav Neurosci* 7:1–15.

Wylie DR, Bischof WF, Frost BJ (1998) Common reference frame for neural coding of translational and rotational optic flow. *Nature* 392, 278–282. doi:10.1038/32648.

Wylie DRW, Brown MR, Barkley RR, Winship IR, Crowder NA, Todd KG (2003a) Zonal Organization of the Vestibulocerebellum in Pigeons (Columba livia): II. Projections of the Rotation Zones of the Flocculus. *J Comp Neurol* 456:140–153.

Wylie DRW, Brown MR, Winship IANR, Crowder NA, Todd KG (2003b) Zonal organization of the vestibulocerebellum in pigeons (Columba livia): III. Projections of the translation zones of the ventral uvula and nodulus. *J Comp Neurol* 465:179–194.

Wylie DRW, Crowder NA (2000) Spatiotemporal properties of fast and slow neurons in the pretectal nucleus lentiformis mesencephali in pigeons. *J Neurophysiol* 84:2529–2540.

Wylie DR, Frost BJ (1991) Purkinje cells in the vestibulocerebellum of the pigeon respond best to either translational or rotational wholefield visual motion. *Exp Brain Res* 86:229–232. doi:10.1007/BF00231059.

Wylie DR, Frost BJ (1993) Responses of pigeon vestibulocerebellar neurons to optokinetic stimulation. II. The 3-dimensional reference frame of rotation neurons in the flocculus. *J Neurophysiol* 70:2647–2659.

Wylie DR, Frost BJ (1999) Complex spike activity of Purkinje cells in the ventral uvula and nodulus of pigeons in response to translational optic flow. *J Neurophysiol* 81:256–266.

Wylie DR, Gutiérrez-Ibáñez C, Corfield JR, Craciun I, Graham DJ, Hurd PL (2017) Inferior olivary projection to the zebrin II stripes in lobule IXcd of the pigeon flocculus: A retrograde tracing study. *J Comp Neurol* 525:3158–3173.

Wylie DR, Hoops D, Aspden JW, Iwaniuk AN (2016) Zebrin II is expressed in sagittal stripes in the cerebellum of dragon lizards (Ctenophorus sp.). *Brain Behav Evol* 88:177–186.

Wylie DR, Jensen M, Gutierrez-Ibanez C, Graham DJ, Iwaniuk AN (2013) Heterogeneity of calretinin expression in the avian cerebellar cortex of pigeons and relationship with zebrin II. *J Chem Neuroanat* 52:95–103.

Wylie DR, Kripalani T, Frost BJ (1993) Responses of pigeon vestibulocerebellar neurons to optokinetic stimulation. I. Functional organization of neurons discriminating between translational and rotational visual flow. *J Neurophysiol* 70:2632–2646.

Wylie DR, Pakan JMP, Elliot CA, Graham DJ, Iwaniuk AN (2007) Projections of the nucleus of the basal optic root in pigeons (Columba livia): A comparison of the morphology and distribution of neurons with different efferent projections. *Vis Neurosci* 24:691–707. doi:10.1017/S0952523807070599.

Wylie DR, Pakan JMP, Huynh H, Graham DJ, Iwaniuk AN (2012) Distribution of zebrin-immunoreactive Purkinje cell terminals in the cerebellar and vestibular nuclei of birds. *J Comp Neurol* 520:1532–1546. doi:10.1002/cne.22810.

Wylie DR, Winship IR, Glover RG (1999) Projections from the medial column of the inferior olive to different classes of rotation-sensitive Purkinje cells in the flocculus of pigeons. *Neurosci Lett* 268:97–100. doi:10.1016/S0304-3940(99)00390-0.

Zhou H, Lin Z, Voges K, Ju C, Gao Z, Bosman LWJ, et al. (2014) Cerebellar modules operate at different frequencies. *Elife* 3, e02536. doi:10.7554/eLife.02536.